Universidade do Minho
Escola de Ciências

Vítor Rafael Miranda Martins

The role of endoplasmic reticulum-mitochondria contact sites on mitochondrial permeabilization and regulated cell death induced by acetic acid

Dissertação de Mestrado

Mestrado em Bioquímica Aplicada, Área de Especialização em Biomedicina

Trabalho efetuado sob a orientação de:

Professora Doutora Maria João Marques Ferreira de Sousa Moreira

Professora Doutora Maria Manuela Sansonetty Gonçalves Côrte-Real

Fevereiro de 2018

DECLARAÇÃO

Nome: Vítor Rafael Miranda Martins

Endereço eletrónico: vitor.rmmartins@gmail.com

Telefone: +351 913 860 748

Número de Cartão do Cidadão: 14411933

Título da Dissertação de Mestrado:

The role of endoplasmic reticulum-mitochondria contact sites on mitochondrial permeabilization and regulated cell death induced by acetic acid.

O papel dos locais de contacto entre o retículo endoplasmático e a mitocôndria na permeabilização mitocondrial e morte celular regulada induzida por ácido acético.

Orientadores:

Professora Doutora Maria João Marques Ferreira Sousa Moreira

Professora Doutora Maria Manuela Sansonetty Gonçalves Côrte-Real

Ano de conclusão: 2018

Designação do Mestrado:

Mestrado em Bioquímica Aplicada, Área de Especialização em Biomedicina

Universidade do Minho, 28 de fevereiro de 2018

_____

(Vítor Rafael Miranda Martins)

ACKNOWLEDGEMENTS

"Find what you love and let it kill you."
–Charles Bukowski?

This journey through college has been both the most amazing experience of my life and the most stressful one. Ending this chapter feels bittersweet. Nonetheless, I am very happy to acknowledge everyone who went through this adventure with me.

To my supervisor, Maria João Sousa, for giving me the chance to work alongside an incredible research group. For always being available to listen to my (sometimes crazy) ideas, that would incessantly come around at least twice a day. For leading by example and showing me the tools to success, for believing in me and in my abilities as a researcher. I greatly benefited from this collaboration, both personally and professionally. To my co-supervisor, Manuela Côrte-Real, thank you for your kindness, help and great contributions to this dissertation. To Doctor Susana Chaves for her help and ideas whenever I needed.

To my Micro I colleagues, thank you for your help in this process and for making our lab such a good workplace. To "Mr. Louis" and "Nuriana", for always responding to my call with a smile and helping me whenever I needed. To "almoços nerds", for all the coffee breaks in between work to take the edge off and for all the conversations about the most ridiculous topics. Particularly, I want to thank Sara: for your ideas and, above all, your cooperative nature and uplifting spirit. To "MENOS BÉ", thank you for your friendship and support; specially to Bruno and Tita for being my partners in crime throughout the last four years. Your friendship means the world to me. To Rita: for your friendship, motivation and contributions to the writing process.

To Rui Pedro: thank you for your incredible support and belief in me, even when I did not have any. I was so deeply rooted into this project that it seemed that there was no way to snap out of it, and yet you stood by me through thick and thin. Thank you for these amazing three years. You have been by far one of the best conquests of my life.

To my parents, brother and sisters. Despite not believing that an education would necessarily bring me a steady future, you supported my decision to try to create a better life for myself and for that I am very grateful. A special thanks to my mother for all the sacrifices she had to make so I would not have to. There is no one in this world that I love more than you. To my sister, Tânia, you fought the hardest and are truly the unsung hero in all of this. I will be forever grateful to and for you.

Lastly, I would also like to acknowledge the Center of Molecular and Environmental Biology (CBMA) and the strategic program UID/BIA/04050/2013 (POCI-01-0145-FEDER-007569) financed by national funds through Fundação para a Ciência e a Tecnologia (FCT) and by Fundo Europeu de Desenvolvimento Regional (FEDER) through COMPETE 2020 – Programa Operacional Competitividade e Internacionalização (POCI).

THE ROLE OF ENDOPLASMIC RETICULUM-MITOCHONDRIA CONTACT SITES ON MITOCHONDRIAL PERMEABILIZATION AND REGULATED CELL DEATH INDUCED BY ACETIC ACID

ABSTRACT

Zones of close membrane apposition function as signaling hubs for interorganelle communication, sustaining organelle homeostasis and exchange of cellular cues. Particularly, endoplasmic reticulum-mitochondria contact sites (ER-MCS) have been the subject of recent scientific interest since the discovery that these structures are disrupted in several pathologies such as cancer and neurodegenerative diseases. Interestingly, these diseases are also characterized by dysregulated apoptosis. Due to the emerging data that correlates ER-MCS function to known events of the apoptotic program, we aimed to dissect this interplay using the yeast *Saccharomyces cerevisiae* as a model organism. Until recently, the only known tethering complex between ER and mitochondria of this yeast was the ER-mitochondria encounter structure (ERMES). We have previously shown that this organism commits to an apoptotic-like mitochondria-dependent cell death process in response to acetic acid, a frequent byproduct of alcoholic fermentation carried out by *S. cerevisiae*. Thus, the main aim of this dissertation was to assess the role of the ERMES complex in the mediation of acetic acid-induced regulated cell death. Preliminary analysis revealed a remarkable role of ERMES in the acid stress response and prompted us to further pursue a phenotypical characterization of the cellular alterations underlying this process. Using mutants deficient in components of the ERMES complex and different techniques, from fluorescence microscopy to flow cytometry, we were able to unveil ERMES as a regulator of cell death and, possibly, its own regulators. In all, this work will aid in the understanding of molecular pathways not yet fully disclosed in apoptosis, namely mitochondrial outer membrane permeabilization. These results come with both biomedical and biotechnological interest since they are expected to further encourage the study of ER-MCS in mammalian cell death as well as the development of more resilient yeast strains in industrial processes.

O PAPEL DOS LOCAIS DE CONTACTO ENTRE O RETÍCULO ENDOPLASMÁTICO E A MITOCÔNDRIA NA PERMEABILIZAÇÃO MITOCONDRIAL E MORTE CELULAR REGULADA INDUZIDA POR ÁCIDO ACÉTICO

RESUMO

As zonas de contacto intermembranar funcionam como centros de sinalização na comunicação interorganelar, assegurando a homeostasia e a troca de informação entre organelos. Em particular, os locais de contacto entre o retículo endoplasmático e a mitocôndria (ER-MCS) têm sido recentemente alvo de grande interesse científico dado que a sua disrupção está associada a várias patologias como cancro e doenças neurodegenerativas. Curiosamente, estas doenças são também caracterizadas por fenómenos de desregulação apoptótica. Atendendo a estudos emergentes que correlacionam o papel dos ER-MCS com funções apoptóticas, o objetivo deste trabalho consistiu em examinar esta interação usando como modelo a levedura *Saccharomyces cerevisiae*. Até recentemente, o único complexo responsável pela ancoragem do retículo endoplasmático à mitocôndria neste organismo era o complexo ERMES (do inglês, *ER-mitochondria encounter structure*). Estudos anteriores demonstraram que *S. cerevisiae* envereda por um processo de morte celular com características típicas da apoptose em resposta a ácido acético, um subproduto frequente da fermentação alcoólica deste organismo. Como tal, o objetivo principal desta dissertação é avaliar o papel do complexo ERMES na morte celular induzida por ácido acético. Análises preliminares revelaram um papel notável na resposta ao stress instigado por este ácido, o que nos levou a enveredar por uma caracterização fenotípica das alterações celulares subjacentes a este processo. Recorrendo à utilização de mutantes cujas subunidades deste complexo foram deletadas e a diferentes técnicas, desde microscopia de fluorescência a citometria de fluxo, foi possível apontar o complexo ERMES como um modulador da morte celular regulada e, possivelmente, os seus próprios reguladores. No seu conjunto, este trabalho irá auxiliar na compreensão dos mecanismos moleculares que ainda não foram completamente desvendados na apoptose, nomeadamente a permeabilização da membrana mitocondrial externa. Os resultados aqui reportados fornecem benefícios em termos biomédicos e biotecnológicos, uma vez que é esperado que encorajem o estudo dos ER-MCS na morte celular em mamíferos bem como o desenvolvimento de estirpes mais resilientes em processos industriais.

TABLE OF CONTENTS

List of Abbreviations and Acronyms

ρ^0 – Cell lacking mitochondrial DNA

$\Delta\Psi_m$ – Mitochondrial transmembrane potential

ANT – Adenine nucleotide translocator

Bcl-2 – B-cell lymphoma 2

CsA – Cyclosporine A

Cyp-D – Cyclophilin D

Cyt *c* – Cytochrome *c*

CL – Cardiolipin

CRC – Colorectal cancer

DHE – Dihydroethidium

$DiOC_6(3)$ – 3,3′-dihexyloxacarbocyanine iodide

EMC – ER membrane protein complex

ER – Endoplasmic reticulum

ER-MCS – ER-mitochondria contact sites

ERMES – ER-mitochondria encounter structure

IMM – Inner mitochondrial membrane

IMS – Mitochondrial intermembrane space

MAC – Mitochondrial apoptosis-induced channel

MAM – Mitochondria-associated membrane

MOMP – Mitochondrial outer membrane permeabilization

mPTP – Mitochondrial permeability transition pore

OMM – Outer mitochondrial membrane

PA – Phosphatidic acid

PC – Phosphatidylcholine

PCD – Programmed cell death

PDH – Pyruvate dehydrogenase

PE – Phosphatidylethanolamine

Pi – Inorganic phosphate

PI – Propidium iodide

PS – Phosphatidylserine

RCD – Regulated cell death

ROS – Reactive oxygen species

SAM – Sorting and assembly machinery

SMP – Synaptogamin-like mitochondrial-lipid-binding protein

tBid – truncated form of Bid protein

TOM – Translocase of the outer membrane

vCLAMP – Vacuole and mitochondria patch

VDAC – Voltage-dependent anion channel

YMUC – Yeast mitochondria unselective channel

LIST OF FIGURES

LIST OF TABLES

CHAPTER 1

INTRODUCTION

1.1. REGULATED CELL DEATH IN METAZOANS AND YEAST

1.1.1. REGULATED CELL DEATH

The term "programmed cell death" (PCD) first came to prominence in 1964, when Lockshin and Williams reported a non-accidental type of cell death (Lockshin & Williams, 1964). Only eight years later, the term "apoptosis" emerged when Kerr and colleagues (1972) described a morphologically different form of cell death that appeared to be complementary to mitosis for the regulation of cell turnover in multicellular organisms. Such form, previously designated as shrinkage necrosis, was categorized as an active and programmed cell phenomenon that occurred both spontaneously and in response to death stimuli (Kerr, Wyllie, & Currie, 1972). Recently, more restrict terminology was established for PCD, characterizing it as one of several types of regulated cell death (RCD). Accordingly, while RCD represents a highly heterogeneous group that encompasses several active cell death mechanisms, the term PCD is now only used when RCD occurs in a physiological context (Galluzzi et al., 2014).

1.1.2. APOPTOSIS

Up until now apoptosis is the best-characterized RCD program, displaying a distinctive morphology and a usually genetically determined and energy-dependent mechanism (Tait, Ichim & Green, 2014). This phenomenon is extremely important to the organism since it represents an integral part of many vital processes such as cell turnover, development and function of the immune system and embryogenesis. Not surprisingly, dysregulated apoptosis can promote damage associated to several pathologies such as cancer, neurodegenerative and autoimmune diseases (Elmore, 2007). When undergoing apoptosis, the cell suffers a series of morphological alterations that allow its death without disturbing the surrounding cells and tissues. In the early stages of apoptosis, both the cell and the nucleus shrink and chromatin condenses in the nucleus peripheral regions (pyknosis), followed by complete nucleic fragmentation (karyorrhexis) and chromatin dissolution throughout the cytosol (karyolysis). The later stages are characterized by externalization of phosphatidylserine (PS), plasma membrane blebbing and formation of apoptotic bodies. PS is normally asymmetrically distributed in the plasma membrane, being mainly present in the inner leaflet. Its externalization, which is controlled by ATP-independent scramblases, functions as a signal for phagocytosis, recruiting macrophages that phagocytize apoptotic bodies

without loss of cellular contents to the extracellular medium and thus preventing the activation of inflammatory responses (Alberts et al., 2002; Saraste & Pulkki, 2000). This type of cell death is distinct from others, such as necrosis, where a higher number of tissue cells are affected. Necrotic responses lead to the swelling of the cell and subsequent rupture of the plasma membrane, resulting in the release of cellular contents and activation of an inflammatory response. Nevertheless, when ATP is depleted or caspase activity is low an apoptotic process can become necrotic (Elmore, 2007; Galluzzi et al., 2014).

The apoptotic process is dependent on a family of enzymes, caspases, which are cysteine proteases that break peptide bonds after an aspartic acid residue in the C-terminal region of a given protein (Lodish et al., 2000). These enzymes are categorized, in humans, as initiators (caspases-2, -8, -9 and -10), effectors (caspase-3, -6 and -7) and inflammatory (caspase-1, -4 and -5), but there are other caspases that have not yet been assorted (Elmore, 2007). Caspases are produced in most cells in the form of zymogens and are activated by other active caspases or by self-aggregation, generating a proteolytic cascade with an amplified signal. The cellular targets of these enzymes are mainly cytoskeleton proteins, the nuclear lamina and deoxyribonucleases, ultimately leading to cell demise (Alberts et al., 2002; Lodish et al., 2000).

1.1.3. Apoptotic pathways

There are two main apoptotic pathways: the extrinsic (or death receptor) pathway and the intrinsic (or mitochondrial) pathway (Figure 1).

The extrinsic pathway involves transmembrane interactions between a specific ligand and a receptor from the tumor necrosis factor/nerve growth factor (TNF/NGF) receptor superfamily. In the extracellular side of the transmembrane domain a cysteine-rich subdomain participates in ligand recognition, whereas in the intracellular side there is a different subdomain, known as death domain, which is responsible for signal transduction. One of the most studied ligands, Fas ligand (FasL) is a homotrimeric protein that leads to Fas receptor (FasR) trimerization. Upon trimerization, the cytosolic protein FADD (Fas-Associated Death Domain) is recruited and binds to the FasR death domain. Then, FADD binds to procaspase-8 by its death effector domain. Altogether, FasR, FADD and procaspase-8 constitute a protein complex known as death-inducing signaling complex (DISC), by which the prodomain of procaspase-8 is cleaved and active caspase-8 is generated (Budihardjo et al., 1999; Locksley, Killeen, & Lenardo, 2001).

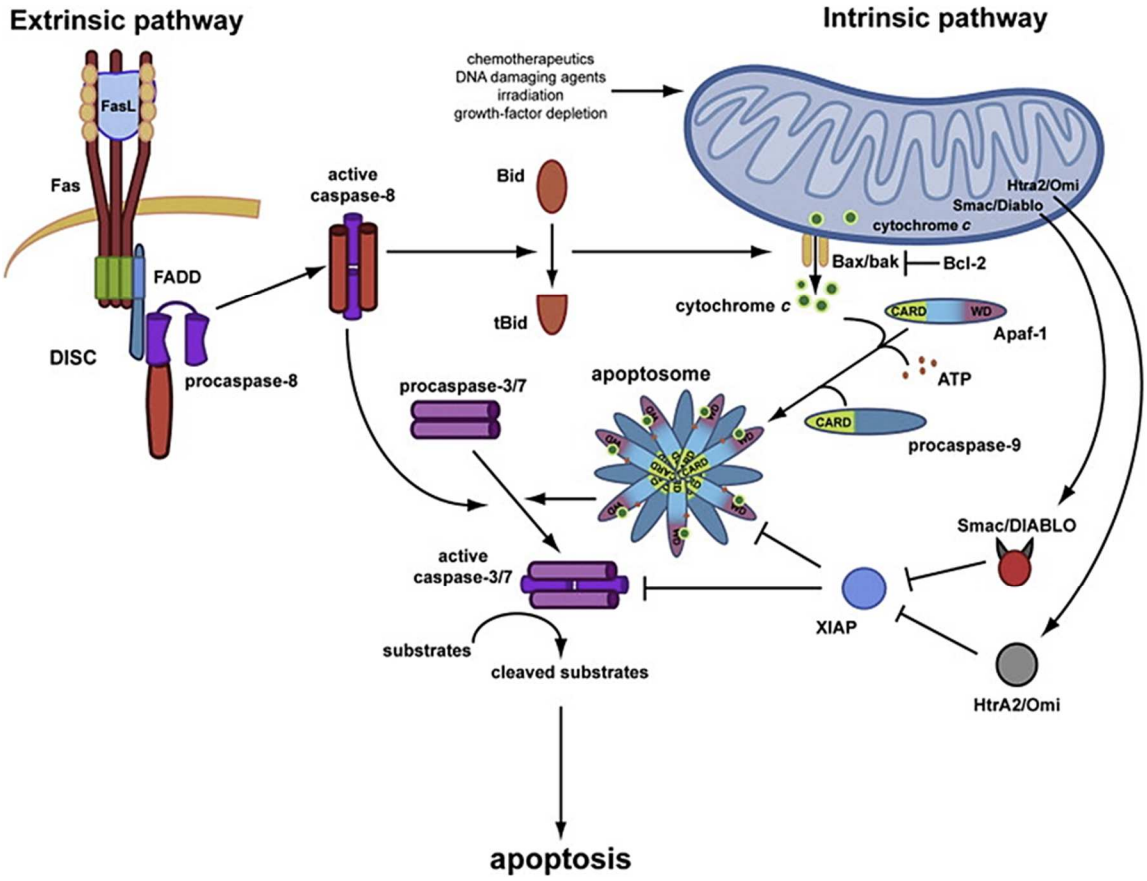

Figure 1. Intrinsic and extrinsic mammalian pathways of apoptosis signaling. Activation of both pathways leads to downstream activation of effector caspases that promote apoptosis either directly, through activation of caspase-8, or indirectly, through Bax/Bak-mediated mitochondrial outer membrane permeabilization and release of apoptogenic factors that activate caspase-9. The crosstalk between both pathways is achieved by caspase-8-mediated cleavage of the pro-apoptotic BH3-only protein Bid. (adapted from Lamkanfi & Dixit, 2010).

The intrinsic pathway begins in mitochondria as a response to intracellular or extracellular stimuli. Such stimuli can be either negative, such as absence of growth factors, hormones and cytokines, leading to the loss of suppressor functions of RCD, or positive, such as radiation, toxins and hypoxia, that directly activate apoptosis (Elmore, 2007). These stimuli promote the permeabilization of the outer mitochondrial membrane (OMM), which in turn promotes the release of pro-apoptotic factors from the intermembrane space (IMS) into the cytosol, such as cytochrome *c* (cyt *c*). Mitochondrial outer membrane permeabilization (MOMP) has been classified as a putative "point of no return" of apoptosis, along with massive caspase activation, loss of mitochondrial transmembrane potential ($\Delta\Psi_m$) and PS exposure (Kroemer et al., 2009). Cyt *c*, a 12 kDa protein that is present in both the IMS and mitochondrial cristae, is involved in the electron transfer through the respiratory complexes of the electron transport chain. Its release promotes loss of $\Delta\Psi_m$ since

the electron transport chain is responsible for the maintenance of the proton gradient across the inner mitochondrial membrane (IMM). MOMP also releases other pro-apoptotic proteins to the cytosol, such as Smac/DIABLO (Second Mitochondria-derived Activator of Caspase/Direct IAP Binding Protein with Low pI) and HtrA2/Omi (High temperature requirement A2 protein), which activate caspases, and AIF (Apoptosis Inducing Factor) and EndoG (Endonuclease G), that mediate chromatin condensation and DNA fragmentation (Saelens et al., 2004). When released to the cytosol, cyt *c* binds to the WD40 domains of the cytosolic protein Apaf-1 (Apoptotic protease activating factor 1), which in turn releases its caspase activation and recruitment domain (CARD). After oligomerization of seven monomers of Apaf-1 and cyt *c*, forming an apoptosome, the CARD of seven procaspase-9 binds to the free CARDs of Apaf-1. Active caspase-9 is generated by procaspase-9 dimerization and can further mediate activation of other caspases (Acehan et al., 2002; Budihardjo et al., 1999).

The extrinsic and intrinsic pathways converge in a crucial point of the apoptotic process, the execution phase, where effector caspases are activated by initiator caspases. Activation of caspase-8 in the extrinsic pathway and of caspase-9 in the intrinsic pathway mark the beginning of this phase, cleaving procaspase-3 and leading to its activation. In turn, caspase-3 activates the cytosolic enzyme CAD, which is translocated to the nucleus leading to DNA fragmentation and to chromatin condensation. The execution phase culminates with the morphological alteration of the plasma membrane, where PS externalization is denoted, and with the formation of apoptotic bodies. These cellular alterations are then recognized by phagocytes which promote degradation of these structures without activation of an inflammatory response (Elmore, 2007; Fadok et al., 1998). In order to amplify the extrinsic pathway signal, cells may integrate the intrinsic pathway through Bid cleavage (Figure 1). Bid, a BH3-only protein from the Bcl-2 family, is cleaved by the extrinsic pathway-activated caspase-8. Consecutively, truncated Bid (tBid) is translocated from the cytosol to mitochondria where it may alter the conformation of the pro-apoptotic protein Bax, inducing MOMP and ensuing cyt *c* release from the IMS (Desagher et al., 1999).

1.1.4. THE BCL-2 FAMILY OF PROTEINS

Proteins of the Bcl-2 (B-cell lymphoma 2) family are considered to be the key regulators of mammalian apoptosis. These proteins are divided in 2 subfamilies, depending on their apoptotic activity: anti- or pro-apoptotic. These proteins can be further divided by account of the homology

level they share with the family founding member Bcl-2: anti-apoptotic proteins exhibit four highly conserved Bcl-2 homology (BH) domains, whereas pro-apoptotic proteins can also present all BH domains though BH4 is less conserved (Shamas-Din et al., 2011). Pro-apoptotic proteins can also be divided in pro-apoptotic multidomain proteins and a special group of proteins called BH3-only proteins which, as their name suggests, only exhibit the BH3 domain.

BH3-only proteins (e.g. Bid, Bad and Bik) are sensitive to cellular stress and activate the pro-apoptotic multidomain proteins (e.g. Bax and Bak), whose action is inhibited by anti-apoptotic proteins (e.g. Bcl-2 and Bcl-xL). However, BH3-only proteins can activate pro-apoptotic proteins by different mechanisms, being divided in two classes: activators, which directly activate pro-apoptotic proteins, and sensitizers, which can stoichiometrically neutralize anti-apoptotic proteins and release the pro-apoptotic proteins from sequestration, therefore activating them (Ghibelli & Diederich, 2010; Shamas-Din et al., 2011). Furthermore, BH3-only proteins have different binding specificities in terms of the anti-apoptotic proteins that they interact with (Vo & Letai, 2010). The mechanism whereby the pro-apoptotic proteins induce apoptosis has not yet been completely established. However, a high number of studies have been performed in order to assess Bax structure and possible interactions with other cellular proteins, hence trying to unmask its regulation mechanism and downstream signaling (Czabotar et al., 2011; Desagher et al., 1999; Sattler et al., 1997; Suzuki, Youle, & Tjandra, 2000).

1.1.5. MITOCHONDRIAL PERMEABILIZATION MODELS

The mitochondrion is a ubiquitous organelle of eukaryotic cells that is accountable for the majority of the cellular energy production. Being the "powerhouse" of the cell, mitochondrion is also a central player in regulated cell death. During apoptosis, there are a series of mitochondrial alterations that take place: alteration of membrane composition and lipid distribution, MOMP formation, loss of $\Delta\Psi_m$, mitochondrial fragmentation and cristae remodeling (Cosentino & García-Sáez, 2014). Although the mechanism through which pro-apoptotic proteins are released to the cytosol is not yet completely understood, several cell death models have been suggested thus far. Among these are formation of protein or lipid pores, oligomerization of ion channels and lipid destabilization (Dewson & Kluck, 2009). In this section, an overview is presented on the current experimental evidence for the most widely accepted mechanisms of MOMP, the mitochondrial permeability transition pore (mPTP) and the mitochondria apoptosis-induced channel (MAC).

1.1.5.1. THE MITOCHONDRIAL PERMEABILITY TRANSITION PORE

The first model proposed for cyt *c* release was the mitochondrial permeability transition pore (mPTP), a non-specific, voltage-sensitive and calcium-dependent channel which crosses both mitochondrial membranes and allows the passage of solutes up to 1.5 kDa (Halestrap, McStay, & Clarke, 2002). The increase in membrane permeability due to mPTP opening causes an equilibrium in the proton electrochemical gradient with consequent depolarization of the IMM and ROS production through direct transfer of electrons to molecular oxygen. As such, the F_0F_1-ATPase starts to hydrolyze ATP and this depletion causes the cell to cease its metabolism. The passage of solutes through this pore also causes a drastic increase in the osmotic pressure of the mitochondrial matrix due to the high protein concentration. In turn, this leads to water entrance in the matrix, mitochondrial swelling and consequent OMM rupture with release of pro-apoptotic proteins to the cytosol (Kinnally & Antonsson, 2007; Rasola, et al., 2010) (Figure 2).

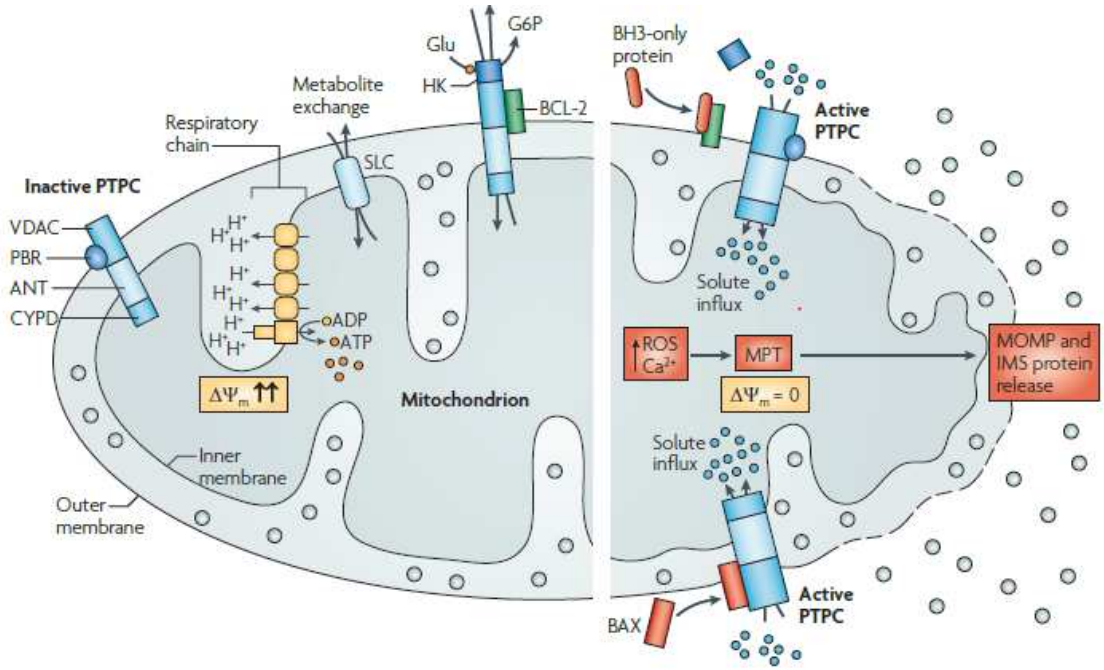

Figure 2. The mitochondrial permeability transition pore (mPTP). The mPTP, in the figure depicted as Permeability Transition Pore Complex (PTPC), is a supramolecular protein complex that is activated in response to stress signals, such as calcium overload or reactive oxygen species (ROS). Some putative constituents of this complex are the voltage-dependent anion channel (VDAC), the peripheral benzodiazepine receptor (PBR), the adenine nucleotide translocase (ANT) and cyclophilin D (CYPD). In otherwise healthy cells, the mPTP opening is inhibited by anti-apoptotic Bcl-2 proteins and hexokinase (HK). After an apoptotic stimulus, pro-apoptotic Bcl-2 proteins interact with the mPTP leading to pore opening. This phenomenon promotes the equilibration of ions between the mitochondrial matrix and the cytosol with ensuing loss of transmembrane potential and water entrance into the matrix. Since the area of inner mitochondrial membrane is greater than that of the outer mitochondrial membrane, the IMM swelling leads to OMM rupture and release of pro-apoptotic proteins to the cytosol (image credit: Fulda et al., 2010).

Despite several efforts the molecular structure of mPTP has not been completely unraveled thus far, with the most-likely components of this complex failing to prevent mPTP formation in experimental attempts. The original models postulated that the mPTP is a protein supercomplex, composed by the voltage-dependent anion channel (VDAC), cyclophilin D (Cyp-D) and the adenine nucleotide translocator (ANT). Furthermore, the mitochondrial phosphate carrier has also been implicated in mPTP formation (Leung, Varanyuwatana, & Halestrap, 2008). The transition between opening and closing of mPTP is highly regulated. Opening is regulated by low inorganic phosphate (Pi) concentration, high calcium concentration and low $\Delta\Psi_m$, whereas closing is regulated by cyclosporine-A (CsA), which binds cyclophilin D (Cyp-D) to the IMM and therefore increases resistance to pore opening (Rasola et al., 2010). However, a study in an ANT-depleted mice model revealed that ANT is not essential for mPTP assembly though it seems to have a role in its regulation (Kokoszka et al., 2004). Indeed, recent evidence was provided for a regulatory role of ANT isoform 1 in mPTP formation (Doczi et al., 2016). Likewise, the onset of mPTP was not compromised in mice lacking one or more VDAC isoforms (Baines et al., 2007). Although research performed in a CyP-D knockout mice model revealed a resistance to calcium-induced permeability transition, as well as oxidative stress, calcium concentrations above a certain threshold still triggered mPTP formation (Baines et al., 2005; Nakagawa et al., 2005). Overall, these results indicate that VDAC is not required for the onset of mPTP and that the only proven regulatory proteins so far are ANT1 and CyP-D. Due to the role of this CyP-D in protein folding, it has also been hypothesized that this protein could act as modulator of mPTP formation through calcium-induced conformational change of an actual mPTP protein (Halestrap, 2009).

A new putative component of the mPTP, the F_0F_1-ATP synthase, has been thoroughly studied in the last few years. With the enormously debated controversies over what are the actual components of mPTP, the work of Bonora and colleagues (2013) paved the way to a new set of discussion, ascribing the c-subunit of the ATP synthase to the supramolecular complex that decides life or death. In this work, the authors demonstrated that silencing of the three genes that code for the c-subunit of F_0F_1-ATPase prevented MOMP formation in response to both oxidative stress and calcium overload in a glycolytic cell model (Bonora et al., 2013). Another hypothesis that has been put forth is that the mPTP is formed by dimers of the F_0F_1-ATPase, as evidenced by the similar electrophysiological properties between mPTP and ATPase dimers in lipid bilayers (Giorgio et al., 2013). Later work would also reveal that c-subunit rings reconstituted into liposomes presented voltage-sensitive conductance (Alavian et al., 2014). However, very recent studies have defied the

notion of mPTP being composed by c-subunit channels. Atomic simulations of a c-subunit channel revealed large discrepancies in conductance and ion selectivity in comparison to what was already determined for mPTP (Zhou et al., 2017). Furthermore, gene disruption studies revealed that the absence of the c-subunit of the F_0F_1-ATPase did not affect mPTP formation, proving that this protein is not essential for the onset of mPTP (He et al., 2017).

Even so, cyt *c* release can also occur without loss of $\Delta\Psi_m$ or mitochondrial integrity, suggesting that an alternative mechanism of permeabilization exists, such as an OMM pore (Dejean et al., 2006). Studies in fibroblasts lacking CyP-D expression revealed that this protein is not involved in apoptosis induced by Bax, TNF-α or staurosporine (Baines et al., 2005). Moreover, wild-type and VDAC-deficient mice were also shown to respond similarly to Bax-induced cell death (Baines et al., 2007). Accordingly, CyP-D and VDAC (and by consequence the mPTP itself) are nowadays mostly ascribed to necrotic cell death (Nakagawa et al., 2005). This led to a new model for cyt *c* release, the mitochondrial apoptosis-induced channel (MAC).

1.1.5.2. THE MITOCHONDRIAL APOPTOSIS-INDUCED CHANNEL

MAC is a high-conductance voltage-independent channel formed by pro-apoptotic multi-domain and BH3-only Bcl-2 proteins and its activity is inhibited by anti-apoptotic Bcl-2 proteins (Dejean et al., 2010; Martinez-Caballero et al., 2005). In light of this model, tBid promotes Bax and Bak oligomerization in the OMM with subsequent production of a pore sufficiently large to diffuse molecules such as cyt *c* to the cytosol, while maintaining $\Delta\Psi_m$ (Dejean et al., 2006; Polčic, Jaká & Mentel, 2015) (Figure 3). Nevertheless, there are small differences in the electrophysiological characteristics between MAC and channels of purified Bax in artificial membranes (Lewis, Bethell, Patel, Martinou, & Antonsson B., 1998; Saito, Korsmeyer, & Schlesinger, 2000). As such, a hypothesis emerged that although Bax may be a crucial constituent of MAC, this channel may have other components (Pavlov et al., 2001). However, up until now the components of MAC have not been completely identified. Taking into account that MAC is a complex with a relatively small pore (approximately 4 nm), this model does not explain how certain apoptogenic molecules cross the OMM (Pavlov et al., 2001; Tait & Green, 2010). Therefore, there is a possibility that mPTP could work alongside MAC in the release of pro-apoptotic factors (Halestrap et al., 2002).

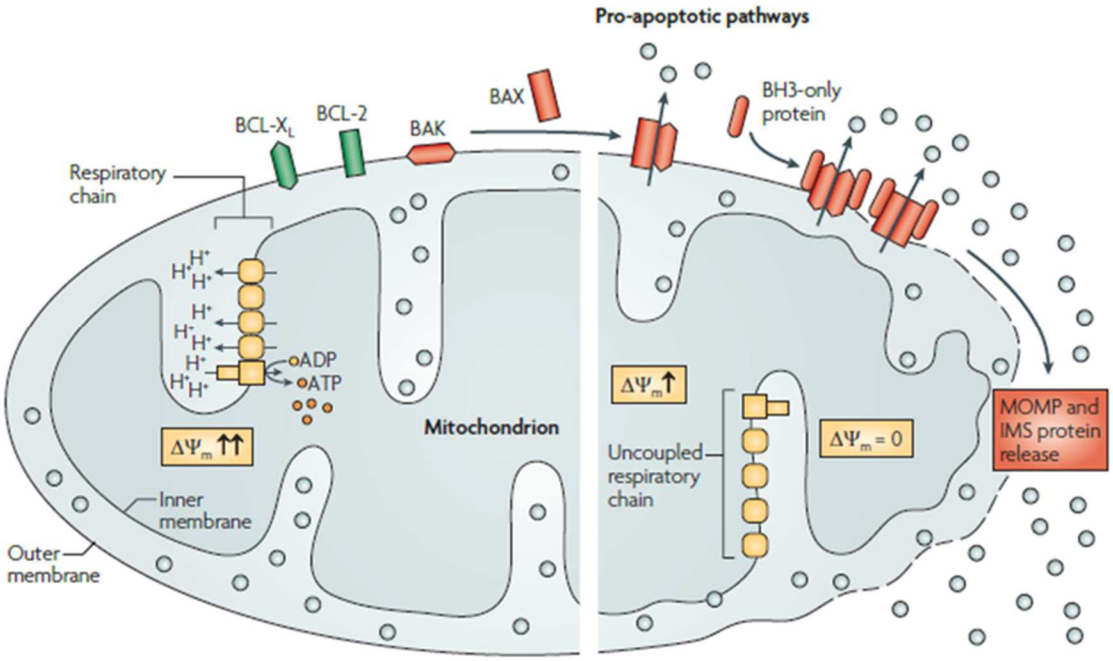

Figure 3. The mitochondria apoptosis-induced channel (MAC). This model postulates that mitochondrial outer membrane permeabilization (MOMP) is regulated by the Bcl-2 family of proteins. In healthy cells, anti-apoptotic Bcl-2 proteins (such as Bcl-2 and Bcl-XL) are inserted in mitochondria and inhibit the mitochondrial targeting of the pro-apoptotic protein Bax. However, upon apoptotic stimuli the BH3-only proteins can neutralize anti-apoptotic factors or directly activate Bax and Bak. In turn, these proteins form homo- or hetero-oligomers that allow the passage of apoptogenic factors from the intermembrane space to the cytosol (image credit: Fulda et al., 2010).

Despite the efforts that have been put into unraveling the molecular machinery that triggers the apoptotic cascade, there is still a large gap to be filled in relation to how pro-apoptotic proteins are released from mitochondria. The reported experimental evidence displays the lack of consensus as to what is the actual mitochondrial permeabilization pathway (or if there is only one) and emphasizes the importance of continuing this line of research.

1.1.6. YEAST AS A COMPLEMENTARY MODEL FOR THE STUDY OF REGULATED CELL DEATH

Saccharomyces cerevisiae is a unicellular eukaryotic organism that has been extensively used to study molecular mechanisms conserved in mammalian cells such as cell division, autophagy and vesicular trafficking (Nasmyth, 1996; Reggiori & Klionsky, 2013; Schekman, 1992). After its genome was completely sequenced, it was found that approximately 30% of the human genes known to cause disease have a yeast orthologue (Foury, 1997). As such, yeast readily became an attractive cell model to study the mechanisms of several human diseases, either by

complementation assays or turning yeast into a humanized system. In this context, it has been extensively used, for example, to assess protein folding dysfunction in many neurodegenerative diseases, such as Alzheimer's, Parkinson's and Huntington's disease (Winderickx et al., 2008)

The term "apoptosis", when referring to *S. cerevisiae*, generated some controversy since this organism does not possess obvious orthologues of the cellular machinery that governs mammalian apoptosis, e.g. the Bcl-2 family of proteins (Weinberger, Ramachandran, & Burhans, 2003). Moreover, the fact that a unicellular organism would willingly commit suicide was thought of as very unlikely, since death of a single cell means the death of the whole organism. However, in 1997, studies performed on a strain of *S. cerevisiae* carrying a mutation in the *CDC48* gene, $CDC48^{S565G}$, which encodes a cell cycle regulatory protein (AAA-ATPase), demonstrated an apoptotic phenotype similar to mammalian cells, namely PS externalization, ROS production, chromatin condensation and nuclear fragmentation (Madeo, Fröhlich, & Fröhlich, 1997). This result, although initially not well-taken, propelled the idea that yeast populations should not be thought of as individuals but as an interacting multicellular community. Indeed, it was demonstrated that RCD in yeast populations occurs whenever the death of a cell represents a benefit to the colony, a phenomenon termed phenoptosis (Skulachev, 2000). It is now known that apoptosis can occur due to several scenarios, such as chronological or replicative aging, as well as after unsuccessful mating (Büttner et al., 2006).

Since in mammalian cells there are innumerous apoptotic regulators that interact with each other, it is difficult to study their individual effects on this model system. Thus, a simpler model was required, where apoptosis could be induced and mammalian proteins studied independently of their regulators. The yeast *Saccharomyces cerevisiae* constitutes a clean background to the heterologous expression of apoptotic proteins since its genome does not encode most of them and, in terms of biochemical and regulation pathways, this organism presents great phylogenetic conservation in comparison to mammalians (Fleury et al., 2002; Madeo et al., 2002). Moreover, this organism has an easy tractability, presenting a fast growth rate in cheap and defined media. Recently, a yeast protein, Ybh3p, was found to contain a functional BH3 domain that interacts with Bcl-xL and activates the intrinsic apoptotic pathway upon apoptotic stimuli (Büttner et al., 2011).

To the extent of current knowledge, the genome of *S. cerevisiae* does not encode any orthologues of metazoan caspases. However, this yeast encodes a type I metacaspase (Mca1p/Yca1p), a cysteine protease with a very similar structure to caspases but with different

cleavage specificity, hydrolyzing peptide bonds after arginine/lysine residues instead of aspartic acid (Tsiatsiani et al., 2011; Wong, Yan, & Chi, 2012). Even so, both enzymes have common substrates suggesting that they are actually functional orthologues (Silva et al., 2011). Nonetheless, RCD in *Saccharomyces cerevisiae* also occurs in a metacaspase-independent manner, hinting the existence of other proteins with similar activities (Madeo et al., 2009). In addition to metacaspase, this yeast has several other orthologues of mammalian apoptotic regulators, such as Aif1p, Ynm3p and Nuc1p which are, respectively, orthologues of AIF, Htr2/Omi and EndoG (Carmona-Gutierrez et al., 2010; Fahrenkrog, Sauder, & Aebi, 2004; Wissing et al., 2004).

The presence of a yeast akin of the mammalian mPTP is still a matter of debate. Even though yeast cells undergo a mitochondria-dependent cell death process that is very similar to its mammalian counterpart, the presence of a mPTP-like structure has not been determined so far (Carraro & Bernardi, 2016). An initially very close candidate was the yeast mPTP, or YMUC (yeast mitochondria unselective channel). Regardless of the fact that, in essence, the mammalian and yeast mPTP appear to have similar physiological roles, their regulation stems from opposing signals. Whilst mPTP opening is stimulated by high Pi and inhibited by CsA and ATP in mammals (Halestrap & Davidson, 1990), its yeast counterpart is opened in response to high ATP levels (Velours, Rigoulet, & Guerin, 1977) and inhibited by high Pi concentrations (Roucou, Manon, & Guérin, 1997), with CsA not affecting the process (Jung, Bradshaw, & Pfeiffer, 1997). However, no components of YMUC have been identified so far. Moreover, the search for a yeast mPTP has been somewhat neglected in recent years due to the fact that no IMM calcium transporter has yet been identified in this organism. Considering the major role of calcium in the activation of the mammalian intrinsic pathway of apoptosis (discussed later in this thesis), efforts are being mostly directed towards unveiling the mammalian mPTP composition and regulation.

1.2. ACETIC ACID AS AN INDUCER OF CELL DEATH

1.2.1. ACETIC ACID

Acetic acid, or ethanoic acid (CH_3COOH), is a frequent by-product of the alcoholic fermentation carried out by *S. cerevisiae* and the main component of volatile acidity in wine. Explored in the food industry as a natural preservative, this and other weak acids can prevent food spoilage due to the cytotoxic effects they exert on several fungi, a frequent and common feature of

weak organic acids. Usually, alcoholic fermentation by *S. cerevisiae* yields low media concentrations of acetic acid ranging from 0.1-0.3 g/L (Zamora, 2009). However, contaminating lactic and acetic acid bacteria can account for higher production of this acid. Acetic acid concentrations above 0.6 g/L can negatively affect the yeast fermentative performance, such as in wine or bioethanol production, leading to ineffective fermentation and, particularly in wine, concentrations above 0.9 g/L can alter its organoleptic qualities (Ribéreau-Gayon et al., 2006; Sousa et al., 2012). As of 2017, the maximum acceptable limit of volatile acidity for the majority of wines is 1.2 g/L of acetic acid (OIV 2017).

Although it was demonstrated that acetic acid treatment results in cell death (Pampulha & Loureiro-Dias, 1989; Pinto et al., 1989), the mechanism through which it impacts cell survival and inhibits cell growth is not yet fully understood. At physiological pH, acetic acid (pKa=4.76) is predominantly in its dissociated form, acetate (CH_3COO^-), but in low pH media such as in fermentative batch cultures this acid is mainly non-dissociated. In glucose-repressed *S. cerevisiae* cells, acetic acid is usually not metabolized until glucose depletion is reached. In low pH media with repressing glucose concentrations, acetic acid is able to cross the cell membrane by simple diffusion. Once inside the cell, and if the intracellular pH is higher than the extracellular pH, the acid dissociates and it can accumulate inside the cell as a function of ΔpH, leading to intracellular acidification and impacting cell metabolic activity and viability (Casal, Cardoso, & Leão, 1998; Pampulha & Loureiro-Dias, 1989).

1.2.2. ACETIC ACID METABOLISM

During aerobic respiration of *S. cerevisiae*, cytosolic pyruvate from the glycolytic pathway is transported to mitochondria and undergoes direct oxidative decarboxylation to acetyl-CoA by the pyruvate dehydrogenase complex (PDH), linking glycolysis to the tricarboxylic acid cycle and further to oxidative phosphorylation. On the other hand, during alcoholic fermentation, pyruvate suffers oxidative decarboxylation to ethanol, a process mediated by the PDH bypass with acetaldehyde as an intermediate (Remize, Andrieu, & Dequin, 2000). The yeast pathway for acetic acid formation in wine, without neglecting possible contributions from other pathways, is its production through the PDH bypass via acetaldehyde, probably because the activity of acetaldehyde dehydrogenase surpasses that of acetyl-CoA synthetase (van den Berg et al., 1996; Vilela-Moura et al., 2011). Notwithstanding, acetate can also be produced to restore cellular redox levels. Under anaerobic

conditions excess NADH is produced during glycolysis, a process which is counteracted by the concomitant production of glycerol and NAD^+. Moreover, in response to hyperosmotic stress induced by high sugar concentrations yeast also produces glycerol as a compatible solute, thus preventing the efflux of water from the intracellular media. As such, the redox balance within the cell is compromised by NAD^+ overproduction and, in order to restore it, yeast cells can convert excess NAD^+ to NADH by oxidizing acetaldehyde to acetate in a reaction catalyzed by a family of enzymes known as aldehyde dehydrogenases (Erasmus, Cliff, & van Vuuren, 2004; Michnick et al., 1997; Remize et al., 1999).

1.2.3. ACETIC ACID-INDUCED REGULATED CELL DEATH

Acetic acid has been studied in our lab as an inducer of apoptotic-like cell death in *S. cerevisiae* for over 18 years. Pioneering work has demonstrated the presence of some functional and structural features in acetic acid-treated *S. cerevisiae* that resemble those of mammalian apoptosis, namely externalization of phosphatidylserine, DNA degradation and chromatin condensation (Ludovico et al., 2001). In this work, it was shown that exponential-phase cells under low acetic acid concentrations (up to 120 mM) commit to an active cell death process that is dependent on protein synthesis (Ludovico et al., 2001), a phenotype that was also found in response to H_2O_2-induced cell death (Madeo et al., 1999).

Since then, evidence was provided for the involvement of mitochondria in acetic acid-induced cell death, describing that yeast cells under treatment display loss of $\Delta\Psi_m$, ROS accumulation, decreased cyt *c* oxidase (COX) activity and cyt *c* release (Ludovico et al., 2002). In this study, it was also shown through an *ATP10* mutant that a fully assembled mitochondrial ATPase complex is required for the release of cyt *c*. The same work also documented the inability of a respiratory-deficient (ρ^0) strain to commit to an RCD program. These phenotypes were determined not to be due to impaired respiration since oligomycin-treated wild-type cells did not display enhanced survival (Ludovico et al., 2002). Moreover, ROS production in response to this death inducer was also shown to mediate the RCD process rather than being a by-product (Giannattasio et al., 2005).

It was previously reported by Pereira and colleagues (2007) that deletion of the Aac1/2/3 protein isoforms (yeast orthologues of ANT) significantly delays acetic acid-induced RCD. The *aac1/2/3*Δ strain revealed a later onset of common apoptotic features in comparison to the control strain, with the exception of ROS accumulation. Furthermore, *aac1/2/3*Δ resistance was proven

not be due to impaired respiration (Pereira et al., 2007). In this work, the role of Por1p (yeast VDAC) and of Cpr3p (yeast mitochondrial cyclophilin) in acetic acid-induced RCD was also assessed. Whilst Por1p deletion increased yeast sensitivity to acetic acid, suggesting that Por1p functions as a negative regulator of the RCD program, Cpr3p deletion did not affect cell survival. A similar study would later reveal that the acetic acid sensitivity displayed by *por1*Δ mutants is abrogated by further deletion of the Aac1/2/3 proteins, suggesting a role of Por1p in the negative regulation of RCD through inhibition of the pro-death role of Aac1/2/3 (Trindade et al., 2016).

In *S. cerevisiae*, Pep4p (human cathepsin D) release from the vacuole was also ascertained in H_2O_2- and acetic acid-induced RCD of *S. cerevisiae* (Mason et al., 2005; Pereira et al., 2010). Genetic ablation of Pep4p sensitized cells to acetic acid and delayed the removal of damaged mitochondria. Overexpression had the opposite effect, suggesting that Pep4p and mitochondrial degradation have a protective role in acetic acid-induced RCD. This, coupled with the observation that the sensitivity to acetic acid shown by *pep4*Δ cells is dependent on the Aac1/2/3 proteins, advocates for an important role of Pep4 and Aac1/2/3 in the mediation of mitochondrial degradation (Pereira et al., 2010). Furthermore, other orthologues of mammalian apoptogenic factors have been also implicated in acetic acid-induced cell death, such as Aif1p (Susin et al., 1999), Ndi1p (Cui et al., 2002), Nuc1p (Büttner et al., 2007) and Yca1p (Guaragnella et al., 2006; Madeo et al., 2002).

A recent proteomic study revealed that acetic acid treatment induces severe amino acid starvation in yeast associated with decreased protein synthesis, suggesting a role for the TOR complex in acetic acid-induced apoptotic-like cell death and which is corroborated by loss of cell viability and enhanced ROS accumulation observed in Δ*tor1* mutants (Almeida et al., 2009). Moreover, the same research demonstrated that upon treatment *S. cerevisiae* also exhibits impaired carbohydrate metabolism and that glycolytic rate is reduced. Others had previously demonstrated that glucose uptake is not inhibited after acetic acid treatment, even though enolase activity is decreased (Pampulha & Loureiro-Dias, 1990). Altogether, these results seem to indicate that metabolic energy is being directed towards stress response rather than growth. In accordance with this postulation, a study with acetic acid-adapted yeast cells from batch cultures suggested that per each mole of acid entering the cell, around 1 mole of ATP is spent, probably to pump H^+ ions out in order to counteract the intracellular acidification caused by the accumulation of the acid (Pampulha & Loureiro-Dias, 2000). Indeed, acetic acid has been found to promote plasma membrane H^+-ATPase activation at low pH (Carmelo, Santos, & Sá-Correia, 1997).

Acetate was also shown to induce apoptosis in colorectal carcinoma (CRC) cell lines. Jan and colleagues (2002) first reported that two dietary *Propionibacterium* species found in the human intestine secrete short-chain fatty acids to the extracellular media and that, among these, acetate and propionate induced high cytotoxicity in two different CRC cell lines at excretion levels, with an effective dose (ED_{50}) of 15 mM. These agents were found to exert typical alterations of apoptosis, namely pyknosis, karyorrhexis, ROS accumulation, loss of $\Delta\Psi_m$ and procaspase-3 cleavage. Co-expression with Bcl-2 was found to partially inhibit acetate-induced RCD, suggesting the involvement of mitochondria in the process. Moreover, mitochondrial swelling was inhibited by the mPTP inhibitor CsA. The authors also determined that acetate is able to permeabilize ANT-containing but not protein-free liposomes, thus indicating a role of ANT in acetate-induced apoptosis, as was later demonstrated in yeast (Pereira et al., 2007). These studies established the baseline for a possible use of acetate as a prophylactic agent in CRC and since then many studies have been conducted to unravel the mechanistic effect of acetate in human CRC cell lines (Ferro et al., 2016; Marques et al., 2013; Oliveira et al., 2015).

1.3. THE ER-MITOCHONDRIA CONTACT SITES AS REGULATORS OF CELL DEATH SIGNALING

1.3.1. INTERORGANELLAR COMMUNICATION

Eukaryotic cells exhibit a highly complex structural organization. These cells are divided into organelles, small membrane-coated compartments that carry out a specific function within the cell. Lipid membranes allow the organelle to regulate the intake and export of cytosolic molecules, creating controlled microenvironments that are required for certain cellular activities and thus making each organelle function as a distinct and specialized microreactor (Alberts et al., 2002). Notwithstanding, no organelle can synthesize every molecule it needs. Hence, molecular flow between the cell and its surrounding environment, as well as between organelles, is required to maintain cellular activity and tissue homeostasis. Vesicular trafficking is perhaps the most well-known cargo delivery process, being the main trafficking route between intra- and extracellular media and between organelles (Alberts et al., 2002). However, not all molecules undergo this type of inter-organelle transport. Instead, communication can be achieved through zones of close apposition between the organelles membranes, which are known as membrane contact sites (MCS). Indeed, the endoplasmic reticulum (ER) and mitochondria can communicate differently,

through the use of several tethering complexes that tighten the organelles together and allow exchange of molecules in a more timely fashion (Kornmann et al., 2009).

1.3.2. THE ER-MITOCHONDRIA CONTACT SITES

The ER is a network of membrane-coated tubules that originates from the nucleus and propagates throughout the cytosol, with its lumen representing around 10% of total cell volume. As the ER membrane spreads throughout the cell, it is not hard to imagine that its membrane contacts with those of other organelles. In fact, a great area of the ER membrane has been demonstrated to contact with other cellular membranes such as the plasma membrane, the Golgi apparatus, the OMM and lysosomes (Levine & Loewen, 2006).

In the late 1950s, Copeland & Dalton referred to a zone of close apposition between the ER and mitochondria, providing the first evidence that inter-organelle contact could occur (Copeland & Dalton, 1959). In 1990, Jean Vance isolated a differentiated ER subcompartment that contacts with mitochondria and that is responsible for their communication: the mitochondria-associated membranes (MAMs). Further studies would reveal that these ER-mitochondria contact sites (ER-MCS) were around 10–20 nm in length (Perkins et al., 1997). These structures occupy up to 20% of the mitochondrial surface and participate in processes such as phospholipid biosynthesis and exchange, as well as calcium signaling (de Brito & Scorrano, 2010; Michel & Kornmann, 2012; Vance, 1990). Since several diseases have been linked to disrupted ER-MCS, such as cancer, Parkinson's and Alzheimer's disease, several studies have been conducted in order to assess the impact of ER-mitochondria connections in health and disease (Hedskog et al., 2013; Paillusson et al., 2016; Zampese et al., 2011).

In metazoans, the ER-MCS are composed of several protein complexes involving mitofusins 1 and 2 (Mfn1/2), the inositol 1,4,5-trisphosphate receptor (IP_3R), the phosphofurin acidic cluster sorting protein 2 (PACS-2), VDAC and several others (Kornmann, 2013; Simmen et al., 2005). Conversely, until recently the only known tethering structure between the ER and mitochondria in *Saccharomyces cerevisiae* was the ERMES (ER-mitochondria encounter structure) complex, a heterotetrameric complex responsible for stabilizing the formation of contact zones between the ER and mitochondria. ERMES, which is localized in discrete foci between the ER and the OMM, is composed of a nucleus of four proteins: Mmm1p, an ER-anchored protein, that interacts with cytosolic Mdm12p and OMM's Mdm10p and Mdm34p (Raturi & Simmen, 2013) (Figure 4). This

complex is regulated by a calcium-binding Miro-GTPase, Gem1p, that controls the number and size of ERMES (Kornmann, Osman, & Walter, 2011; Stroud et al., 2011). Mmm1p, Mdm12p and Mdm34p exhibit SMP (synaptotagmin-like mitochondrial lipid-binding protein) domains that are homologous to the tubular lipid-binding protein (TULIP) superfamily and that probably participate in the lipid exchange function of ERMES, which is in agreement with a reduced conversion rate of PS to phosphatidylcholine (PC) in ERMES mutants (Kopec, Alva, & Lupas, 2010; Kornmann et al., 2009). In addition to being implicated in lipid and calcium exchange, ERMES has also been correlated with anchoring mtDNA nucleoids and mtDNA replication (Hanekamp et al., 2002; Hobbs et al., 2001; Murley et al., 2013), mitochondrial inheritance (Burgess, Delannoy, & Jensen, 1994), mitochondrial protein import and assembly of β-barrel proteins in the OMM (Meisinger et al., 2007), mitophagy (Böckler & Westermann, 2014) and in the association of mitochondria to the actin cytoskeleton (Boldogh et al., 1998).

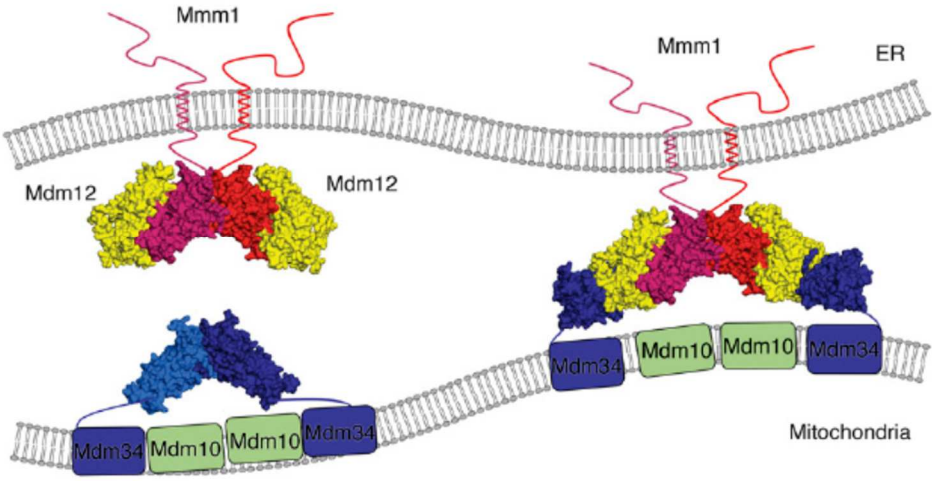

Figure 4. The endoplasmic reticulum-mitochondria encounter structure (ERMES). Schematic view of ERMES subunits: the ER-anchored protein Mmm1, the cytosolic protein Mdm12, the integral outer mitochondrial membrane (OMM) proteins Mdm10 and Mdm34. Interaction between ER and mitochondria during phospholipid transport is thought to be mediated by Mdm12p, which associates with Mmm1p dimers in the ER and Mdm34p in the OMM (image credit: Jeong, Park, & Lee, 2016).

Although being generally regarded as a facilitator of ER-mitochondria lipid and calcium transfer, each component of this tethering complex has been studied individually. Not surprisingly, there are several reports that link the absence of each of these proteins to a common phenotype, namely to altered mitochondrial morphology (Burgess et al., 1994; Esposito et al., 2011; Sogo & Yaffe, 1994) and mitochondrial phospholipid composition (Kornmann et al., 2009; Nguyen et al.,

2012; Osman et al., 2009). If these two phenotypes are somewhat related is a question that remains unanswered. Nonetheless, each protein also exerts their function elsewhere.

Lack of each ERMES protein has been correlated with defective mitochondria segregation to daughter cells (Boldogh et al., 2003; Burgess et al., 1994; Sogo & Yaffe, 1994). Presence of a multibudded phenotype has been reported for cells deficient in either Mmm1p or Mdm10p when grown in non-fermentable carbon sources (Burgess et al., 1994; Sogo & Yaffe, 1994). Considering that these mutants exhibit giant and spherical mitochondria, it is hypothesized that mitochondria segregation is a size-limited process that can function as a checkpoint for cytokinesis to occur. It was also shown that *mdm10*Δ cells enter the G_2 phase of the cell cycle 20 minutes later than the wild-type, similarly to what occurs in ρ^0 cells. The authors demonstrated that the delay is in fact not due to mtDNA or septation defects but to flawed contractile ring closure (García-Rodríguez et al., 2009). In *mdm34*Δ cells, but not cells lacking any other ERMES subunit, the defective morphology of mitochondria is moderately reversed after overexpression of Cdc14p, a protein phosphatase required for mitotic exit (Esposito et al., 2011). Combined with the aforementioned reports from the Burgess (1994) and García-Rodríguez (2009) groups, a reasonable body of evidence exists for an interplay between cell cycle and mitochondrial inheritance that appears to be activated in response to abnormal mitochondrial morphology.

Furthermore, Mdm10p has an important role on mitochondrial protein import, namely in its association with the sorting assembly machinery (SAM) and the translocase of the outer membrane (TOM). This protein was shown to interact with the SAM complex and to be required for the late steps of Tom40 assembly into the TOM complex (Meisinger et al., 2004; Yamano, Tanaka-Yamano, & Endo, 2010). The same was demonstrated for Mmm1p and Mdm12p, which seem to participate downstream of Mdm10p in β-barrel assembly (Meisinger et al., 2007). Interestingly, deletion of either Mmm1p, Mdm10p or Mdm34p also results in peroxisomal abnormality. During exponential and stationary growth, 33% and 22% of peroxisomes were found to co-localize with ERMES, respectively (Cohen et al., 2014). Indeed, the peroxisomal protein Pex11 was found to establish the connection between mitochondria and peroxisomes through the ERMES complex (Ušaj et al., 2015).

A recent study demonstrated that neither Gem1p or ERMES were directly required for PS transport or mitochondrial DNA inheritance, therefore suggesting that ERMES may only provide structural contact between ER and mitochondria and that there may be other protein complexes

involved in these contact sites (Nguyen et al., 2012). In fact, Lahiri and colleagues (2014) showed the existence of a ER membrane protein complex (EMC), composed of 6 proteins (Emc1-6), that was required for PS transfer from the ER to mitochondria. In this study, it was shown that genetic ablation of ERMES did not significantly reduce PS transport but, in cells lacking EMC and Mmm1p, viability was drastically decreased. As such, it was proposed that ERMES and EMC could be both tethering complexes that are responsible for different types of transport (Lahiri et al., 2014). This complex, with the additional subunits Emc7, 8a, 8b and 10, was also shown to be present in mammals (Wideman, 2015).

Upon ERMES deletion, there is an increase in the number of contact sites between vacuoles and mitochondria (vCLAMP, vacuole and mitochondria patch). Likewise, ablation of vCLAMP increases the number of ERMES foci (Elbaz-Alon et al., 2014). The study also shows that complete abrogation of both ERMES and vCLAMP is lethal, with cells lacking ERMES and carrying a repressed vCLAMP presenting impaired phospholipid transport. Phospholipidic profiling demonstrated a nearly 40% decrease in phosphatidylethanolamine (PE) and cardiolipin (CL) levels (synthesized in mitochondria) and a near doubling increase in phosphatidylinositol (PI; synthesized in the ER), indicating a potential defect in phosphatidic acid (PA) transport between ER and mitochondria. In support of this theory, after double deletion PS accumulates in the ER and PC production is more than halved. These findings demonstrate that ERMES and vCLAMP foci are co-regulated and that both assure the correct functioning of phospholipid transfer between ER and mitochondria (Elbaz-Alon et al., 2014).

1.3.3. THE ER-MITOCHONDRIA CONTACT SITES IN CELL DEATH SIGNALING

The ER and the mitochondrion are fundamental organelles in the apoptotic process. As above-mentioned, the mitochondrion actively participates in apoptosis through the release of pro-apoptotic factors such as cyt *c.* However, the trigger for mitochondria to commit to apoptosis may also rest on its interaction with the ER. The majority of studies that propose a putative role of ER-MCS in cell death have been performed on mammalian cells. On the other hand, to our current knowledge very few studies have provided experimental evidence for a role of each subunit of ERMES in the signaling pathway of apoptosis in *S. cerevisiae*. As such, in this subsection we will focus on the evidence provided for a role of ER-MCS on the mediation of cell death in higher eukaryotes, while trying to unveil possible connections to their yeast counterpart (Figure 5).

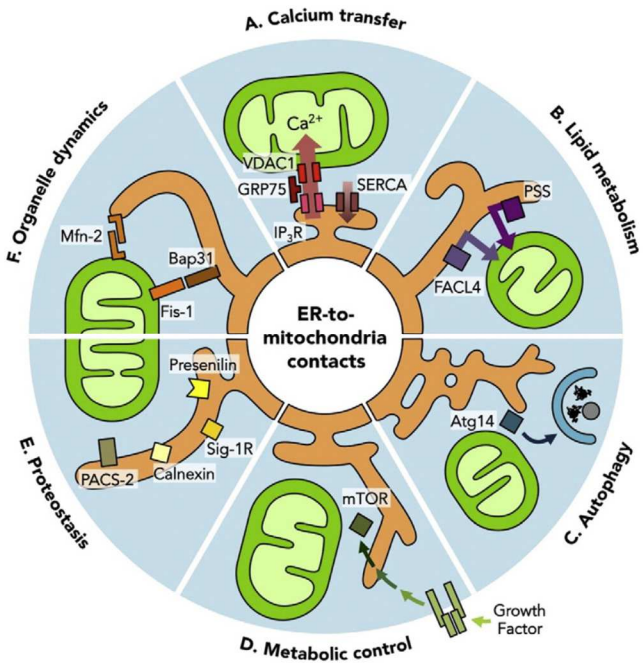

Figure 5. The wide-ranging functions of ER-mitochondria contact sites (ER-MCS). (A) The ER-MCS have been implicated in calcium transfer between ER and mitochondria through the ER-anchored inositol-triphosphate receptor (IP_3R) receptor, the cytosolic chaperone GRP75 and the voltage dependent anion channel isoform 1 (VDAC1). The sarco/endoplasmic reticulum calcium ATPase (SERCA) is also localized to ER-MCS. **(B)** These contact sites are enriched in enzymes required for lipid biosynthesis such as phosphatidylserine synthase (PSS). **(C)** ER-MCS have been suggested to provide the lipids required for autophagosome formation during autophagy. **(D)** The mTOR complex, a proteinaceous structure which senses the metabolic status of the cell, is enriched at ER-MCS. **(E)** There are several components of these contact sites that participate in protein homeostasis. **(F)** ER-MCS have also been shown to regulate mitochondrial morphology, as well as fusion and fission mechanisms (image credit: López-Crisosto et al., 2015).

1.3.3.1. CALCIUM SIGNALING

Calcium release from the ER stores and its uptake by mitochondria is a known hallmark of the apoptotic process (Pinton et al., 2008). The ER is the major calcium store within the cell and, in metazoans, its mobilization to the cytosol via inositol 1,4,5-trisphosphate receptors (IP_3R) is concomitant with a large increase in mitochondrial calcium (Giacomello et al., 2007). Although mitochondrial calcium increase is responsible for an augmented respiratory rate, prolonged exposure to this ion at concentrations above a critical threshold can lead to cell death, namely due to its role in the regulation of mPTP opening and subsequent release of pro-apoptogenic factors (Marchi, Patergnani, & Pinton, 2014). Indeed, IP_3R is a putative component of ER-MCS, suggesting a role for these sites in the signaling pathways of apoptosis (Kornmann, 2013).

Upon release from the ER, calcium is effectively taken up by mitochondria. The mitochondrial calcium uniporter (MCU) has been found to be responsible for calcium traffic between the IMM and the mitochondrial matrix, whereas VDAC is responsible for its uptake through the OMM (De Stefani et al., 2011). The former carrier has a low affinity to calcium (K_D = 20-50 μM), so it is hard to think that this is the sole responsible for mitochondrial matrix calcium increase (Marchi, Patergnani, & Pinton, 2014). Since the time lapse between the release of calcium from the ER and its uptake by mitochondria is estimated to be nearly 500 ms, a very high calcium concentration surrounding mitochondria would be required for such a quick uptake (Csordás et al., 2010). Indeed, it had been hypothesized that there are transient cytosolic microdomains where calcium concentrations are very high (> 10 μM) and thus allow extensive calcium uptake by mitochondria (Rizzuto et al., 1993). The subcellular localization of these microdomains was discovered to be in sites where the ER and mitochondria are in close proximity (Giacomello et al., 2007). In agreement with this, silencing or ablation of Mfn2, a putative component of the metazoan ER-mitochondria tether, caused impairment of calcium uptake by mitochondria in HeLa cells and mouse embryonic fibroblasts (de Brito & Scorrano, 2008). Moreover, cytosolic calcium concentrations above 1 μM were also shown to tighten the gap between ER and mitochondria, probably adding to its effective uptake by mitochondria (Wang et al., 2000).

However, the role of calcium in yeast mitochondria-dependent cell death has not been ascertained yet since this organism does not display an apparent orthologue of the mammalian MCU (Kovács-Bogdán et al., 2014). Even though it has been demonstrated that a rise in cytosolic calcium triggers an apoptotic response in yeast, how calcium ions enter mitochondria is still a subject of debate. Contrarily to what happens in mammalian cells, the major calcium store in yeast is the vacuole and not the ER. However, it has been shown that the ER is able to store calcium and that yeast mitochondria detain a calcium concentration equivalent to rat liver mitochondria (Carraro & Bernardi, 2016). As such, it is possible that a yet unknown mitochondrial calcium transporter exists in yeast mitochondria. Similar to mammals, yeast ER-MCS could provide the spatial proximity required for calcium exchange between the ER and the OMM, while a yet unknown transporter could account for the uptake of calcium into the mitochondrial matrix. However, experimental evidence to prove this hypothesis is still missing.

Curiously, in mammals, cyt *c* seems to amplify the apoptotic response at an early stage of the apoptotic process by enhancing calcium signaling. As aforementioned, cyt *c* is released to the cytosol upon apoptotic stimuli and forms the apoptosome, a protein complex responsible for the

activation of caspase-9. When released from mitochondria, cyt *c* was also shown to be an agonist for calcium release, blocking the calcium-dependent inhibition of IP_3R and thus promoting the efflux of even more calcium from the ER, which subsequently leads to an even more pronounced permeability transition (Boehning et al., 2005). Nonetheless, this phenomenon has not yet been demonstrated in yeast.

1.3.3.2. AUTOPHAGY

The ER-MCS have also been associated with autophagy, a process in which cellular components are degraded on a selective or non-selective manner. The role of autophagy in cell death is still controversial, with some regarding it as an RCD program that promotes cellular demise and others proposing that it is solely a survival mechanism to eliminate defective organelles or invading pathogens (Carmona-Gutierrez et al., 2018). Nevertheless, there have been reports claiming that proteins required for autophagosome formation are localized at the MAMs under nutrient starving conditions, such as Rab32 and mTORC1/C2. Furthermore, dissociation of mTORC2 leads to MAM disruption (Marchi, Patergnani, & Pinton, 2014). In yeast, ERMES was found to be required for mitophagy but not bulk autophagy (Böckler & Westermann, 2014). Artificial tethering of ER and mitochondria in deletion mutants restored mitophagy levels, proposing that mitophagy requires close apposition of these two organelles. Indeed, the authors determined that the ERMES complex localizes with mitophagosome formation sites and co-localizes with autophagic proteins Atg5, Atg8, Atg9, Atg14 and Atg32. Moreover, ERMES mutants display immature autophagosomes, which is in agreement with a model where ERMES could provide the lipids required for autophagosome formation (Böckler & Westermann, 2014).

1.3.3.3. PHOSPHOLIPIDS

The ER and mitochondria display an extensive interplay of phospholipid traffic between their membranes. PS synthesized in the ER by phosphatidylserine synthase (Psd1) is transported to mitochondria and used as a precursor for PE synthesis. In turn, PE is translocated to the ER to form PC, which then heads back to mitochondria. The ERMES complex has been implicated in lipid traffic between the ER and the OMM since its discovery (Kornmann et al., 2009). Even though it is not known if ERMES is responsible for this lipidic flow, it is regarded as a suitable candidate. Considering that Mmm1p, Mdm12p and Mdm34p present lipid-binding domains and that genetic

interaction maps show a strong correlation with enzymes from phospholipid biosynthesis pathways, ERMES could be responsible for this molecular flow between membranes (Hoppins et al., 2011; Kopec et al., 2010; Kornmann et al., 2009).

It is widely accepted that certain lipids participate in mammalian apoptosis, as it is the case of MOMP-inducing ceramide pores (Woodcock, 2006). The role of phospholipids in this cell death process, namely CL and PS, has also been attested for. To date, the only function ascribed to PS in this process is its externalization at the plasma membrane in the late steps of apoptosis, signaling apoptotic bodies for phagocytosis (Segawa & Nagata, 2015). In yeast, PS externalization has been reported under apoptotic stimuli (Madeo et al., 1997), demonstrating that the mechanisms underlying PS exposure are likely conserved and appeared early in evolution. However, a role for this phenotypical trait in the yeast apoptotic process remains elusive since yeast is a unicellular organism and therefore does not engage in phagocytosis.

Cardiolipin also participates in the apoptotic process. This unique anionic diglycerophospholipid is almost exclusive of the IMM and is responsible for the stabilization of the quaternary structure of complexes III and IV of the electron transport chain and of complex V (Eble et al., 1990; Gomez & Robinson, 1999; Pfeiffer et al., 2003). CL is typically bound to 15–20% of the cyt *c* at the IMM. This association is caused by insertion of one acyl chain of CL into a hydrophobic pocket of cyt *c*, which destabilizes the heme group and partially unfolds the protein. ROS generated by the apoptotic cascade, especially H_2O_2, can convert the unfolded cyt *c* into a CL-specific peroxidase system. In turn, cyt *c* is capable of oxidizing CL which then loses its affinity for cyt *c*, releasing it to the IMS (Li et al., 2015). However, in yeast this phenomenon has not yet been identified. Studies have shown that CL promotes Bax insertion in the OMM (Eble et al., 1990; Gomez & Robinson, 1999; Pfeiffer et al., 2003) and, in agreement, CL is required for tBid/Bax-induced permeabilization of liposomes (Kuwana et al., 2002; Lutter et al., 2000; Terrones et al., 2004). Moreover, the contact zones between the IMM and the OMM are CL-rich and therefore it is possible that the local concentration of CL is enough to interact with tBid and induce MOMP (Lutter, Perkins, & Wang, 2001).

1.3.3.4. MITOCHONDRIAL FRAGMENTATION

Mitochondria are remarkably plastic organelles and their shape can fluctuate between tubular and punctiform structures either through fusion or fission mechanisms, respectively, which are mediated by guanosine triphosphatases from the dynamin family (Alberts, 2002; Cosentino & García-Sáez, 2014). As such, mitochondria form dynamic interconnecting networks where fusion mechanisms (mediated in mammals by Mfn1/2 and Opa1 proteins, and in yeast by Fzo1p and Mgm1p) promote neutralization of damaged mitochondrial components and fission mechanisms (mediated in mammals by Drp1 proteins, and in yeast by Dnm1p) allow the network to get rid of damaged mitochondria (Cosentino & García-Sáez, 2014; Suen, Norris, & Youle, 2008). The mitochondrial fusion machinery is thought to be a defense mechanism to avoid ROS-induced damage. ROS can promote mtDNA mutations that are thought to lead, over time, to age-related diseases. As such, mitochondrial fusion can attenuate this by allowing several copies of mtDNA in one compartment, thus expressing more normal gene products than mutant ones (Westermann, 2008).

Mitochondrial fission occurs early in apoptosis, before plasma membrane blebbing (Suen et al., 2008). A study performed by Murley and colleagues (2013) revealed that the ERMES complex is present in mitochondrial fragmentation sites. This postulate came to support the previous evidence that ER tubules provide constriction for mitochondrial fragmentation, a phenomenon termed ER-associated Mitochondrial Division (Friedman et al., 2011). As such, it is hypothesized that the ERMES complex functions as a hotspot for Dnm1 recruitment and ensuing mitochondrial fission. Moreover, the pro-apoptotic protein Bax colocalizes with Drp1 and it was demonstrated that the two proteins are actually binding partners (Wang et al., 2015). Therefore, besides the apparent role of ERMES in regulating mitochondrial fission, it could also be that these ER-MCS are required for Bax mitochondrial addressing and induction of MOMP in yeast heterologously expressing human Bax.

CHAPTER 2

RESEARCH OBJECTIVES

A screening of the EUROSCARF haploid mutant collection was performed in our laboratory, identifying genes whose deletion caused altered sensitivity to acetic acid-induced regulated cell death (Sousa et al., 2013). The results showed that cells lacking genes involved in mitochondrial function were the most affected by this death inducer, as well as cells lacking known apoptotic regulators. Since *S. cerevisiae* commits to a mitochondria-dependent cell death program in response to acetic acid (Ludovico et al., 2002), we investigated genes that encode proteins of the outer mitochondrial membrane and that could potentially be involved in the intricate molecular machinery that promotes MOMP.

In the screening, abrogation of two subunits of the ERMES complex, Mdm10p and Mdm12p, rendered cells with an altered sensitivity to this stressor. As such, we hypothesized that the ERMES complex could be involved in the mediation of acetic acid-induced cell death. With the purpose of testing this hypothesis, we ambitioned to:

1. Gain better insight on the phenotypical traits of ERMES mutants;
2. Evaluate cell survival and both functional and structural alterations typical of mammalian apoptosis in ERMES-deficient strains after acetic acid treatment.

Due to the emerging data that is now connecting several pathologies to dysfunctional ER-MCS, as well as the industrial requirement for acetic acid-resistant strains, we hope to enlighten the current knowledge on acetic acid-induced regulated cell death and provide solid ground for the study of ER-MCS in cell death, with both biomedical and biotechnological interest.

CHAPTER 3

MATERIALS AND METHODS

3.1. YEAST STRAINS AND PLASMIDS

The wild-type strain used in this study was *Saccharomyces cerevisiae* BY4741 (*MATa his3Δ1 leu2Δ0 met15Δ0 ura3Δ0*). All strains, along with their respective genotype and source, are listed on Table I. Wild-type and mutant strains are part of a series of deleted strains with auxotrophic markers for adjacent gene expression (Brachmann et al., 1998) and belong to the haploid mutant knockout collection from "EUROSCARF" (Frankfurt, Germany).

Table I. *Saccharomyces cerevisiae* strains used in this study. Auxotrophic selection markers are depicted in parenthesis. *KanMX4* confers geneticin-418 resistance.

***S. cerevisiae* strain**	**Genotype**	**Source**
BY4741	*MATa his3Δ1 leu2Δ0 met15Δ0 ura3Δ0*	EUROSCARF
BY4741 ρ^0	BY4741 lacking mtDNA	Sousa, F.
BY4741 mtGFP	BY4741 + pYX242-mtGFP (*LEU2*)	This study
BY4741 *mmm1*Δ	BY4741 + *YLL006W::KanMX4*	EUROSCARF
BY4741 *mdm10*Δ	BY4741 + *YAL010C::KanMX4*	EUROSCARF
BY4741 *mdm10*Δ mtGFP	BY4741 *mdm10*Δ + pYX242-mtGFP (*LEU2*)	This study
BY4741 *mdm12*Δ	BY4741 + *YOL009C::KanMX4*	EUROSCARF
BY4741 *mdm12*Δ mtGFP	BY4741 *mdm12*Δ + pYX242-mtGFP (*LEU2*)	This study
BY4741 *mdm34*Δ	BY4741 + *YGL219C::KanMX4*	EUROSCARF
BY4741 *mdm34*Δ mtGFP	BY4741 *mdm34*Δ + pYX242-mtGFP (*LEU2*)	This study
BY4741 *por1*Δ	BY4741 + *YNL055C::KanMX4*	EUROSCARF
BY4741 *por1*Δ *mdm34*Δ	BY4741 *POR1*::*URA3 MDM34*::KanMX4	This study

In order to assess the effect of acetic acid on mitochondrial morphology and degradation, the wild-type and deleted strains described above were transformed with a plasmid (pYX242) encoding a mitochondrial matrix-targeted green fluorescent protein (mtGFP) and carrying the *LEU2* gene for auxotrophic selection.

3.2. GROWTH CONDITIONS AND MEDIA COMPOSITION

Yeast strains were grown in liquid YEP medium (0.5% (w/v) yeast extract, 1% (w/v) peptone) supplemented with the appropriate carbon sources (YEPD: 2% (w/v) glucose; YEPG: 2% (v/v) glycerol; YEPGal: 2% (w/v) galactose) and maintained on solid YEPDA plates (YEPD plus 2% (w/v) agar). Exceptionally, to assess respiratory capacity strains were grown in solid selective complete

medium (SC; 0.17% (w/v) yeast nitrogen base without amino acids or ammonium sulfate, 0.5% (w/v) ammonium sulfate, 0.2% (w/v) Ramsdale drop-out mix, 0.01% appropriate auxotrophic requirements) with 2% (w/v) glycerol and 2% (w/v) agar. Yeast strains carrying pYX424-mtGFP were selected and grown in SC medium with 2% glucose (SC Glucose) lacking leucine, whereas *mdm34*Δ *por1*Δ mutants were selected and grown in medium lacking uracil. For plasmid transformation, yeast cells were grown in liquid YEPD 2xGlu medium (YEPD with 4% (w/v) glucose). Growth in liquid media and treatments of wild-type and mutant strains were always performed at 30 °C and 200 revolutions per minute (rpm) in an orbital shaker. Competent *Escherichia coli* XL-1 Blue cells carrying the pYX242 vector were grown in both liquid and solid LB medium (1% (w/v) NaCl, 0.5% (w/v) yeast extract, 1% (w/v) tryptone and 2% (w/v) agar) supplemented with 100 µg/mL ampicillin (Formedium). All centrifugations were performed at 5 000 rpm for 3 minutes at room temperature and all wash steps were performed with sterile deionized water unless stated otherwise.

3.3. ACETIC ACID TREATMENT

For the treatment with acetic acid, cells grown in YEPD and SC Glucose media were harvested by centrifugation and transferred to YEPD pH 3.0 media (set with HCl), whereas cells grown in YEPGal media were shifted to YEPGal pH 3.0 media (set with HCl). Strains were then treated with 100 or 120 mM acetic acid (Panreac). At this particular pH, approximately 82.6% of acetic acid (pKa=4.76) is in its undissociated form.

3.4. PLASMID ISOLATION AND BACTERIAL TRANSFECTION

For pYX242-mtGFP isolation, BY4741 cells carrying the plasmid were grown overnight in SC Glucose medium to an $O.D._{640\ nm}$ of 2. Cells were then harvested, washed and suspended in resuspension buffer (50 mM Tris-HCl pH 8.0, 100 mM ethylenediaminetetraacetic acid (EDTA) and 100 µg/mL RNase A). Cell wall disruption was achieved by vigorously shaking the suspension with 500 µm glass beads, using five vortex pulses of 1 minute with a 1-minute interval on ice. Then, an isovolume of lysis buffer (200 mM NaOH, 1% (w/v) sodium dodecyl sulfate (SDS)) was added and the suspension was carefully mixed and incubated at room temperature for 5 minutes. To remove cellular debris, an isovolume of neutralization solution (3 M potassium acetate pH 5.5) was added and the suspension was centrifuged at 14 000 rpm for 2 minutes. Afterwards, an equal amount of

100% (v/v) isopropanol was added to the supernatant, mixed by inversion and the precipitated DNA was harvested by centrifugation (15 000 rpm, 15 minutes). Finally, the DNA was washed twice with 70% (v/v) ethanol and once with absolute ethanol and dried in an incubator at 55 °C for 1 h. Samples were suspended in TE buffer (100 mM Tris, 10 mM EDTA, pH 8.0) and stored at -20 °C.

Subsequently, competent *E. coli* XL-1 Blue cells were transfected with pYX242-mtGFP. For that purpose, approximately 50 ng of plasmid were added to a 100 µL aliquot of competent cells. The mixture was incubated on ice for 40 minutes before a quick thermal shock in a water bath at 42 °C for 2 minutes, and then kept on ice for an additional 2 minutes. Afterwards, LB medium was added to the mix and cells were allowed to grow for 1 hour at 37 °C, 200 rpm. Cells were then harvested, suspended in LB medium and plated in solid LB plates supplemented with 100 µg/mL ampicillin. After growth at 37 °C for 16 h, the plates were stored at 4 °C.

3.5. YEAST TRANSFORMATION

Plasmid isolation from *E. coli* cells carrying pYX242-mtGFP was achieved by using the GenElute Plasmid Miniprep kit (Sigma-Aldrich) according to manufacturer's instructions. Finally, wild-type and mutant strains were transformed with the purified plasmid through the Gietz and Woods method (2006). Following transformation, cell suspensions were spotted on solid SC Glucose media lacking leucine and grown at 30 °C for three days. Efficiency of transformation was assessed by fluorescence microscopy.

3.6. CONFIRMATION OF CORRECT DELETION OF TARGET GENES

3.6.1. GENOMIC DNA EXTRACTION

Genomic DNA of wild-type and mutant strains was extracted from YEPD-grown yeast at an $O.D._{640nm}$ of 2.0. Cells were harvested, washed and suspended in 1 M sorbitol with 0.1 M EDTA pH 7.5. For cell wall digestion, 25 U zymolyase-20T was added to the suspension, incubated for 1 hour at 37 °C, and then mixed with an isovolume of Tris-HCl 50 mM with EDTA 20 mM. Afterwards, SDS was added to a final concentration of 0.24% (w/v) and the suspension was incubated for 5 minutes at 65 °C. The resulting spheroplast suspension was next treated with 1.4 M potassium

acetate and cells were pelleted (15 000 rpm, 30 minutes, 4 °C). The supernatant was transferred to a plastic tube where an isovolume of 100% (v/v) isopropanol was added and the DNA was harvested (15 000 rpm, 15 minutes, 4 °C) and washed with 70% (v/v) ethanol. The pellet was dried for 1 hour in an incubator at 55 °C and suspended in TE before storage at -20 °C.

3.6.2. Polymerase Chain Reaction

Assessment of correct *KanMX4* insertion was achieved through the use of primers that anneal in the sequence flanking the target ORF (F1 and R1) and within the *KanMX4* cassette (KanB and KanC). As such, the primer sets F1/R1, F1/KanB and KanC/R1 were used. The F1 and R1 primers for each mutant (Table II) were carefully designed with strict criteria, whereas the KanB (5'-CTGCAGCGAGGAGCCGTAAT-3') and KanC (5'-TGATTTTGATGACGAGCGTAAT-3') primers were already established and purchased by the lab. All PCR programs (Table III) were carried out in a T100 Thermal Cycler (Bio-Rad) and the reactions were set as advised in the Thermo Scientific DreamTaq DNA Polymerase product information. The resulting PCR products were then loaded into an agarose gel (1% with TBE (0.54% (w/v) Tris base, 0.275% (w/v) boric acid and 0.2% (v/v) 50 mM EDTA pH 8.0)) and run with TBE at 100 V. Post-staining of DNA fragments was achieved by incubation in a 0.025% (v/v) Midori Green Advanced DNA Stain (Nippon Genetics) solution in TBE. Visualization of the fragments was performed in a VWR Genosmart UV transilluminator.

Table II. List of primers used for KanMX4 confirmation (F1/R1) and amplification (F2/R2). The primers F1 and R1 anneal approximately 200 bp upstream/downstream of the target ORF and are used along with KanB (reverse) and KanC (forward) primers, respectively, which anneal within the KanMX4 cassette. The primers F2 and R2 anneal closer (18 to 98 bp) to the target ORF. F1/F2: forward primers; R1/R2: reverse primers.

Strain	Forward Primer (F1) 5'–3'	Reverse Primer (R1) 5'–3'
***mmm1*Δ**	GGGTTGCCCTTGTATACATTTCAG	GCTACCAAGGGACAAACTAGGAAT
***mdm10*Δ**	CTGGCTCCATGACCTCCTT	GATGAAGCTTTGAGCGAAAGT
***mdm12*Δ**	TCAATGTCTGTGAGGGCCTTAT	ACGGACAACTGTCTAGAGTATGAGAT
***mdm34*Δ**	GGGCCATGAAGCCTTGTAG	TCATGCCTTTAGCTGCAAGT

Table III. PCR programs used for confirmation and amplification of KanMX4. The PCR programs for each set of primers were the same for all strains.

Primer set	Initial denaturation	Denaturation	Annealing	Extension	Final Extension
F1/KanB	94 °C 4 min	94 °C 30 s	55 °C, 30 s	72 °C, 1 min	72 °C 10 min
KanC/R1			53 °C, 30 s	72 °C, 1 min	
F1/R1			55 °C, 30 s	72 °C, 2 min	
	1 cycle	**35 cycles**			**1 cycle**

3.7. GENERATION OF A *mdm34Δ por1Δ* DOUBLE MUTANT

A *mdm34*Δ *por1*Δ double mutant was generated through homologous recombination. Briefly, genomic DNA was extracted from a *por1*Δ strain from EUROSCARF whose selective marker had been changed from *KanMX4* to *URA3.* Then, a PCR was performed in order to amplify the *POR1*::*URA3* cassette using the primers iPor1 (5'-TTATAGCCAGCAGAGCACGA-3') and iPor2 (5'-ATGATTATGAGAACCAGCCG-3'). Homologous recombination was achieved by transformation of *mdm34*Δ cells with the PCR product through the above-mentioned Gietz & Woods method (2006). Following transformation, cells were plated on SC Glucose medium lacking uracil and allowed to grow for 3 days at 30 °C. Afterwards, each colony was simultaneously streaked onto YEPD plates supplemented with 200 μg/mL geneticin-418 (Sigma-Aldrich) and SC Glucose plates lacking uracil and grown for 2 days at 30 °C. Colonies that were able to grow on both plates were deemed possible candidates. For certainty, this experiment was repeated once more. Final assessment of deletion was achieved by analyzing Por1p expression by western blot.

3.8. CLONOGENIC SURVIVAL ASSAYS

For the evaluation of cell viability after acetic acid treatment, strains were cultured overnight in YEPD or YEPGal medium until the exponential growth phase was reached ($O.D._{640nm}$=0.5–0.8). Cells were then harvested and resuspended in either YEPD or YEPGal at pH 3.0 (set with HCl), treated with either 100 or 120 mM acetic acid and incubated under the same conditions for 200 minutes. A sample of 50 μL (yielding a concentration of approximately 10^7 cells/mL) was collected at specific time points (0, 60, 120, 180 and 200 minutes) and four serial dilutions of 1:10 were performed in sterile dH_2O. Five drops from the last dilution (30 μL each) were spotted on YEPDA

plates and incubated for 48 hours at 30 °C, after which colony forming units (CFU) were counted. Cell survival percentage for each time point was assessed by calculating the percentage of CFU counts in relation to those of the initial time point, which was considered to represent 100% of cell viability.

3.9. ANALYSIS OF FUNCTIONAL AND STRUCTURAL APOPTOTIC-LIKE MARKERS

3.9.1. FLOW CYTOMETRY ANALYSIS

Flow cytometry analysis of several apoptotic-like functional and structural markers was performed using an Epics® XL-MCL™ (Beckman COULTER®) flow cytometer equipped with an argon ion laser emitting a 488 nm beam at 15 mW. Yeast cell populations were gated in a histogram of Side Scatter (SS) x Forward Scatter (FS) in order to select high frequency and homogeneity subpopulations for fluorescence analysis. Fluorescence was acquired in a four-decade logarithmic scale. Approximately thirty thousand cells were analyzed per sample and data were analyzed in FlowJo X 10.0.7r2.

3.9.1.1. ASSESSMENT OF PLASMA MEMBRANE INTEGRITY BY PROPIDIUM IODIDE STAINING

Maintenance of plasma membrane integrity was assessed by staining cells with propidium iodide (PI; Sigma-Aldrich). This red-fluorescent DNA intercalating agent is unable to cross the plasma membrane of live cells and thus only dead cells, with compromised plasma membrane, are stained. Yeast cells were grown and treated as described in 3.8. At the indicated time points, both wild-type and mutant strains were harvested and suspended in phosphate buffer saline (PBS; 37 mM NaCl; 2.7 mM KCl; 10 mM Na_2HPO_4 and 1.8 mM KH_2PO_4, pH 7.4) to a final concentration of 10^6 cells/mL. Afterwards, cells were incubated with 1 µg/mL PI for 10 minutes at room temperature in the dark, and quickly analyzed by flow cytometry. Monoparametric detection of PI fluorescence was achieved by collecting red fluorescence through a 675 nm band-pass filter (FL-4 channel).

3.9.1.2. MEASUREMENT OF MITOCHONDRIAL MEMBRANE POTENTIAL BY $DiOC_6(3)$/PI STAINING

Alterations in mitochondrial membrane potential were assessed by staining with both 3,3'-dihexyloxacarbocyanine iodide ($DiOC_6(3)$, Thermo Fisher Scientific) and PI. As previously mentioned, only cells with compromised plasma membrane are stained with PI. Therefore, this probe was used to exclude dead cells from analysis since the aim was to evaluate mitochondrial membrane potential alterations in live cells. $DiOC_6(3)$ is a potential-sensitive lipophilic dye that when used at low concentrations accumulates in mitochondria due to the difference in potential between the cytosol and the mitochondrial matrix. For this purpose, yeast cells were grown and treated as described in 3.8., harvested at the indicated time points and suspended in $DiOC_6(3)$ buffer (10 mM MES (2-(N-morpholino)ethanesulfonic acid); 0.1 mM $MgCl_2$; 2% (w/v) glucose, pH 6 adjusted with $Ca(OH)_2$) to a final concentration of 10^6 cells per mL. Then, cells were stained with 1 nM $DiOC_6(3)$ and incubated at 30 °C for 30 minutes in the dark, with addition of 1 µg/mL PI 10 minutes prior to analysis. After staining, all samples were quickly analyzed by flow cytometry. Monoparametric detection of PI fluorescence was achieved through the FL-4 channel and only PI-negative cells were selected for further analysis. Monoparametric detection of $DiOC_6(3)$ fluorescence was attained through a 525 nm band-pass (FL1-channel). A monoparametric histogram [FL-1 (log)/FS (log)] was designed in order to correct for fluorescence variations due to cell size. The mean of the [FL-1 (log)/FS (log)] ratio was considered as the state of mitochondrial potential at that specific time point. Data were normalized by relating the ratio mean at a specific time point to that of time 0.

3.9.1.3. EVALUATION OF CYTOSOLIC SUPEROXIDE ANION ACCUMULATION BY DHE STAINING

Superoxide anion accumulation was assessed by staining acetic acid-treated cells with the probe dihydroethidium (DHE; Sigma-Aldrich). While cytosolic DHE exhibits blue fluorescence, when in the presence of superoxide anion it is oxidized to ethidium, a DNA intercalating agent which stains the nuclei with a bright red fluorescence. In order to evaluate the cellular levels of this anion following acetic acid treatment, cells were grown and treated as described in 3.8, harvested and suspended in PBS to a final concentration of 10^6 cells/mL. Subsequently, samples were stained with 2 µg/mL DHE for 20 minutes at room temperature and in the dark and quickly analyzed by flow cytometry. Monoparametric detection of DHE fluorescence was achieved by a 675 nm band-pass filter (FL-4 channel).

3.9.1.4. ASSESSMENT OF MITOCHONDRIAL DEGRADATION

To characterize the pattern of mitochondrial degradation in ERMES mutants, wild-type and deleted strains transformed with pYX242-mtGFP were subjected to flow cytometry analysis after treatment with acetic acid. Yeast cells were grown as described in 3.8., but on SC glucose medium. For acetic acid treatment, cells were harvested and suspended on YEPD at pH 3.0. At the indicated time points, samples were collected and suspended in PBS to a final concentration of 10^6 cells/mL. Mitochondrial degradation was determined in a biparametric histogram [ratio (FL-1 (log)/FS (log)) × GFP fluorescence (FL-1 peak)]. Similarly to $DiOC_6(3)$ staining, the ratio was used to eliminate fluorescence variations due to cellular volume. Additionally, given that untreated cells (time 0) virtually exhibit intact mitochondria and that mitochondrial degradation will lead to a decrease in GFP fluorescence, the FL1-peak was used as a quantitative parameter for the integrity of mitochondria by discriminating between spots of intense mitochondrial GFP signal and diffuse cytoplasmic GFP resultant from mitochondrial degradation. As such, time 0 populations were perceived as maintaining 100% of mitochondrial integrity and loss of GFP fluorescence was considered as mitochondrial degradation.

3.9.2. FLUORESCENCE MICROSCOPY

An automated Leica Microsystems DM-5000B epifluorescence microscope coupled to a Leica DCF350 FXR2-193510309 digital camera was used to assess mitochondrial morphology in live cells. Photomicrographs were acquired and processed using Leica Application Suite (LAS) AF 6000 LX Microsystems software with a 100x oil immersion objective lens with numerical aperture of 1.3 and 1.6x magnification-change. For each cell analyzed, images were taken using appropriate filter settings for differential phase contrast (DIC) and green fluorescence (GFP). The produced photomicrographs were further managed with the LAS X v. 3.3.0.16799, GIMP v.2.8.22 and ImageJ v. 1.51j8 software.

3.9.2.1. MITOCHONDRIAL MORPHOLOGY AND FRAGMENTATION

For the assessment of mitochondrial morphology before and after acetic acid treatment, all strains carrying pYX242-mtGFP were grown in SC media lacking leucine to an $O.D._{640nm}$ = 0.8–1.0

and then shifted to YEPD pH 3.0 media. Then, 50 µL of untreated cells were collected and suspended in sterile dH_2O, while the remaining culture was treated with 100 mM acetic acid for 1 h. After treatment, sampling occurred in the same manner as described before. Cell suspensions were transferred to glass slides, mounted carefully with a coverslip and quickly visualized on a fluorescence microscope.

3.10. CHRONOLOGICAL AGING ASSAY

To evaluate if the mutations inserted into BY4741 affected the chronological lifespan, strains were grown in 20 mL of SC Glu medium for 72 h. Afterwards, cells were diluted in sterile dH_2O to an $O.D._{640nm}$ of 0.5 and 10-fold serial dilutions were performed five times. Three drops of 75 µL from the last dilution were spotted on YEPDA plates and counted after 48 hours of growth at 30 °C. This was considered to be the time 0 of the experiment. Sampling was repeated periodically (every 2/3 days) for 17 days. Clonogenic survival at any given time point was normalized to that of time 0.

3.11. RESPIRATORY ABILITY AND TEMPERATURE SENSITIVITY

In order to assess the mutant's respiratory ability and temperature sensitivity, wild-type and mutant strains were grown in YEPD medium until an $O.D._{640nm}$ = 1.5 was reached. Cultures were then diluted to an $O.D._{640nm}$ of 1.0 in sterile dH_2O and four 1:10 serial dilutions were performed. For the assessment of respiratory capacity, 5 µL drops of all dilutions were spotted on a SC Glycerol plate and incubated for 72 hours at 30 °C. Strains that grew on this non-fermentable media were scored as respiratory-competent. Temperature sensitivity of the mutants was evaluated by simultaneous growth at 30 °C and 37 °C. For this purpose, 5 µL spots of all dilutions were performed on YEPDA plates and allowed to grow for 48 hours at 30 °C or 37 °C. Strains that were able to grow at 30 °C but not at 37 °C were considered as temperature-sensitive.

3.12. PETITE INDUCTION

To measure the rate at which mutants lose their respiratory ability (petite induction), strains were grown overnight in YEPG medium to select only respiring cells. Cell suspensions were diluted to an $O.D._{640nm}$ = 1.0 in sterile dH_2O and four serial dilutions (1:10) were performed. 75 µL from the

last dilution were plated on YEPDA plates and homogeneously spread with 1 mm glass beads. After growth for 96 hours at 30 °C, assessment of respiratory-competent colonies was performed by the tetrazolium assay (Ogur et al., 1957). Briefly, plates were overlaid with 15 mL of 1.5% agar and 0.1% 2,3,5-tetrazolium chloride in 0.067 M potassium phosphate buffer at pH 7.0. After 3 hours, non-respiring cells remain white while in respiring cells tetrazolium is reduced to 1,3,5-triphenylformazan, which gives the colony a red tonality. YEPD-grown ρ^0 cells were used as negative control.

3.13. MITOCHONDRIAL FRACTIONING

For mitochondria isolation, wild-type and mutant strains were cultured overnight on YEPGal medium in 3 L flasks with a flask/medium volume ratio of 5:1 until $O.D._{640nm}$ = 1.5–1.8. For each strain, 1.2 L of culture were grown, from which half was used as control and the other half was harvested, washed and treated with 100 mM acetic acid. Incubation time of wild-type and mutant strains was 60 and 90 minutes, respectively. The subsequent steps were performed for both treated and non-treated strains. Cells were harvested and washed, followed by determination of cellular wet weight. Then, the pellet was suspended in DTT buffer (100 mM Tris/H_2SO_4 pH 9.4, 10 mM dithiothreitol) in a proportion of 2 mL of buffer per gram of wet weight and incubated for 30 minutes at 30 °C with gentle shaking (80 rpm). Cells were then harvested, washed and suspended in Zymolyase buffer (20 mM potassium phosphate buffer pH 7.4, 1.2 mM sorbitol) in a 1:7 (g:mL) proportion. From our previous experience, we have determined that acetic acid-treated yeast cells strengthen their cell wall, rendering cell wall digestion more difficult. As such, 10 mg Zymolyase-20T (GRiSP Research Solutions) were added per gram of non-treated cells and 20 mg per gram of acetic acid-treated cells. For optimal cell wall disruption, the suspension was incubated for 30 minutes at 32 °C, 80 rpm, and spheroplast formation was evaluated by monitoring cell lysis in the optical microscope upon addition of 1% SDS. Afterwards, the resulting spheroplast suspension was centrifuged (5 000 rpm, 8 minutes, 4 °C), washed and suspended in ice-cold homogenization buffer (10 mM Tris-HCl pH 7.4, 0.6 M sorbitol, 1 mM EDTA and 1 mM phenylmethylsulfonyl fluoride (PMSF): 2 mL per gram of wet weight). The suspension was then transferred to an ice-cold glass Dounce homogenizer and cautious strokes were performed with a tight-fitting pestle until cells were lysed and free organelles could be seen in the optical microscope. Finally, cellular debris were pelleted twice (5 000 rpm, 5 minutes, 4 °C) and the resulting supernatant was further centrifuged

four times (12 000 rpm, 15 minutes, 4 °C) in order to isolate both mitochondrial and post-mitochondrial fractions. Both fractions were resuspended in 200 µL of homogenization buffer before being instantly frozen with liquid nitrogen and stored at -80 °C.

3.14. PREPARATION OF CELLULAR PROTEIN EXTRACTS

3.14.1. TOTAL PROTEIN EXTRACTS

For the preparation of whole cell extracts, samples were collected in order to yield a suspension of $O.D._{640nm} = 1$ in 1 mL of dH_2O. The suspension was washed twice and cells were lysed with 3.5% (v/v) β-mercaptoethanol in 2 M NaOH for 15 minutes on ice. An isovolume of 50% trichloroacetic acid (TCA) was added to the suspension in order to precipitate the proteins and incubated on ice for an additional 15 minutes. Afterwards, cells were harvested (15 000 rpm, 3 minutes) and suspended in 50 µL of Laemmli buffer (0.0625 M Tris-HCl, 2.3% (w/v) SDS, 10% (v/v) glycerol, 1.25% (v/v) β-mercaptoethanol, 0.125% (w/v) bromophenol blue), yielding a bright blue-colored protein suspension. However, some samples presented a yellow color that probably arose from the acidity of any possible remaining TCA. As such, to maintain proper pH, when required each sample was further titrated with 1 M Tris-HCl pH 9.8 until the sample turned blue. After protein extraction, all samples were further thermally denatured at 95 °C for 5 minutes and stored at -20 °C.

3.14.2. MITOCHONDRIAL AND CYTOSOLIC PROTEIN EXTRACTS

Protein concentration was determined through the previously described Bradford method (Bradford, 1976), using bovine serum albumin (BSA) as standard in a Varian Carry 50® UV-Visible spectrophotometer. Approximately 75 µg of protein from both mitochondrial and cytosolic fractions were precipitated using a variant of the method described above for total protein extracts. The respective sample volumes were collected and 50% TCA was added to the suspension and incubated for 15 minutes on ice. Afterwards, samples were washed with acetone and centrifuged at 15 000 rpm for 3 minutes before addition of 50 µL of Laemmli buffer. As previously stated, if necessary samples were titrated with 1 M Tris-HCl pH 9.8 until a blue color was visible. Protein samples were then denatured at 95 °C for 5 minutes and stored at -20 °C until used.

3.15. WESTERN BLOT ANALYSIS

Protein samples from homogenates and isolated mitochondrial or cytosolic fractions were separated by SDS 12.5% polyacrylamide gel electrophoresis (SDS-PAGE) using a Mini-Protean III electrophoresis system (Bio-Rad). Previously frozen samples were thawed on ice, centrifuged at 5 000 rpm for 3 minutes and 10 µL were introduced into the wells. Electrophoresis was run for approximately 1 hour at 20 mA per gel. After separation, the proteins were transferred from the gels to polyvinylidene fluoride (PVDF) membranes (Amersham Hybond-P, GE Healthcare Life Sciences) using a Semi-dry TE77X Transfer Unit (Hoefer). The membranes were then blocked for 1 hour with 5% (w/v) non-fat milk in PBS-T (PBS with 0.1% Tween-20) in an orbital shaker at room temperature before an overnight incubation with primary antibodies at 4 °C. Primary antibodies used were rabbit polyclonal anti-human Bax (1:5000, Sigma), rabbit polyclonal anti-yeast cyt *c* (1:1000, kindly provided by Stéphen Manon and custom-made by Millegen), mouse monoclonal anti-yeast phosphoglycerate kinase (1:5000, Invitrogen) and mouse monoclonal anti-yeast porin (1:5000, Invitrogen). The following day membranes were washed for 15 minutes with PBS-T and incubated with secondary antibodies against rabbit or mouse immunoglobulin G coupled to horse radish peroxidase (1:5000, Jackson ImmunoResearch) for 1 hour at room temperature. Membranes were then washed every 15 minutes with PBS-T four times at room temperature and band detection was achieved by chemiluminescence using the ECL detection system (Merck Millipore) and visualized in a ChemiDoc XRS Imaging System (Bio-Rad). Derivatizations of protein content by band intensity were performed using the ImageJ v. 1.51j8 software.

3.16. STATISTICAL ANALYSIS

Reported data are expressed as mean ± standard deviation (SD) of independent experiments. Statistical analysis was performed on GraphPad Prism v. 6.01 (GraphPad Software Inc, La Jolla California USA) and statistical tests used are referenced in the figure captions. Significance was considered whenever $p<0.05$.

CHAPTER 4

RESULTS

4.1. PRELIMINARY RESULTS AND STUDY OVERVIEW

Following a genetic screening performed in our lab where *mdm10*Δ and *mdm12*Δ revealed altered sensitivity after acetic acid treatment, we started to hypothesize a possible role for these proteins in acetic acid-induced cell death (Sousa et al., 2013). Further work would come to characterize the phenotypical alterations displayed by these mutants through analysis of known apoptotic hallmarks (Fernandes, 2013). This study was conducted with the prospection that proteins commanding mitochondrial phospholipid composition could be involved in the yeast response to acetic acid. Accordingly, follow-up studies would soon conduct mitochondrial phospholipidic profiling experiments on these strains, before and after treatment, in order to determine if variations in phospholipid content of mitochondria could correlate with cell survival (Afonso, 2016). At the moment, the data collected by our lab for these mutant strains proposes a role for both in the mediation of cell death induced by acetic acid. In this work, we aimed to unravel the role of the ERMES complex in acetic acid-induced cell death. For that purpose, we used deletion mutants of all known ERMES components, namely the above-mentioned proteins, Mdm10p and Mdm12p, as well as Mmm1p and Mdm34p.

4.2. THE ERMES COMPLEX IS REQUIRED FOR ACETIC ACID-INDUCED CELL DEATH

To better characterize the role of this complex, we started by monitoring cell survival of *Saccharomyces cerevisiae* wild-type and *mmm1*Δ, *mdm10*Δ, *mdm12*Δ and *mdm34*Δ strains after exposure to 100 and 120 mM acetic acid for 200 minutes.

For the former concentration, results showed that within 60 minutes the viability of the wild-type strain was drastically decreased, with a staggering reduction of approximately 94 ± 5.70% (Figure 6A). On the other hand, all deleted strains displayed high resistance to cell death induced by this acid, with cell survival percentages ranging between 93.9 ± 9.0% for *mmm1*Δ and 67.3 ± 12.6% for *mdm12*Δ at that particular time point. Not surprisingly, although at 120 minutes of treatment survival of the wild-type strain was completely abolished, the mutants still exhibited a significant resistance to this stressor, apart from *mdm12*Δ. As expected, cell survival was higher for every strain at any time point when 100 mM acetic acid was used (Figure 6B). Complete death of the wild-type strain was delayed for an additional time point, allowing better comparison between this strain and the deleted mutants. Survival of the wild-type strain at 180 and 200 minutes was

0.3 ± 0.2% and 0.1 ± 0.2%, respectively. Notwithstanding, *mmm1*Δ and *mdm34*Δ displayed tremendous resistance to acetic acid with 75.8 ± 10.7% and 84.2 ± 11.2% of cell survival, respectively, even after 200 minutes of treatment. Albeit more sensitive to this stressor than the other mutants, *mdm10*Δ and *mdm12*Δ still showed significant delay in cell death, with CFU counts revealing 42.7 ± 12.9% and 35.9 ± 9.0% of survival after two hours of exposure to acetic acid.

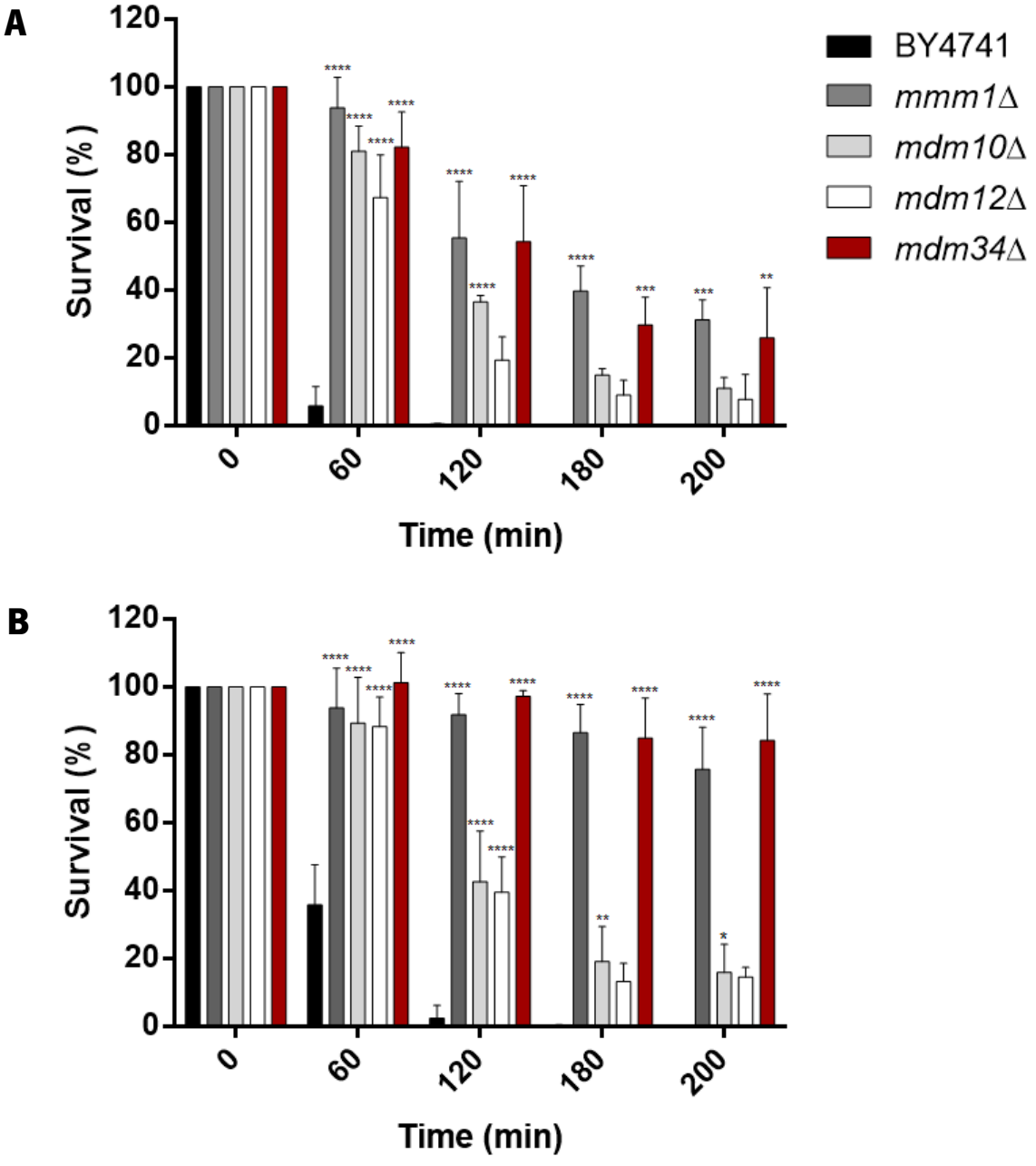

Figure 6. Absence of the ERMES complex enhances cell survival after acetic acid treatment. Relative cell survival of exponential phase cells after 200 minutes of exposure to 120 (A) or 100 mM (B) acetic acid, assessed by CFU counts on YEPDA plates. The results are expressed as mean ± S.D. of three independent experiments. Time zero was considered 100% of cell viability. A two-way ANOVA was performed and comparison between the wild-type (BY4741) and deleted strains in each time point was assessed using Dunnett's test: **p<0.01, ***p<0.001, ****p<0.0001.

Due to the drastic decrease of survival observed in the wild-type strain after 120 mM acetic acid challenge, we considered the hypothesis that at this particular concentration acetic acid could be triggering a necrotic cell death. Since apoptotic cells are known to maintain their plasma membrane integrity, whilst necrotic cells display an earlier membranal demise, we assessed plasma membrane integrity by propidium iodide (PI) staining for both concentrations (Figure 7). This dye can only enter the cell if the plasma membrane is disrupted and therefore fluorescent signals represent cells with compromised membranes.

The results obtained indicated that these strains were dying through a non-necrotic death process since cell survival did not proportionally correlate with PI staining, i.e., the percentage of unviable cells did not equal the percentage of PI-positive cells at any given time point for any given strain (Figure 7). Furthermore, all mutants revealed a significant delay in loss of plasma membrane integrity until the end of the treatment, corroborating an active role in acetic acid-induced cell death. After 60 minutes of 100 mM acetic acid treatment, 2.1 ± 1.0% of wild-type cells had lost membrane integrity even though cell survival had declined 64.2 ± 10.3% (Figure 7C). Likewise, after two hours only 10.4 ± 0.3% of cells exhibited plasma membrane disruption whilst 97.6 ± 3.3% of cells were unviable, suggesting that cell death at this acetic acid concentration is non-necrotic. The same is to be said regarding the mutant strains. Surprisingly, *mdm10*Δ and *mdm12*Δ revealed no significant differences in PI staining in comparison to the wild-type strain for the first two hours of treatment even though cell survival revealed great differences (42.7 ± 12.9% for *mdm10*Δ and 35.9 ± 9.0% for *mdm12*Δ *vs.* 2.4 ± 3.3% for BY4741). These differences in PI exclusion were enhanced for the last two time points. While 99.1 ± 0.6% of wild-type cells exhibited compromised membrane integrity, only 35.3 ± 7.7% of *mdm10*Δ and 31.1 ± 4.9% of *mdm12*Δ cells displayed this phenotype after 200 minutes of treatment which is also in agreement with the survival results.

Even though cell death induced by 120 mM acetic acid revealed itself to be non-necrotic, survival of the wild-type strain was very low after 1 hour of treatment. As such, we could not kinetically determine the delay in cell death rate of the mutant strains due to the lack of variation in survival of the wild-type strain for the last three time points, in which it was virtually 0%. Previous reports from Ludovico and colleagues (2001) state that a 120 mM concentration of acetic acid is borderline necrotic and survival is practically unrecoverable by cycloheximide treatment. Additionally, we wanted to maintain the same cell death rate as reported by Fernandes (2013) as a mean to compare our results for *mdm10*Δ and *mdm12*Δ. Thus, in order to attain a more gradual cell death we chose to use a 100 mM acetic acid concentration throughout this work.

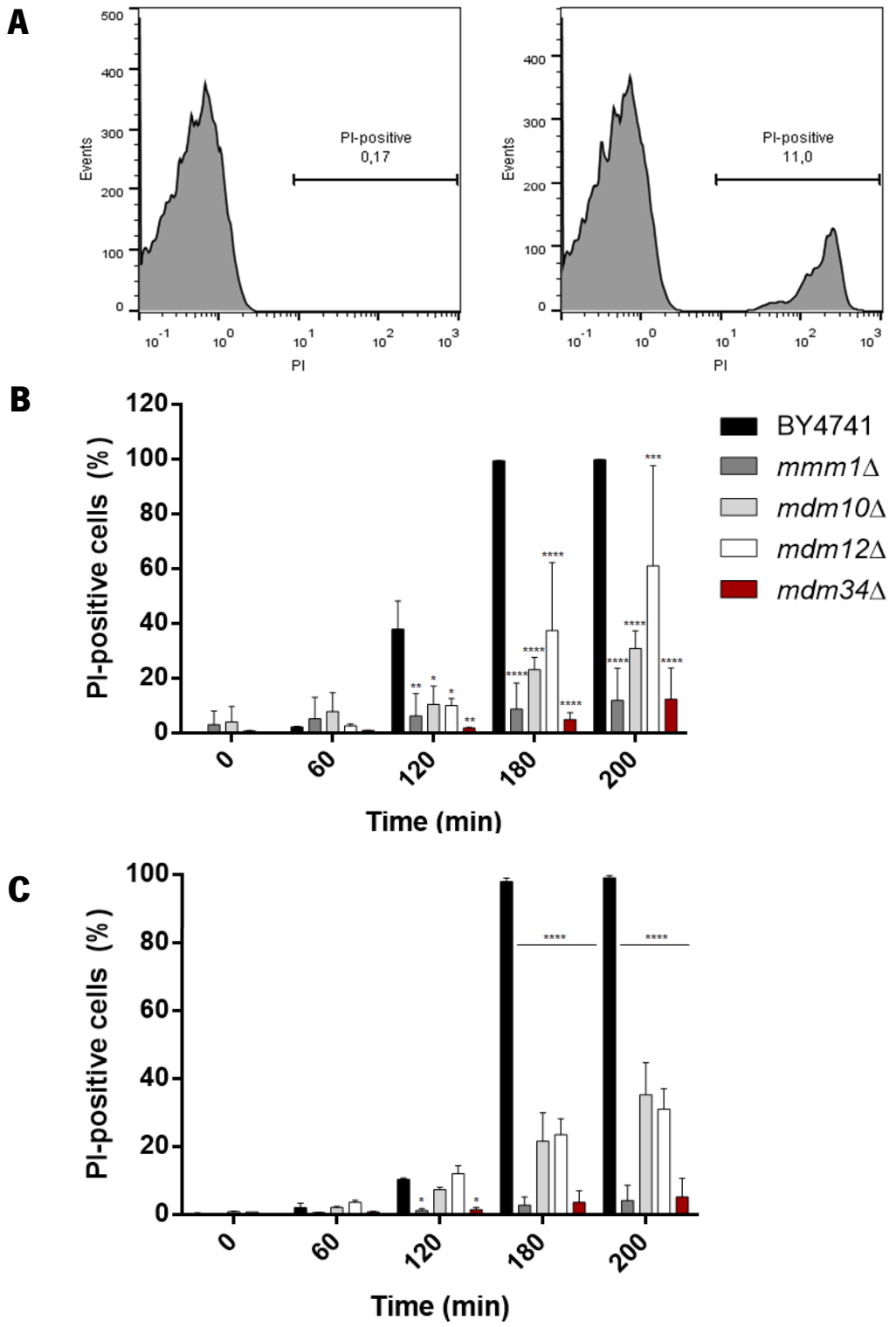

Figure 7. Disruption of plasma membrane integrity is delayed in acetic acid-treated *S. cerevisiae* lacking ERMES components. Exponential phase cells were treated with acetic acid for 200 minutes. At each time point, cells were harvested and stained with 1 µg/mL PI for 10 minutes to evaluate loss of plasma membrane integrity by flow cytometry. **(A)** Representative monoparametric histograms obtained by flow cytometry analysis before (left) and after 180 minutes (right) of acetic acid treatment for the *mdm34*Δ strain. **(B and C)** Kinetic assay of PI staining for 200 minutes after 120 or 100 mM acetic acid treatment, respectively. The results are reported as mean ± S.D. of three independent experiments. A two-way ANOVA was performed and comparison between the wild-type (BY4741) and deleted strains was assessed using Dunnett's test: *p<0.05, **p<0.01, ***p<0.001, ****p<0.0001.

Our results indicate that every ERMES-deleted strain exhibits a higher resistance to acetic acid, as formerly reported for *mdm10*Δ and *mdm12*Δ (Fernandes, 2013). Although our results for the latter are in line with the ones found by Fernandes, the ones obtained for *mdm10*Δ show that this strain is less resistant in comparison with the wild-type strain than previously reported. As such, to eliminate the possibility that we were working with strains with a different deletion we extracted genomic DNA from every strain and performed a standard confirmation PCR. Since the EUROSCARF haploid mutant deletion has the non-essential genes interrupted with a *KanMX4* cassette, we assessed the presence of the *KanMX4* cassette on the target gene (Figure 8).

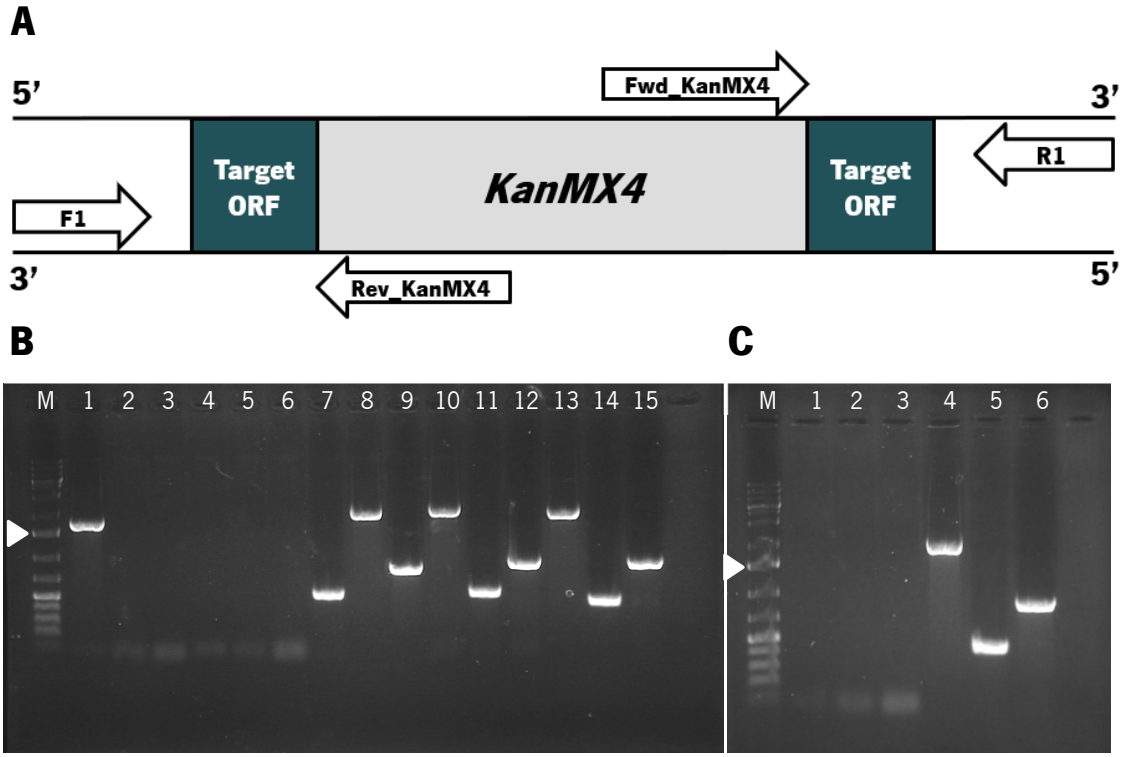

Figure 8. Confirmation of correct *KanMX4* cassette insertion in ERMES-deleted strains. Genomic DNA (gDNA) was extracted from each strain and *KanMX4* insertion was assessed by PCR. **(A)** Schematic representation of the strategy used for evaluation of *KanMX4* presence. Primers upstream (F1) or downstream (R1) of the target ORF were used along with primers that anneal within the *KanMX4* cassette (Fw_KanMX4 and Rv_KanMX4). **(B)** The PCR products ran on an 1% agarose gel visualized under UV light after staining. M: molecular marker; 1–3: BY4741 gDNA with primers F1/R1, F1/KanB & KanC/R1 from *mmm1*Δ, respectively; 4–6: *mmm1*Δ gDNA with primers F1/R1, F1/KanB & KanC/R1, respectively; 7–9: *mdm10*Δ gDNA with primers F1/KanB, F1/R1 & KanC/R1, respectively; 10–12: *mdm12*Δ gDNA with primers F1/R1, F1/KanB & KanC/R1, respectively; 13–15: *mdm34*Δ gDNA with primers F1/R1, F1/KanB & KanC/R1, respectively. **(C)** M: molecular marker; 1–3: Sample without DNA with primers F1/R1, F1/KanB & KanC/R1 (negative control); 4–6: *mdm34*Δ gDNA with primers F1/R1, F1/KanB & KanC/R1. Arrows indicate 1 500 bp band.

Surprisingly, we were able to confirm proper deletion of *mdm10*Δ, *mdm12*Δ and *mdm34*Δ but not *mmm1*Δ using primers sets that anneal approximately 200 bp upstream and downstream

of the initiation and stop codon of the target ORF, respectively (Figure 8). Presence of *KanMX4* on the *mmm1*Δ strain was attempted three more times using new PCR reagents and newly extracted genomic DNA, as well as using primers that anneal around 250 bp far from the target gene. However, every experiment was unsuccessful. Considering that the inexistence of a kanamycin-resistance cassette in the wild-type strain was assessed using *mmm1*Δ primers, the problem of finding *KanMX4* insertion was not due to inaccurate primer design. Moreover, the alleged *mmm1*Δ strain grew on YEPDA plates supplemented with 200 µg/mL geneticin-418, indicating that *KanMX4* was present. As such, it is probable that in this strain *KanMX4* may have recombined elsewhere in the genome other than the target gene.

4.3. ERMES DEFICIENCY IMPAIRS MITOCHONDRIAL APOPTOTIC EVENTS AFTER ACETIC ACID CHALLENGE

We next assessed if the mutant strains presented alterations in mitochondrial transmembrane potential following acetic acid treatment, as it has been reported before for W303-1A and BY4741 (Fernandes, 2013; Ludovico et al., 2002). Since the strains in study are mitochondrial mutants we wanted to compare them with the wild-type to evaluate if differences in $\Delta\Psi m$ could be associated with higher survival rates. For that purpose, cells were stained with the potential-sensitive probe $DiOC_6(3)$ for 200 minutes after acetic acid treatment. In order to evaluate this parameter in live cells exclusively, we co-stained each sample with PI. Since mitochondrial mass within cells from the same culture is not constant, we tried to avoid variations by normalizing fluorescent signal over cell size.

Our results with BY4741 using $DiOC_6(3)$ show that the $\Delta\Psi m$ suffered a quick hyperpolarization after 60 minutes of treatment and reached a plateau throughout the assay, slightly dropping at 200 minutes (Figure 9). Not surprisingly, the $\Delta\Psi m$ of the mutant strains remained practically unchanged for the first hour of treatment. Thereafter, $\Delta\Psi m$ of *mdm10*Δ and *mdm12*Δ seemed to follow in the same fashion as that of the wild-type strain while *mdm34*Δ mitochondria appeared to only slightly hyperpolarize throughout treatment. These results are in agreement with our cell survival assays (see Figure 6), demonstrating that cells lacking ERMES

components are more resistant to acetic acid and that clonogenic survival can correlate with alterations in mitochondrial transmembrane potential.

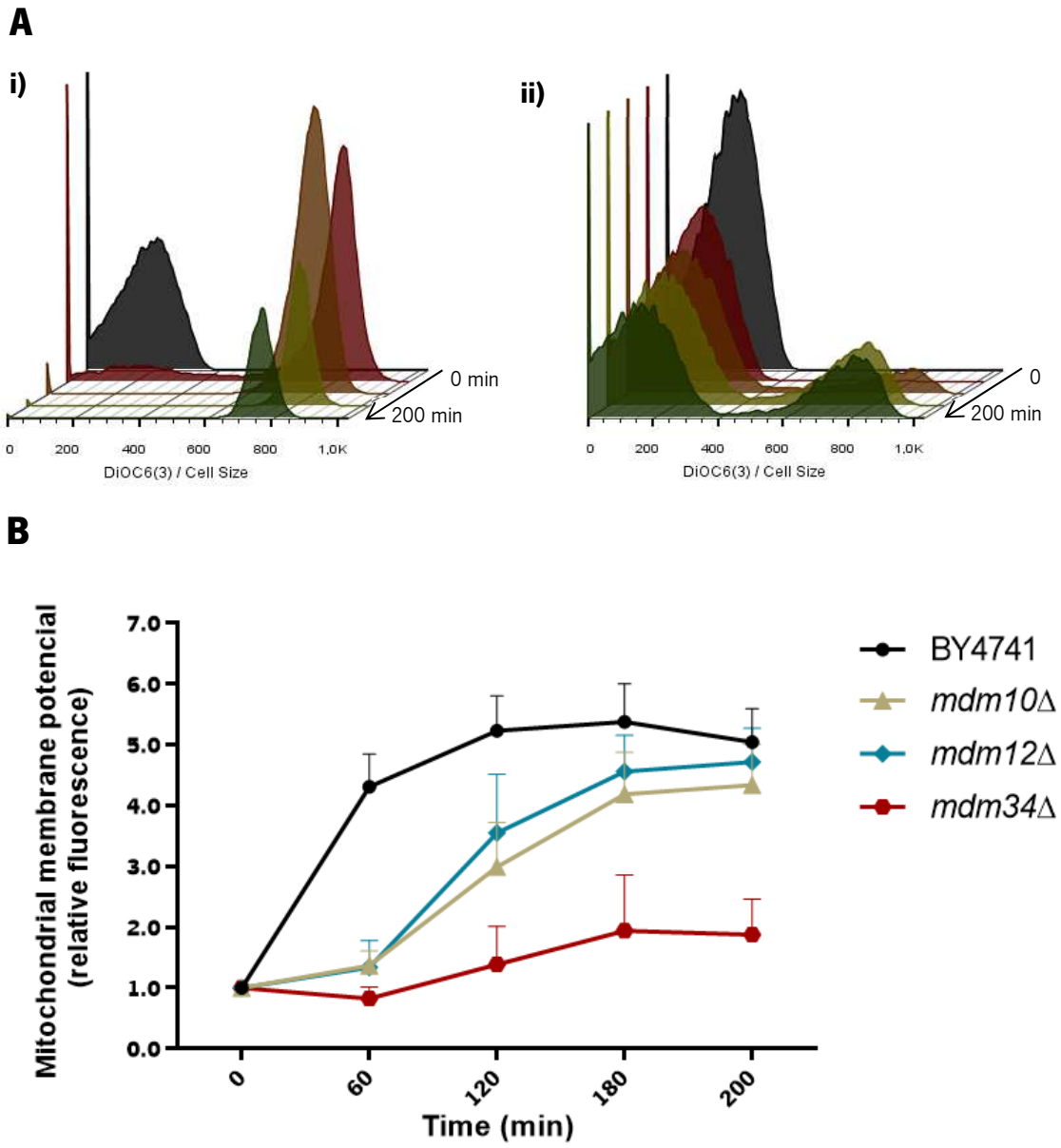

Figure 10. Alteration of mitochondrial transmembrane potential is significantly delayed in yeast lacking ERMES subunits after acetic acid treatment. Relative $DiOC_6(3)$ fluorescence of exponential phase-grown cells exposed to 100 mM acetic acid for 200 minutes. At each time point, cells were harvested, stained with 1 nM $DiOC_6(3)$ and analyzed by flow cytometry. **(A)** Representative histograms of monoparametric detection of $DiOC_6(3)$ fluorescence for (i) BY4741 and (ii) *mdm34*Δ. Mean fluorescence intensity of $DiOC_6(3)$ signal was normalized to cell size. **(B)** Kinetic assessment of mitochondrial transmembrane potential in response to acetic acid. Ratio between DiOC6(3) signal and cell size at each time point was further normalized to time 0, which represents normal mitochondrial transmembrane potential. Results represent mean ± S.D. of three independent experiments.

Mitochondrial fragmentation is a known hallmark of apoptosis which has already been described in acetic acid-treated yeast cells (Fannjiang et al., 2004). As such, we questioned if this phenomenon still occurred in cells lacking ERMES since these are mitochondrial mutants. For that purpose, all mutants were transfected with a plasmid carrying a mitochondrial matrix-targeted green fluorescent protein (pYX242-mtGFP). Mitochondrial morphology and fragmentation was visualized in a fluorescence microscope (Figure 10).

As expected, wild-type BY4741 cells were found to exhibit mitochondrial networks in the form of linear threads. On the other hand, a very little percentage of ERMES-deficient cells revealed a similar phenotype. The results are in line with previous studies where cells lacking ERMES components exhibited spherical mitochondria (Burgess et al., 1994; Esposito et al., 2011; Sogo & Yaffe, 1994). Due to time constraints, we could not quantitatively estimate the percentage of each morphotype displayed by the strains. However, our qualitative analysis shows that, in some cases, very short tubular mitochondria were present and occasionally accompanied by mitochondria with a spherical morphology. While the *mdm10*Δ and *mdm12*Δ strains predominantly revealed large and round mitochondria, with just a few cells exhibiting small punctae and/or short tubules, this morphotype was not found for the *mdm34*Δ strain, which only exhibited either punctate or tubular mitochondria (Figure 10).

Albeit mitochondrial fragmentation upon acetic acid treatment was assessed for both wild-type and mutant strains, we were unable to determine if fragmentation was occurring in the deleted strains by fluorescence microscopy. Considering that ERMES mutants have impaired mitochondrial morphology and predominantly display spherical or punctate mitochondria, evaluating mitochondrial breakage would only generate either short tubules or punctae which could not be distinguished from mitochondria of untreated cells. We first evaluated if this particular acetic acid concentration could induce mitochondrial fragmentation in the wild-type strain. Indeed, after 60 minutes of treatment the pattern of tubular mitochondria previously detected turned into a punctate structure (Figure 10). The same phenotype was encountered for all ERMES-deficient cells under treatment (not shown).

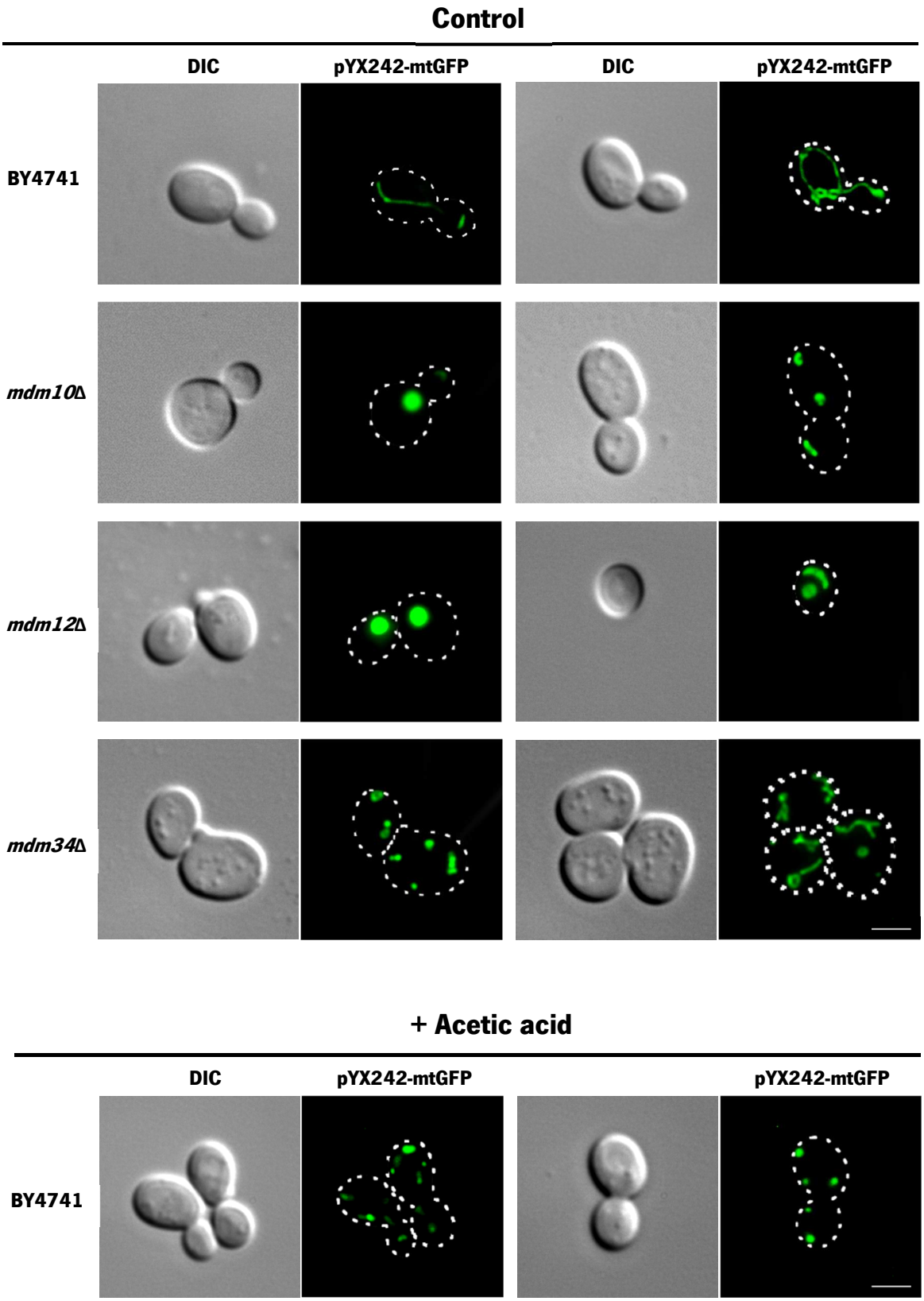

Figure 10. Photomicrographs of ERMES-deficient yeast cells reveal impaired mitochondrial morphology. Wild-type and ERMES-deficient cells were transformed with a plasmid encoding a mitochondrial matrix-targeted green fluorescent protein (pYX242-mtGFP). Mitochondrial morphology of exponential phase yeast cells carrying the plasmid was assessed by fluorescence microscopy. The wild-type strain was further treated with 100 mM acetic acid for 60 minutes. Photomicrographs shown are representative of three independent experiments. Bar, 5 µm.

We next assessed if the mutant strains presented differences in mitochondrial degradation upon acetic acid treatment in comparison to the wild-type strain. We monitored mitochondrial degradation by flow cytometry using the decrease of GFP fluorescence as a marker of mitochondrial breakdown. To do so, we followed a gating strategy that allowed us to differentiate the fluorescence derived from mitochondrial networks from that of cytosolic GFP resultant from mitochondrial degradation (Figure 11A).

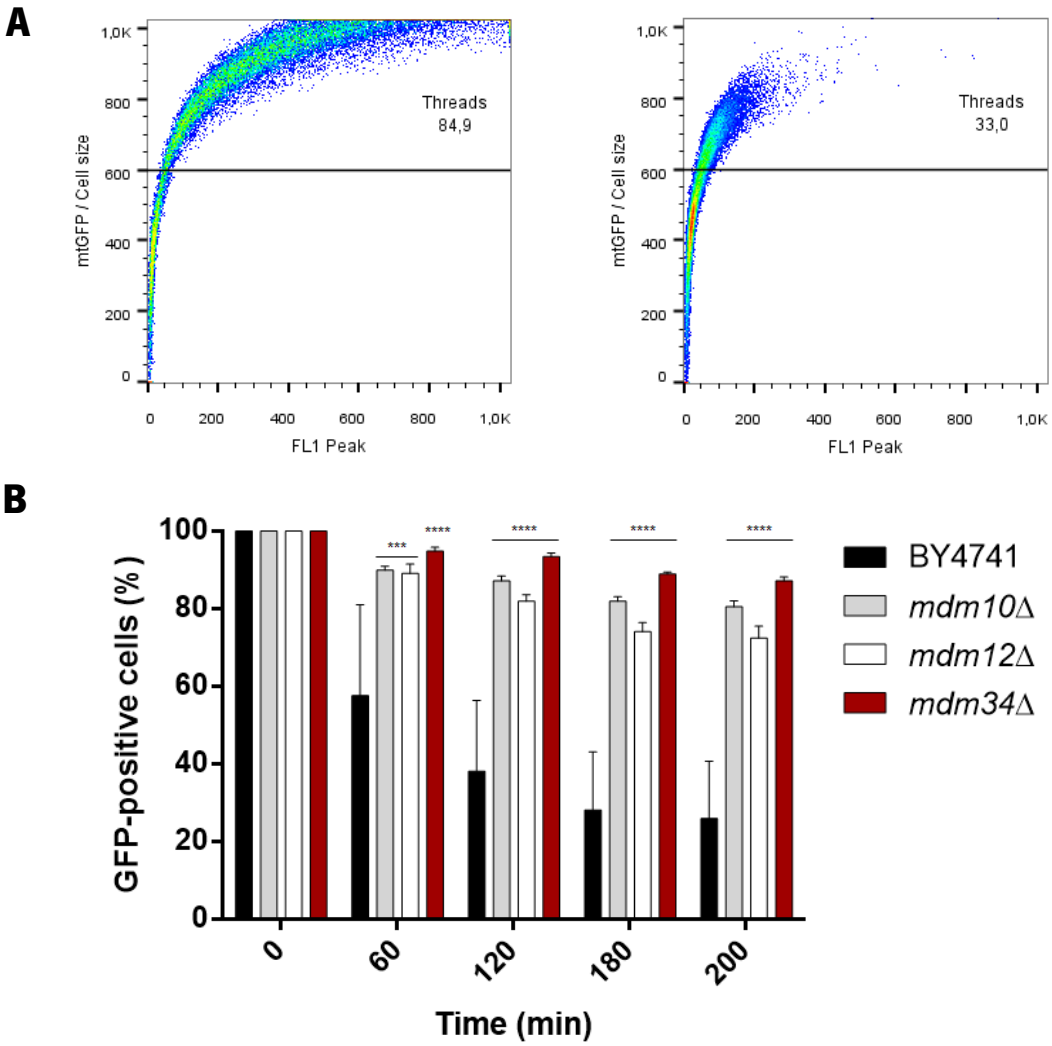

Figure 11. Mitochondrial degradation is significantly delayed in *S. cerevisiae* lacking ERMES components after acetic acid treatment. Wild-type and mutant strains carrying the pYX242-mtGFP plasmid were grown to exponential phase and treated with 100 mM acetic acid for 200 minutes. At each time point, cells were harvested and analyzed by flow cytometry. **(A)** Representative histograms of the gating strategy for biparametric detection of GFP fluorescence for the wild-type strain before (left panel) and after 200 minutes of acetic acid treatment (right panel). Mean fluorescence intensity of GFP signal was normalized to cell size and then used in a biparametric histogram along with the peak fluorescence. **(B)** Kinetic evaluation of mitochondrial degradation upon acetic acid treatment. The percentage of intact mitochondria at time 0 was considered 100% and values obtained for each time point were normalized to those of time 0. Values represent mean ± S.D. of three independent experiments. Statistical analysis was achieved by performing a two-way ANOVA coupled to a Dunnett's post-hoc test for comparison between wild-type (BY4741) and mutant strains: ***p<0.001, ****p<0.0001.

The results revealed a quick increase in mitochondrial degradation for the wild-type strain that was not evidenced for the mutant strains (Figure 11B). Whilst the wild-type strain exhibited 57.6 ± 19.1% of cells with preserved mitochondrial GFP after 60 minutes of acetic acid challenge, the mutant strains presented a minimum of 89.2 ± 1.9%. Throughout time, wild-type GFP-positive cells would further decrease to approximately 25.9 ± 12.0% after 200 minutes of treatment, whereas the more sensitive mutant, *mdm12*Δ, still exhibited 72.5 ± 2.5% cells with GFP fluorescence.

4.4. LACK OF ERMES COMPLEX DELAYS THE ACCUMULATION OF CYTOSOLIC SUPEROXIDE ANION

To further characterize the apoptotic-like response of these strains, we assessed if the mutants displayed accumulation of reactive oxygen species, namely superoxide anion. This anionic species is a common byproduct of cellular respiration that is generated by leakage of electrons from the respiratory complexes that directly reduce molecular oxygen. Moreover, it has been reported that acetic acid-induced cell death of *S. cerevisiae* is accompanied by an increase of ROS formation, specifically superoxide anion (Guaragnella et al., 2011; Ludovico et al., 2002). With that intent, wild-type and mutant strains were stained with dihydroethidium after acetic acid treatment and accumulation of superoxide anion was evaluated by flow cytometry.

The results showed an earlier increase in superoxide anion in the wild-type strain in comparison to the deletion mutants (Figure 12). Although there was no considerable difference between BY4741 and *mdm10*Δ after one hour of treatment, from that point on that difference was exacerbated with a percentage of DHE-positive cells of 94.1 ± 1.0% for BY4741 and 56.6 ± 2.1% for *mdm10*Δ after 120 minutes. Not surprisingly, at that particular time point *mdm34*Δ revealed a significant delay in superoxide anion accumulation with a percentage of DHE-positive cells of 13.7 ± 4.5%, approximately seven times lower than the wild-type. While BY4741 reached almost 100% of DHE-stained cells after 2 hours of treatment, even after 200 minutes the mutants did not display such percentages. Altogether, the results show that superoxide anion accumulation is significantly delayed in cells lacking the ERMES complex after acetic acid challenge.

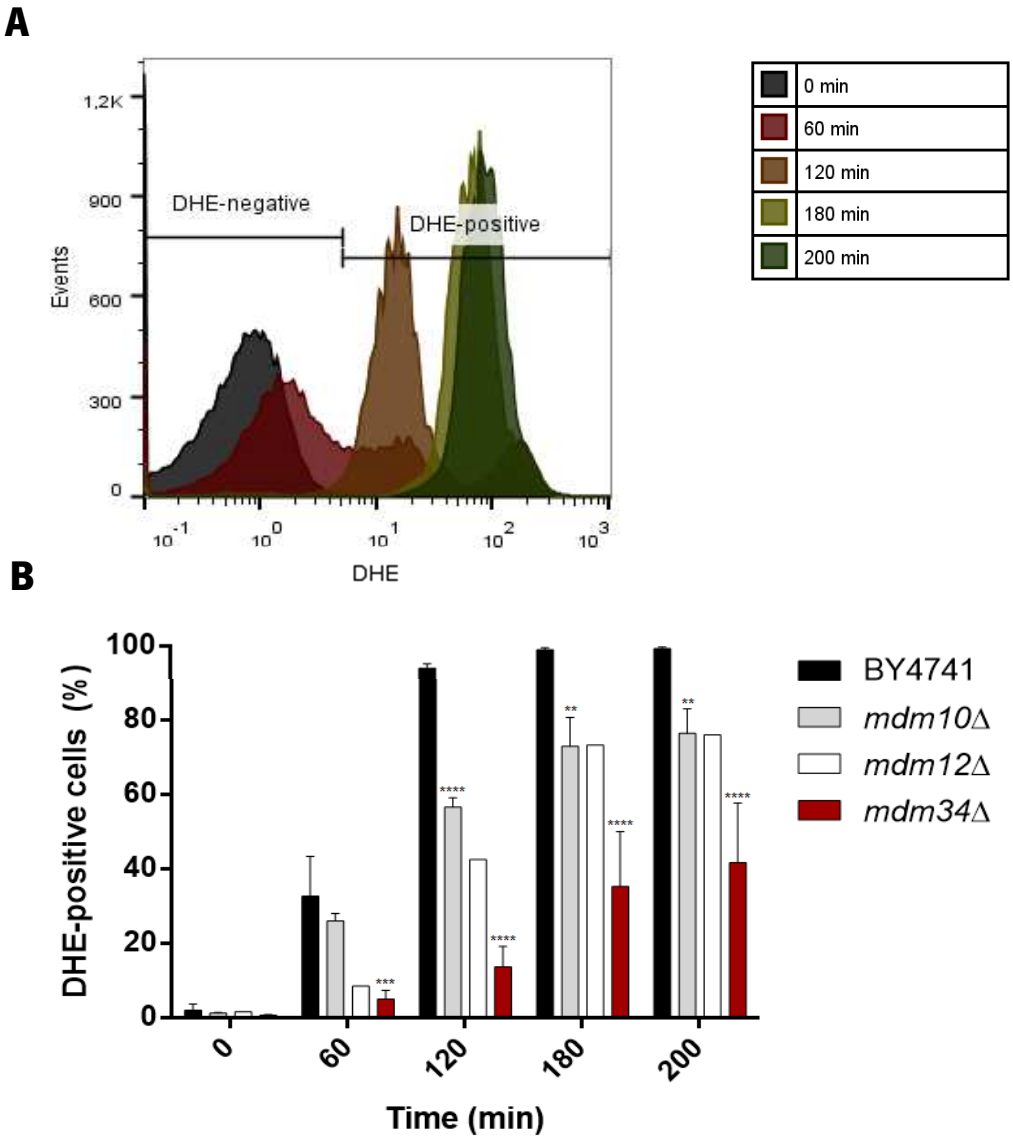

Figure 12. Evaluation of total superoxide anion accumulation after acetic acid treatment by dihydroethidium (DHE) staining. Exponential phase cells were treated with 100 mM acetic acid for 200 minutes. At each time point, cells were harvested and stained with 2 µg/mL DHE for 20 minutes to evaluate accumulation of superoxide anion by flow cytometry. **(A)** Representative monoparametric histograms with respective gating strategy obtained by flow cytometry analysis at each time point for the wild-type strain (BY4741). **(B)** Percentage of DHE-positive cells after acetic acid treatment. Results are reported as mean ± S.D. of three independent experiments with the exception of *mdm12*Δ (n=1). A two-way ANOVA was performed and comparison between the wild-type (BY4741) and deleted strains was assessed using Dunnett's test: **p<0.01, ***p<0.001, ****p<0.0001.

4.5. ERMES-DEFICIENT YEAST CELLS ARE ABLE TO RESPIRE ON A BY4741 BACKGROUND

Several reports have described that ERMES-deleted strains exhibit impaired respiratory ability (Jin et al., 2015.; Kornmann et al., 2009; Tan et al., 2013). Bearing in mind that respiratory-deficient mutants are unable to grow on non-fermentable carbon sources and form small colonies

on fermentable media (Day, 2013), we expected to see *petite* colonies. However, growing these strains on solid YEPDA plates we found that the colony size of yeast lacking ERMES components was comparable to that of the wild-type. Therefore, we assessed the respiratory ability of the mutants in this particular background strain. Moreover, considering that ρ^0 strains have increased resistance to acetic acid (Ludovico et al., 2002), it was also necessary to assess if the resistance of these mutants could be due to an inability to respire. For this purpose, wild-type and mutant strains were grown in YEPD medium and drop dilution assays were performed on SC plates with 2% glycerol (Figure 13).

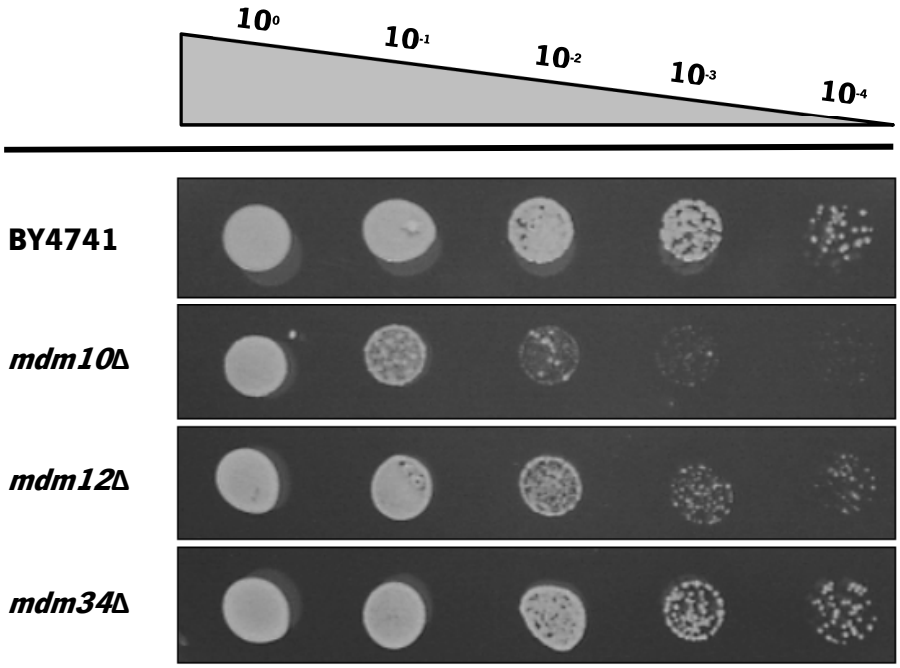

Figure 13. Growth assessment of ERMES-deleted strains on a non-fermentable carbon source. Wild-type and mutant strains were grown in liquid YEPD medium, diluted to an $O.D._{640nm}$=1 in sterile deionized water and serial diluted in a 1:10 proportion in the same solvent. Thereafter, a 5 µL drop of each dilution was plated on solid SC medium containing 2% glycerol and incubated at 30 °C for 72 hours. Data represents one of three independent experiments.

The results show that *mdm10*Δ and *mdm12*Δ seem to have deficiencies in their respiratory capacities, while *mdm34*Δ exhibits a wild-type-like phenotype (Figure 13). The mutants also grew in liquid SC glycerol media, albeit more slowly than the wild-type. With our previous characterization of mitochondrial morphotypes by fluorescence microscopy (see Figure 10), these results demonstrate that the defective mitochondrial morphology of *mdm10*Δ and *mdm12*Δ is associated with decreased ability to respire, while *mdm34*Δ exhibited near-normal morphology and respiration. Moreover, these results confirm that resistance to acetic acid treatment is not a consequence of respiratory inability.

Taking into account that certain point mutations in ERMES proteins generate temperature-sensitive mutants (Burgess et al., 1994; Sogo & Yaffe, 1994) and to further characterize these strains, we sought to determine if null mutants were able to grow at non-permissive temperatures on glucose media. Therefore, exponential phase-grown cells were subjected to drop dilution assays on YEPDA plates and simultaneously allowed to grow for two days at 30 °C and 37 °C (Figure 14).

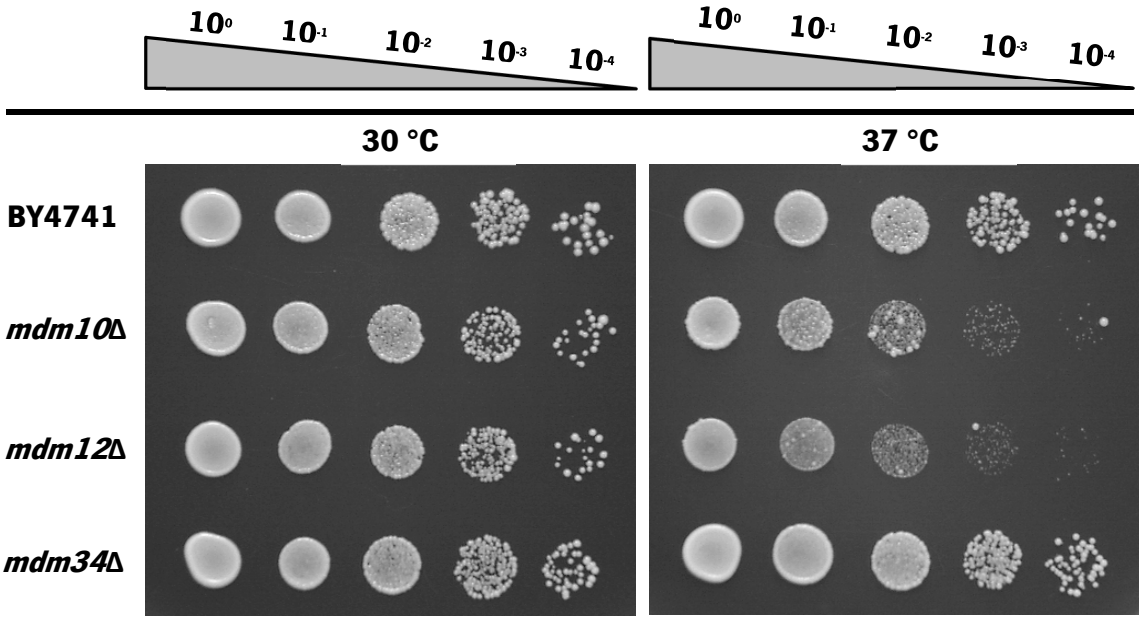

Figure 14. ERMES-deleted strains are sensitive to growth at restrictive temperature. YEPD-grown cultures were serial diluted and 5 µL spot dilutions were performed on YEPDA plates. The plates were simultaneously incubated at 30 °C and 37 °C for 48 hours. Data represents one of three independent experiments.

As anticipated, the results revealed normal growth of both wild-type and mutant strains at the permissive temperature (Figure 14). On the other hand, at 37 °C the *mdm10*Δ and *mdm12*Δ strains displayed impaired growth whilst *mdm34*Δ exhibited wild-type-like behavior. Of note, more than a decrease in colony number for the former strains we rather observed a drastic reduction in colony size for the former strains, similarly to what had occurred when growing these strains on glycerol plates. Occasionally, from the second to the last dilutions we were able to observe that some *mdm10*Δ and *mdm12*Δ colonies displayed a wild-type-like size. Altogether, these results demonstrate that these strains grow poorly at non-permissive temperature with a very high rate of *petite* formation.

As aforementioned, the ERMES complex has been linked to anchoring mtDNA nucleoids and mtDNA replication (Hanekamp et al., 2002; Hobbs et al., 2001; Murley et al., 2013). Since loss of mtDNA is one of the causes for *petite* formation, we evaluated the rate at which ERMES-deficient cells lost their respiratory capacity by measuring the appearance of colonies with a *petite* phenotype. With that intent, wild-type and mutant strains were grown in liquid YEPG medium to select only respiratory-sufficient (ρ^+) cells and spread onto YEPDA plates. After 4 days of growth, assessment of *petite* colonies was performed by the tetrazolium overlay technique (Ogur et al., 1957). White colonies were scored as *petite* and red colonies as respiratory-competent (Figure 15).

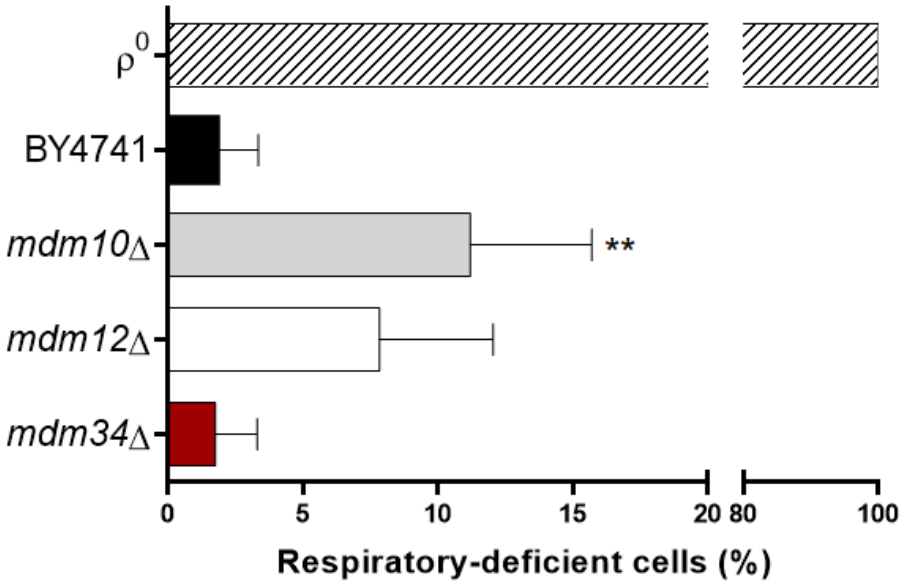

Figure 15. Lack of *MDM10* promotes *petite* formation in *Saccharomyces cerevisiae*. YEPG-grown wild-type and mutant strains were spread onto YEPDA plates and allowed to grow for 4 days. Thereafter, colonies were overlaid with 0.1% (w/v) 2,3,5-triphenyl tetrazolium chloride and reserved for 3 hours. Actively respiring colonies are able to reduce the compound and gain a red tonality, while respiratory-deficient cells remain white. A respiratory-deficient (ρ^0) strain was used as positive control. Reported values represent the mean ± S.D. of three independent experiments. A one-way ANOVA was performed and Dunnett's post-hoc test was used for comparison between wild-type (BY4741) and mutant strains: **p<0.01.

In agreement with our results regarding respiratory ability, we observed that *mdm34*Δ exhibited a similar phenotype in comparison to the wild-type strain, with *petite* induction percentages of 1.78 ± 1.27% and 1.74 ± 1.27%, respectively (Figure 15). Not surprisingly, the *mdm10*Δ and *mdm12*Δ strains displayed a higher loss of respiratory ability with 11.2 ± 3.7% and 7.8 ± 3.4% of colonies remaining white after 3 hours. To ensure proper white/red screening, we repeated the scoring process after 72 hours and observed no differences in the results. Moreover,

the use of a mtDNA-deficient strain in this experiment attested for the efficacy of the assay with not a single colony turning red after 72 hours.

4.6. LACK OF ERMES COMPLEX REDUCES THE YEAST CHRONOLOGICAL LIFESPAN

Aiming to investigate if the resistance phenotype we encountered after acetic acid challenge could be due to an unspecific hindrance of the mutants to commit to a cell death program, we evaluated if ERMES deficiency could impact the overall lifespan of *S. cerevisiae*. To unveil the effects of *MDM10*, *MDM12* and *MDM34* deletions on the yeast chronological lifespan, we performed a chronological aging assay for 17 days and evaluated cell viability by CFU counts. Our results indicate that cells lacking the ERMES complex are more prone to lose viability than the wild-type strain (Figure 16).

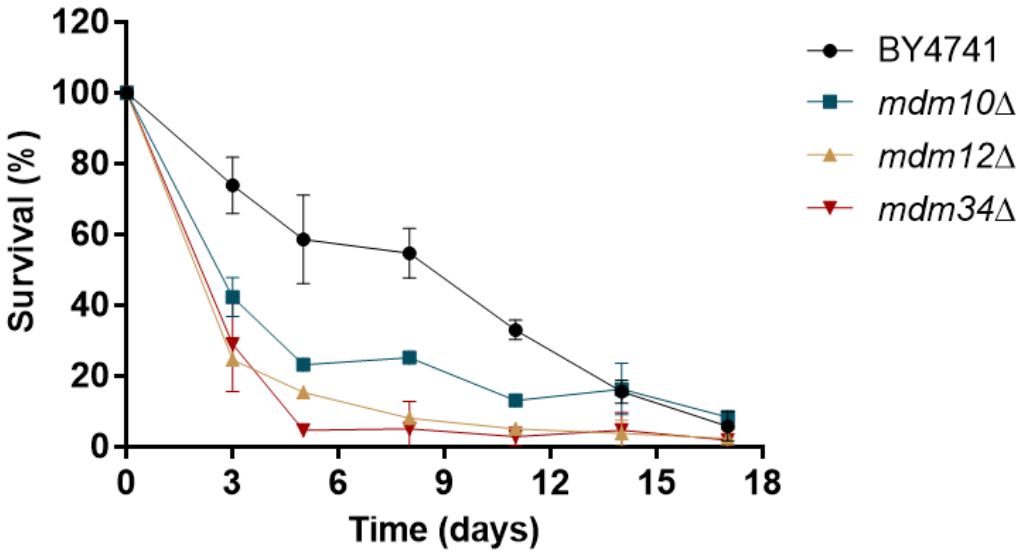

Figure 16. Ablation of ERMES complex reduces the chronological lifespan of *Saccharomyces cerevisiae*. Wild-type and mutant strains were grown in SC glucose media to stationary phase for three days, by the end of which the first samples were collected (time 0). The experiment was carried out for 17 days and survival was evaluated by CFU counts on YEPDA plates. Time 0 was considered 100% of viability. Results are expressed as mean ± S.D. of two independent experiments.

4.7. THE ERMES COMPLEX MEDIATES CYTOCHROME *C* RELEASE UPON ACETIC ACID TREATMENT

Cyt *c* release from mitochondria and its association with procaspase-9 to form the apoptosome is a known hallmark of mammalian apoptosis (Budihardjo et al., 1999). Furthermore, cyt *c* release has been implicated in the mediation of apoptotic-like cell death of acetic acid-treated yeast cells (Ludovico et al., 2002). Thus far, our results with yeast cells lacking the ERMES complex are indicative for a role of this structure in the signaling cascade that decides life or death in this organism. To continue this characterization, we evaluated the release of cyt *c* from the mitochondrial intermembrane space, where it is loosely bound to the IMM and participates in oxidative phosphorylation. In order to do so, a change of carbon source was required.

Glucose is the preferred energy and carbon source of *S. cerevisiae*. Even when oxygen is available, this yeast employs this monosaccharide in alcoholic fermentation to yield a quick energy source in the form of ATP and allow rapid cell growth and replication. However, glucose acts as a repressor of mitochondrial respiration. *S. cerevisiae* is able to sense intra- and extracellular levels of this sugar and modulate the expression of genes involved in the breakdown of other carbon sources, as well as by post-transcriptional and post-translational mechanisms (Kayikci & Nielsen, 2015). While under fermentative conditions mitochondrial mass is scarce, an aerobic metabolism yields a larger number of mitochondria per cell (Westermann, 2012). Considering our interest in evaluating cyt *c* release from the mitochondrial reservoirs, a higher mitochondrial mass was required for better detection of cyt *c*. For that purpose, we changed the carbon source from glucose to galactose. Galactose is a weaker repressor of mitochondrial respiration in comparison to glucose, allowing a respiro-fermentative metabolism that yields a higher amount of cyt *c* (Herrero et al., 1985).

Due to this change in carbon source, we needed to ensure that the resistance to acetic acid previously shown in glucose media was not affected by the change in media composition. As such, we performed clonogenic survival assays after growing all strains in media containing 2% galactose instead of glucose (Figure 17).

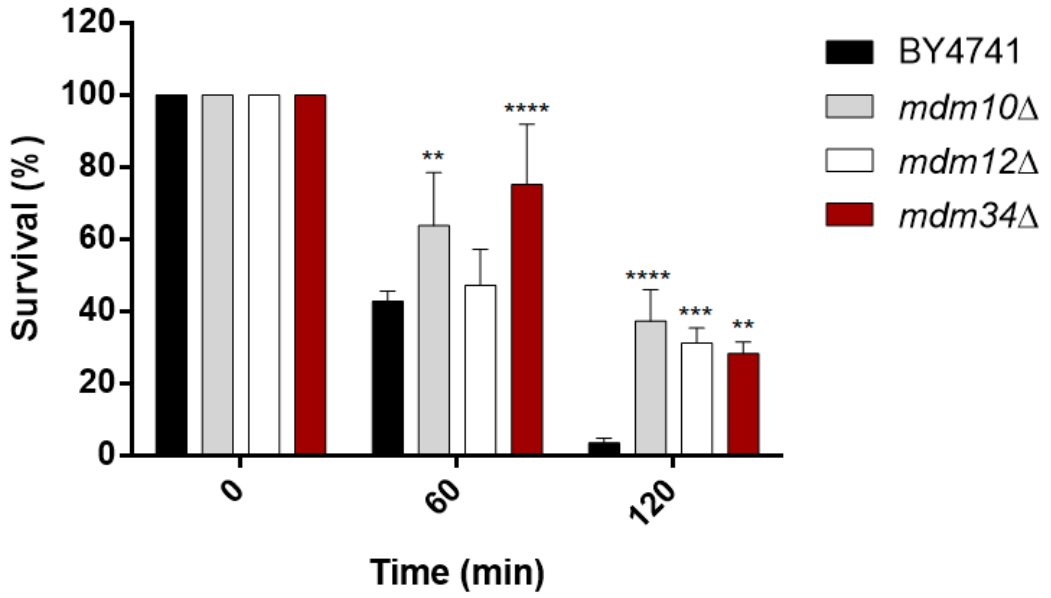

Figure 17. Absence of ERMES complex induces resistance to acetic acid treatment in galactose media. Wild-type and mutant strains were grown to exponential phase in YEPGal media and shifted to YEPGal pH 3.0 media before 100 mM acetic acid treatment for 200 minutes. Clonogenic survival was evaluated by CFU counts on YEPDA plates, where time 0 was considered 100% of viability. The results are expressed as mean ± S.D. of three independent experiments. A two-way ANOVA was performed and Dunnett's post-hoc test was used for comparison between wild-type (BY4741) and mutant strains: **p<0.01, ***p<0.001, ****p<0.0001.

After one hour of exposure to acetic acid only the *mdm10*Δ and *mdm34*Δ strains exhibited a higher resistance to treatment, with 63.8 ± 12.0% and 73.5 ± 13.6% of survival, respectively (Figure 17). On the other hand, survival of *mdm12*Δ cells did not significantly differ in comparison to the wild-type strain. Nonetheless, after two hours of treatment all strains revealed a significant resistance phenotype. While only 3.6 ± 1.1% of wild-type cells were able to resist acetic acid-induced cell death, all the mutant strains exhibited much higher survival rates with 37.3 ± 7.1% for *mdm10*Δ, 31.2 ± 3.5% for *mdm12*Δ and 28.4 ± 2.6% for *mdm34*Δ cells.

For the evaluation of cyt *c*, wild-type and mutant strains were grown in YEPGal medium and shifted to YEPGal pH 3.0 media before treatment with 100 mM acetic acid. After treatment, untreated and treated cells were subjected to mitochondria fractioning from which mitochondrial and cytosolic fractions were isolated. Release of cyt *c* was assessed by western blot analysis and the extent of release was measured by band intensity normalized to the respective loading control (Figure 18).

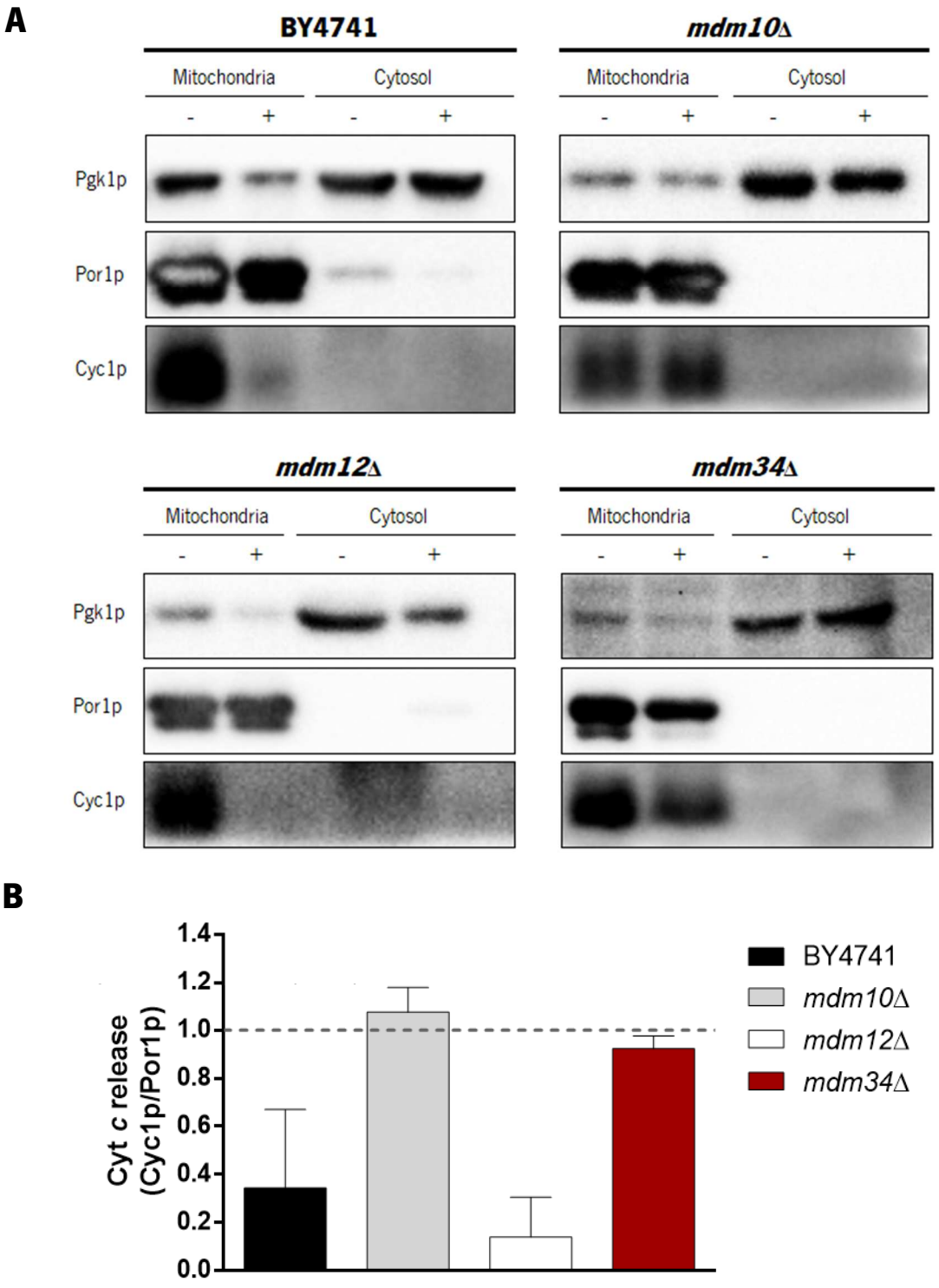

Figure 18. Cytochrome *c* release is abrogated in *mdm10*Δ and *mdm34*Δ mutants. Wild-type and mutant strains were subjected to mitochondrial fractioning in YEPGal medium before (-) and after (+) exposure to 100 mM acetic acid treatment. Wild-type cells were treated for 60 minutes, whereas mutant strains were treated for 90 minutes. **(A)** Release of cytochrome *c* (Cyc1p) was evaluated by western blot analysis. Phosphoglycerate kinase 1 (Pgk1p) and mitochondrial porin 1 (Por1) were used as loading controls for mitochondrial and cytosolic fractions, respectively. A representative experiment is shown for each strain of two independent experiments. **(B)** Cytochrome *c* levels on mitochondrial fractions before and after treatment were quantified by band intensity using the ImageJ software. Protein levels were normalized to the corresponding loading control, Por1p. Values are the mean ± S.D. of two independent experiments. Dashed grey line represents a Cyc1p/Por1p ratio of 1, meaning no cytochrome *c* was released.

The results clearly demonstrate that the absence of ERMES has an impact on cyt *c* release (Figure 20). Notably, we found that absence of both *mdm10*Δ and *mdm34*Δ prevented the efflux of cyt *c* from mitochondria almost completely, with Cyc1p/Por1p ratios of 1.07 ± 0.07 and 0.92 ± 0.04, respectively, in comparison to untreated samples. On the other hand, the wild-type and *mdm12*Δ strains exhibited a high degree of cyt *c* release from mitochondria after acetic acid treatment. In these strains, relative Cyc1p/Por1p ratios obtained were 0.34 ± 0.23 and 0.14 ± 0.12, respectively. Curiously, no cyt *c* was detected on the cytosolic fractions of both treated or untreated samples of wild-type and *mdm12*Δ strains, hinting that cytosolic cyt *c* may have been subject of proteolysis.

4.8. THE YEAST VOLTAGE-DEPENDENT ANION CHANNEL IS A NEGATIVE REGULATOR OF Mdm34p-MEDIATED CELL DEATH

Our laboratory has previously ascribed a protective role for the mitochondrial porin (Por1p) in acetic acid-induced cell death. Cells lacking Por1p were shown to enter an apoptotic-like cell death program earlier than the respective wild-type strain, with significant loss of viability, ROS production, chromatin condensation, DNA fragmentation and loss of plasma membrane integrity (Pereira et al., 2007). Later work would determine that abrogation of the Aac1/2/3 proteins largely increased the resistance of *por1*Δ cells to acetic acid treatment and hypothesized that the mitochondrial porin may act as a negative regulator of Aac1/2/3-mediated cell death (Trindade et al., 2016).

To perform a more in-depth characterization of ERMES-mediated resistance to cell death induced by acetic acid, we engineered a yeast double mutant in order to study the effect of *POR1* deletion in an ERMES-deleted strain. The *mdm34*Δ strain was used in this context since, in our experimental conditions, these cells displayed the highest resistance to acetic acid treatment and could provide better phenotypical differentiation. We generated a *mdm34*Δ *por1*Δ double mutant through homologous recombination of a *POR1::URA3* cassette in a *MDM34::KanMX4* strain. After a thorough selection process of auxotrophy and antibiotic resistance, the selected colonies were subjected to western blot analysis for final assessment of Por1p expression (Figure 19).

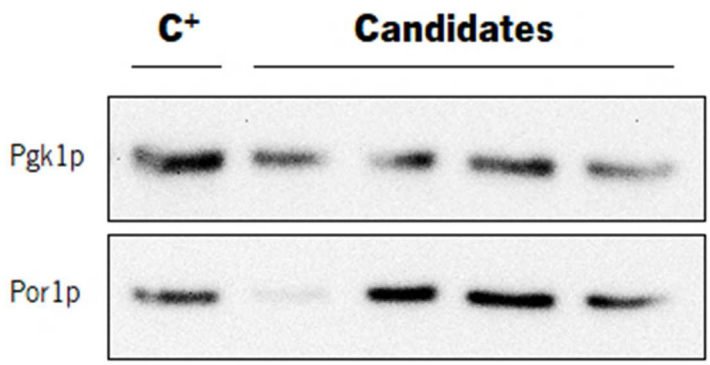

Figure 19. Generation of a *mdm34*Δ *por1*Δ double mutant through homologous recombination. *MDM34*::*KanMX4* cells were transformed with a *POR1*::*URA3* cassette. After selection of transformants by simultaneous growth in SC glucose medium lacking uracil and YEPD medium supplemented with 200 µg/mL geneticin-418, the apparent positive colonies were subjected to western blot analysis for evaluation of the levels of Por1p expression. Phosphoglycerate kinase 1 (Pgk1p) was used as loading control for whole cell extract and BY4741 cells were used as positive control (C^+).

After selecting the positive *mdm34*Δ *por1*Δ clone, we performed a survival assay in order to determine if a *POR1* deletion could alter the resistance phenotype of the *mdm34*Δ strain. With that purpose, we used a wild-type strain along with *por1*Δ, *mdm34*Δ and *mdm34*Δ *por1*Δ deletion mutants (Figure 20).

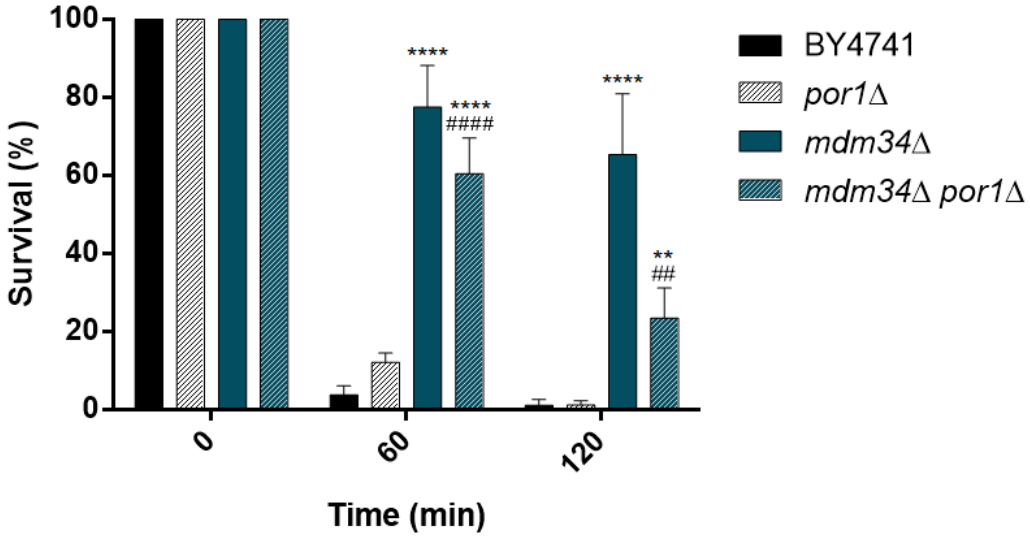

Figure 20. Deletion of *MDM34* enhances cell survival of *por1*Δ cells. Relative cell survival of YEPD-grown exponential phase cells treated with 120 mM acetic acid for 120 minutes. Survival was evaluated by CFU counts on YEPDA plates. Results are expressed as mean ± S.D. of three independent experiments. A two-way ANOVA was performed and multiple comparisons were assessed using Dunnett's post-hoc test. Statistically significance is displayed in comparison to BY4741 (*) or *por1*Δ (#) strains: **/##, $p<0.01$; ****/####, $p<0.0001$.

Our results demonstrate that *mdm34*Δ *por1*Δ cells displayed much higher resistance to acetic acid challenge when compared to wild-type or *por1*Δ strains (Figure 20). As expected, the *mdm34*Δ strain also exhibited a resistance phenotype. Throughout treatment, no significant differences were found between wild-type and *por1*Δ cells, which displayed 1.3 ± 1.1% and 1.2 ± 0.9% after two hours of incubation, respectively. However, by the first hour of treatment the *mdm34*Δ *por1*Δ double mutant revealed an increased resistance to treatment in comparison to the *por1*Δ strain, with survival percentages of 60.5 ± 7.44 vs. 12.1 ± 2.0%, respectively. These differences in clonogenic survival were still visible after 120 minutes although less significant. Altogether, these results suggest a possible role of Por1p in the modulation of Mdm34-mediated cell death.

CHAPTER 5

DISCUSSION

The involvement of ER-MCS in disease has been previously attested in pathologies such as neurodegenerative diseases and cancer (Hedskog et al., 2013; Paillusson et al., 2016; Zampese et al., 2011). Interestingly, these diseases are also characterized by dysregulation of apoptosis. In this context, the possible involvement of ER-MCS in cell death has been the subject of recent interest. While there are some studies linking ER-MCS with mammalian apoptosis, to the extent of our knowledge no experimental data has been put forth evidencing a regulatory role of the ERMES complex in yeast cell death. We have previously shown that acetic acid, a frequent byproduct of alcoholic fermentation of *S. cerevisiae*, is able to induce a mitochondria-dependent apoptotic-like cell death that exhibits several of the morphological and functional alterations of mammalian apoptosis (Ludovico et al., 2002). In the same fashion, acetate was also shown to induce apoptosis in colorectal carcinoma cell lines (Jan et al., 2002). Therefore, unraveling the cell death process induced by acetic acid is of utmost importance, with both biomedical and biotechnological interest.

Previous work from our laboratory has hinted that the ERMES complex could be involved in the modulation of cell death induced by acetic acid (Fernandes, 2013). Nevertheless, this study solely encompassed two of the four known proteins that compose this complex, Mdm10p and Mdm12p, ascribing a delay in the appearance of known apoptotic markers in cells lacking these two proteins. Another study would later unveil the mitochondrial phospholipidic composition of these deletion mutants before and after acetic acid challenge in order to understand if resistance to this stressor was due to the role of ERMES in phospholipid traffic (Afonso, 2016). In this work, we attempted to further characterize the phenotypical traits of ERMES-deficient yeast cells, as well as to uncover if this complex could modulate cell death triggered by acetic acid.

Our initial analysis on clonogenic survival after acetic acid challenge demonstrated that ERMES-deficient yeast cells exhibit a high resistance to this stressor, therefore establishing the baseline for a possible role of these proteins in acetic acid-induced cell death. To ensure that this resistance was not intrinsically acquired upon mutation, we monitored the chronological lifespan of each strain. The results evidenced that ablation of any ERMES component reduced the chronological lifespan of *S. cerevisiae* in a similar manner, evidencing that the phenotypes observed were not due to unspecific resistance. The similar death rate of these strains also hinted that the decrease of survival could be attributed to the loss of a common function, emphasizing that the identical chronological lifespan is probably due to ERMES loss.

There have been reports that ablation of any of the ERMES components leads to the disruption of the whole complex (Kornmann et al., 2009), so it should be borne in mind that by evaluating the phenotype of each deletion mutant we may be ascertaining either a direct or indirect role of the deleted protein, e.g., the role of the protein or the role of the whole complex, respectively. Still, disparities between the phenotypes found for each mutant can account for a direct role in the mediation of cell death, as will be examined throughout this discussion. Indeed, it was interesting that the four deletion mutants did not exhibit similar survival upon acetic acid treatment, as it would be expected if the complex itself was the responsible for resistance. Instead, *mdm34*Δ cells were extremely resistant to acetic acid challenge in glucose media, while *mdm10*Δ and *mdm12*Δ viability was more affected. Even though cell survival of the latter strains was significantly higher in comparison to the wild-type strain, it was still very different from the one displayed by *mdm34*Δ cells after 200 minutes of acetic acid exposure (Two-way ANOVA, Tukey's post-hoc test, $p<0.0001$).

Interestingly, screening assays have reported either loss or recovery of clonogenic survival in yeast strains lacking some ERMES components. Mdm10p deletion was shown to sensitize yeast cells to C2-ceramide but not cisplatin or cadmium dichloride-mediated cell death (Galluzzi et al., 2012). Likewise, *mmm1*Δ and *mdm10*Δ cells displayed some sensitivity to 2,4-dichlorophenol stress (Yadav et al., 2011). However, all ERMES-deficient strains were found to be highly tolerant to Te(IV)-induced toxicity (Ottosson et al., 2010). Thus, it appears that Mdm10p is able to exert both protective and aggravating roles in response to different death stimuli. Our results suggest that this and the other ERMES proteins are required for acetic acid-induced cell death.

In this work, we also assessed the emergence of several death markers of yeast cells undergoing apoptosis. We demonstrated that all ERMES mutants exhibited a delay in loss of plasma membrane integrity, alteration of mitochondrial transmembrane potential, mitochondrial degradation and superoxide anion accumulation. Moreover, we showed that cyt *c* release was impaired in *mdm10*Δ and *mdm34*Δ mutants. Though all mutants displayed a common resistance phenotype, in almost all assays this appeared to be a consequence of a protein-specific function rather than ERMES disruption.

Indeed, the extent of the loss of plasma membrane integrity in *mdm34*Δ cells was very different from that of *mdm10*Δ and *mdm12*Δ (Two-way ANOVA, Tukey's post-hoc test, $p<0.0001$). Furthermore, our analysis using $DiOC_6(3)$ for the assessment of mitochondrial transmembrane potential suggests that *mdm10*Δ and *mdm12*Δ cells follow in the same pattern as the wild-type

strain (even though delayed), whereas *mdm34*Δ mitochondria were unable to hyperpolarize to an equivalent degree after 100 mM acetic acid challenge. It has been documented that upon acetic acid treatment, mitochondria of *S. cerevisiae* W303-1A suffer an initial hyperpolarization followed by depolarization (Ludovico et al., 2002). Additionally, the same phenotype was reported on a BY4741 background using our exact conditions, with *mdm10*Δ and *mdm12*Δ mitochondria slightly hyperpolarizing even though survival was decreased (Fernandes, 2013). To further confirm our results, we evaluated this phenotype using Mitotracker Green as an indicator of mitochondrial mass and Mitotracker Deep Red as a potential-sensitive dye. The results attained with this methodology were in agreement with our previous findings (data not shown).

Our results regarding the accumulation of superoxide anion also revealed significant differences between mutant strains and the respective wild-type, as well as a great disparity between *mdm10*Δ and *mdm34*Δ cells (Two-way ANOVA, Tukey's post-hoc test, $p<0.0001$). Even though this was a great indicator of the overall oxidative status of the cell upon acetic acid treatment, the probe used in this study measures cellular superoxide anion. Considering the mutations in study, we also intend to assess mitochondrial ROS generation by using an organelle-specific superoxide probe, such as MitoSOX Red.

Several studies have reported that ERMES-deficient strains exhibit giant spherical mitochondria (Burgess et al., 1994; Esposito et al., 2011; Sogo & Yaffe, 1994). While in our experiments this phenotype was encountered for *mdm10*Δ and *mdm12*Δ, the same did not occur regarding *mdm34*Δ. Instead, short tubular mitochondria or small punctae were frequently found in this strain, which is in agreement with previous studies (Youngman et al., 2004). Mitochondrial degradation of ERMES-deleted yeast cells was one of the most noteworthy hallmarks studied, with all mutants displaying much higher percentages of GFP-positive cells after 200 minutes of treatment in comparison to the wild-type strain. It could be argued that, due to the altered mitochondrial morphology of ERMES-deficient strains, mitochondrial degradation could somehow be impaired. However, the strain with higher resemblance to the wild-type mitochondrial morphotype, *mdm34*Δ, was actually the one with the higher percentage of GFP-positive cells, suggesting that mitochondrial degradation occurs in a morphology-independent manner in these mutants.

Evaluation of clonogenic survival after acetic acid challenge in galactose media also revealed a resistance phenotype for ERMES-deficient strains. However, the resistance of glucose-repressed

*mdm34*Δ cells was decreased upon treatment in galactose media, though still significantly higher than that of the wild-type strain. Since galactose is a weaker repressor of mitochondrial respiration (Herrero et al., 1985), we hypothesized that this phenotype could be due to a higher respiratory activity. Hence, we conducted survival assays in the presence of an oxidative phosphorylation and an electron transport chain inhibitor, respectively, oligomycin (inhibitor of the F_0 part of the F_0F_1-ATPase) and antimycin A (inhibitor of the cytochrome bc_1 complex). A one-hour pre-incubation period with either inhibitor, or with their respective solvents, did not induce differences in the resistance of *mdm34*Δ to cell death mediated by acetic acid (data not shown). Thus, we concluded that the higher susceptibility to acetic acid of *mdm34*Δ in galactose medium, when compared with glucose medium, was not due to an increased respiration rate.

Cytochrome *c* release from mitochondria during an apoptotic process has been well described in both mammalian and yeast cells (Liu et al., 1996; Ludovico et al., 2002). Accordingly, we followed cyt *c* release after acetic acid challenge. The results showed a high decrease in cyt *c* content in both wild-type and *mdm12*Δ mitochondria, while this phenomenon was severely impaired in *mdm10*Δ and *mdm34*Δ mutants. The fact that cell viability at the time of harvest was approximately equal in all cases assured that in both *mdm10*Δ and *mdm34*Δ cells cyt *c* release was in fact impaired. In order to assure that cyt *c* was release in wild-type and *mdm12*Δ cells was not due to mitochondrial damage during isolation, we measured the activity of the mitochondrial matrix enzyme citrate synthase. By doing so, we would be able to assess the integrity of the IMM during the isolation protocol and exclude protein release due to rupture of the membrane. However, our assays were not reproducible probably due to the low protein concentration and further experiments have to be conducted. Notwithstanding, the above-mentioned results corroborate our initial premise that the ERMES complex, namely its outer mitochondrial membrane components, could be required for MOMP and ensuing cyt *c* release.

During the development of this thesis we also performed a more thorough analysis on the phenotypical traits of ERMES-deleted strains. Since ERMES mutant strains have been described to display characteristic respiratory-deficient features (Day, 2013; Jin et al., 2015; Kornmann et al., 2009; Tan et al., 2013), we evaluated the respiratory capacities of our mutants by assessing their ability to grow on a non-fermentable carbon source. Results revealed that both *mdm10*Δ and *mdm12*Δ strains bore respiratory deficiencies while *mdm34*Δ cells did not. Of note, we did not observe an obvious reduction in colony number. Instead, *mdm10*Δ and *mdm12*Δ colonies

exhibited a predominantly *petite* phenotype, a feature that was also present after growing these strains at restrictive temperature. Since it has been documented that cells lacking the ERMES complex lose mtDNA with a high frequency (Hobbs et al., 2001), we further assessed the rate at which these strains lost their respiratory function. Our results demonstrated that only the *mdm10*Δ strain exhibited a significantly higher rate of *petite* induction in comparison to the wild-type. These results were in line with our previous data on the respiratory ability of the mutant strains. To ensure that these defects are in fact due to mtDNA loss, we will be assessing the presence of mtDNA in colonies scored as respiratory-deficient through 4',6-diamidino-2-phenylindole (DAPI) staining. Given that both *mdm10*Δ and *mdm12*Δ exhibit severely impaired mitochondrial morphology, whereas in *mdm34*Δ this appears to be a moderate phenotype, it seems likely that defects in respiration and growth at restrictive temperature are associated to an abnormal mitochondrial morphotype.

The yeast mitochondrial porin (Por1p) was previously shown to protect yeast cells against acetic acid challenge (Pereira et al., 2007) and to negatively regulate Aac1/2/3-mediated cell death (Trindade et al., 2016). As such, we were interested in disclosing if abrogation of Por1p in an ERMES-deleted strain could revert the *por1*Δ phenotype in the same fashion. Hence, we engineered a *mdm34*Δ *por1*Δ double mutant and assessed cell survival upon acetic acid treatment. The double mutation largely increased the resistance of *por1*Δ cells after one hour of treatment, similarly to the single *mdm34*Δ deletion. However, after 120 minutes the viability of the double mutant was more than halved in comparison to the *mdm34*Δ strain, though still significantly different from the wild-type and *por1*Δ strains. The difference between *mdm34*Δ and *mdm34*Δ *por1*Δ mutants after two hours of treatment (Two-way ANOVA, Tukey's post-hoc test, $p<0.0001$) indicates that double deletion does not appear to have an additive effect on cell viability, therefore unveiling a possible regulatory role of Por1p in Mdm34p-mediated cell death. The phenotype encountered for the double mutant strain hints that Por1p is required for resistance of *mdm34*Δ cells to acetic acid challenge, i.e., Mdm34-driven cell death could be counteracted by Por1p and, as such, Por1p could function as a negative regulator of the cell death process mediated by Mdm34p. In fact, studies have shown genetic interactions between *POR1* and ERMES (Hoppins et al., 2011; Jin et al., 2015) as well as co-immunoprecipitation of both (Murley et al., 2015), which further corroborate our results regarding the interplay between Por1p and Mdm34p in cell death. To ascertain if and how Por1p impairs Mdm34p-mediated cell death, new analysis of apoptotic markers, including detection of cyt *c*, release will be required.

Overall, these results hint that each protein must also exert its functions elsewhere other than ERMES, as described earlier in this thesis (see Chapter 1, subsection 1.3.2.). In fact, we have previously referred to the role of Mdm10p on the sorting and assembly machinery (SAM), a protein complex that mediates the insertion of β-barrel proteins into the outer mitochondrial membrane. The SAM complex and Mdm10p are thought to play a role in the maturation of the TOM complex in the OMM. Interestingly, this complex has been deemed as required for Bax-induced cyt *c* release (Ott et al., 2007), though this subject has been disputed (Szklarz et al., 2007). Thus, ablation of Mdm10p has pleiotropic effects that could be masking the role of ERMES in acetic acid-induced cell death. Looking back, this could also explain the different phenotypes encountered in screening experiments, i.e., the sensitivity shown by Mdm10p to certain stressors could arise from protein import defects. In the future, it would be interesting to follow the strategy used by Yamano and colleagues (2010) and perform site-directed mutagenesis on the carboxy-terminal portion of *MDM10*, that encodes the signaling sequence required for its association with the SAM complex. In this way, we could evaluate the contributions of Mdm10p independently of its association with SAM to the yeast response to acetic acid and therefore infer the true role of Mdm10p in ERMES-driven cell death induced by this stressor.

Genetically engineered strains may engage in synthetic rescue to cope with unfavorable phenotypes. In this regard, ERMES-deficient strains are no different. It has been reported that ERMES mutants lose phenotype over time and develop suppressor mutations (Lang et al., 2015). Such suppressors include the Mdm10p complementary proteins (Mcp) 1, 2 and 3, Sot1p and Vps13p. In all, these suppressing mutations are able to rescue, at least partially, the defective mitochondrial morphotype, growth impairment in non-fermentable carbon sources and at restrictive temperature and mtDNA maintenance (Berger et al., 1997; Lang et al., 2015; Sinzel et al., 2016; Tan et al, 2013). However, it seems somewhat unlikely that these suppressor mutations have occurred in these strains considering that growth impairment at restrictive temperature and mitochondrial morphology defects were visible, except in *mdm34*Δ cells. Furthermore, under our experimental conditions mitochondrial morphology does not appear to contribute for the resistance to acetic acid, since *mdm34*Δ mitochondria exhibit an intermediate phenotype between wild-type and *mdm10*Δ or *mdm12*Δ while displaying much higher resistance than the other strains. Notwithstanding, screening for the activation of suppressor mutations would surely clarify these assumptions.

At a protein level, all ERMES components were found to be required for cell death, displaying a similar survival phenotype after treatment with acetic acid in galactose media. Of note, absence of Mdm10p and Mdm34p severely impaired cyt *c* release from mitochondria whereas Mdm12p ablation did not. These findings came to corroborate our initial hypothesis that OMM-anchored ERMES proteins are required for cyt *c* release. In light of this, while Mdm12p does not appear to be important for the onset of MOMP, it is likely that the resistance shown stems from disruption of ERMES function.

Mitochondrial degradation appeared to be significantly impaired in these mutants. Thus, it appears that although ERMES mutants are able to resist acetic acid challenge in different degrees, the similar mitochondrial degradation profile indicates a possible role of the whole complex in this process. Pep4p, a vacuole protease that is released from the vacuole to the cytosol upon acetic acid treatment, is thought to mediate the mitochondrial degradation process (Pereira et al., 2010). In this line, we will assess whether Pep4p is released from the vacuole and mediates mitochondrial degradation in ERMES-deficient yeast cells after acetic acid challenge. If so, by measuring Pep4p cytosolic activity we will surely provide complementary data that could further enlighten the role of ERMES in mitochondrial degradation.

Ascribed functions of ERMES encompass phospholipid and calcium traffic between the ER and the OMM, roles that have been previously detailed in this thesis (see Chapter 1, subsection 1.3.3). Calcium is a known signaling molecule of cell death in metazoans, where it is mobilized from the ER to mitochondria through ER-MCS (De Stefani et al., 2011; Giacomello et al., 2007). Likewise, phospholipids such as PS and CL have already been implicated in both mammalian and yeast apoptosis (Li et al., 2015; Madeo et al., 1997; Segawa & Nagata, 2015). Thus, it is possible that these functions could modulate the yeast response to acetic acid and, at least in part, explain the acquired resistance of all mutants. Accordingly, in the final stage of this thesis the isolated mitochondrial samples from untreated ERMES-deficient strains were sent for phospholipid analysis at the University of Aveiro (Aveiro, Portugal). By unraveling the phospholipidic profile of mitochondrial membranes, we hope to further characterize these strains and perhaps connect these phenotypes with a possible involvement of the lipid function of ERMES in cell death. Moreover, Mdm12p has been proposed to mediate phospholipid transfer by connecting Mmm1p dimers in the ER to Mdm34p in the OMM (Jeong, Park, & Lee, 2016). Considering that Mdm10p does not seem to possess lipid-binding domains (Jeong et al., 2016), the similar survival phenotype of Mdm10p and Mdm12p could stem from different aspects, namely protein import defects and

impaired lipid exchange, respectively. Notwithstanding, in the future we also intend to assess the role of both cytosolic and mitochondrial calcium levels in the mediation of cell death in these mutants.

Acetic acid has been very recently shown to induce ER stress and activation of the unfolded protein response (Kawazoe et al., 2017). When this pathway fails to prevent the cell from coping with the stressor, apoptosis is induced. Since ERMES is responsible for connecting the ER to mitochondria, it is possible that the resistance shown by the mutants could arise from an ineffective signaling from ER to mitochondria. As such, the involvement of ERMES in mitochondrial dysfunctions and subsequent apoptosis induced by acetic acid-mediated ER stress should also be assessed in the future.

Considering that other ER-MCS have more recently been found in yeast (see Chapter 1, subsection 1.3.2), it would also be of great use to explore if their abrogation interferes in cell death mediated by acetic acid. Moreover, since EMC also exhibits lipid exchange properties, we would further infer with more certainty a role of phospholipid traffic in this process. Given that interorganellar communication appears to have a major role in apoptosis, other contact sites pertaining mitochondria and other organelles should also be evaluated. Specifically, studying vacuole- and peroxisome-mitochondria contact sites should bring about new insights on the magnitude of cross-talk between interorganelle communication and apoptosis. The vCLAMP has already been established as an alternative complex for the traffic of mitochondrial lipids in the absence of ERMES (Elbaz-Alon et al., 2014). Likewise, Pex11 was found to provide the connection between peroxisomes and mitochondria through the ERMES complex (Cohen et al., 2014; Ušaj et al., 2015). Thus, it is possible that an intricate interorganelle signaling network that goes beyond ER-mitochondria contacts could actively participate in cell death.

Apart from other possible functions, above all ERMES is a tethering complex. Even though EMC is proposed to tether the ER to mitochondria through its interaction with Tom5, ablation of either EMC or ERMES leads to a similar decrease in ER-mitochondria association (Lahiri et al., 2014). In turn, dismantling these contacts alters the structure of mitochondria, resulting in the abnormal mitochondrial morphotype of ERMES mutants (Kornmann et al., 2009). Thus, studies where an artificial tether is used will bring about new insights on how the loss of ER-mitochondria tethering could impact cell death, as well as pinpoint the importance of ERMES-mediated signaling in this process.

In summary, herein we report experimental evidence for a role of the ERMES complex in the intricate signaling network that decides life or death. Through the use of single deletion mutants, we were able to determine a delay in several apoptotic hallmarks such as loss of plasma membrane integrity, mitochondrial transmembrane polarization status, mitochondrial degradation and accumulation of superoxide anion. Flow cytometry analysis revealed itself to be a valuable tool in this context. We have also demonstrated that cytochrome *c* release from mitochondria is impaired in cells lacking either Mdm10p or Mdm34p. Considering that these two proteins are embedded in the outer mitochondrial membrane, we propose a role for these proteins in the molecular machinery that promotes mitochondrial outer membrane permeabilization and ensuing cytochrome *c* release. Additionally, our preliminary analysis revealed that resistance mediated by Mdm34p deficiency appears to be dependent on the mitochondrial porin (Por1p), which acts as a negative regulator.

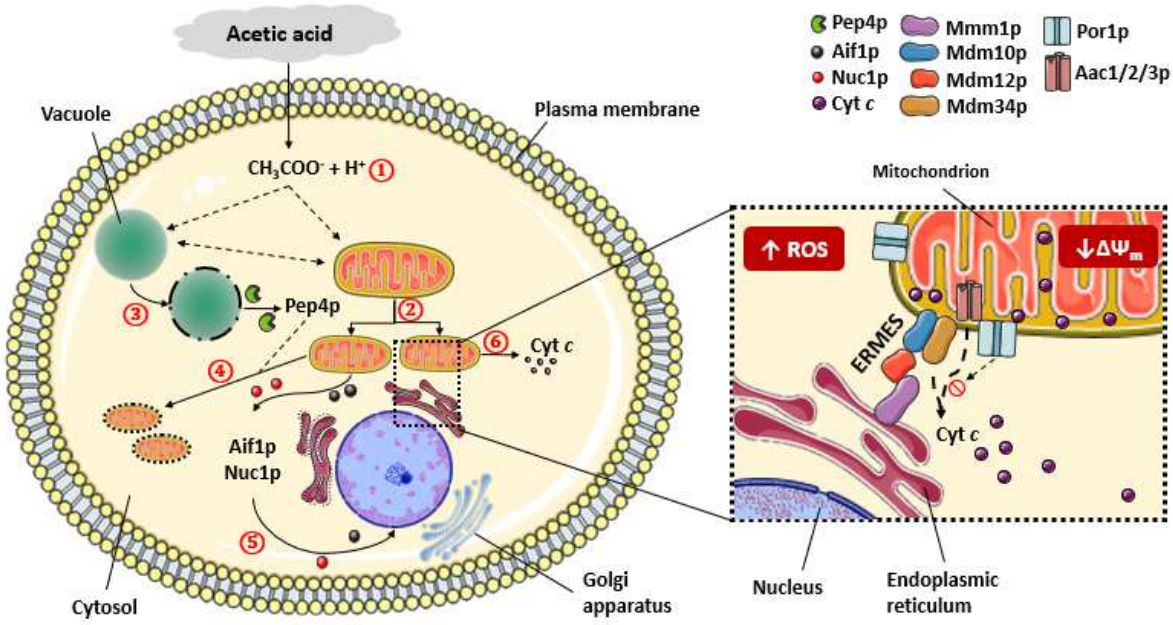

Figure 21. Current working model of death effectors involved in acetic acid-induced cell death of *Saccharomyces cerevisiae*. Acetic acid enters glucose-repressed cells by simple diffusion. Once in the cytosol, this weak acid dissociates. **(1)** If the intracellular pH is higher than the extracellular pH, acetate ions accumulate leading to acidification of the cytosol. **(2)** Mitochondrial fragmentation is an early event in apoptosis. **(3)** Acetate induces partial vacuolar permeabilization and the release of hydrolases to the cytosol. **(4)** Pep4p is thought to mediate mitochondrial degradation. **(5)** After mitochondrial outer membrane permeabilizaton (MOMP), pro-apoptotic effectors are released to the cytosol. Aif1p and Nuc1p are thereupon translocated to the nucleus where they mediate DNA fragmentation. **(6)** MOMP also promotes the release of cytochrome *c* (cyt *c*) to the cytosol. *Close-up:* Acetic acid triggers an increase of ROS accumulation in the cytosol as well as a decrease in mitochondrial transmembrane potential ($\Delta\Psi_m$). Cyt *c* release appears to be mediated by the ERMES complex and Aac1/2/3 proteins, while Por1p seems to function as a negative regulator of this process. Dashed lines represent putative mechanisms or processes that are not yet fully disclosed.

CHAPTER 6

CONCLUDING REMARKS AND FUTURE PERSPECTIVES

In this thesis, we aimed to dissect the role of ER-mitochondria contact sites (ER-MCS) in mitochondrial outer membrane permeabilization and acetic acid-induced cell death. We have previously shown that acetic acid is able to induce a mitochondria-dependent cell death process in *Saccharomyces cerevisiae*, a unicellular organism in which the apoptotic program appears to be conserved (Ludovico et al., 2002). In mammals, dysregulation of apoptosis has curiously been linked to several pathologies where disrupted ER-MCS have also been reported, such as cancer and neurodegenerative diseases (van Vliet, Verfaillie & Agostinis, 2014). Thus, we used yeast as a model system to infer how cell death induced by acetic acid is impacted by absence of the (until recently) only known ER-mitochondria tethering complex, the ER-mitochondria encounter structure (ERMES).

Resorting to techniques ranging from standard plate counts to flow cytometry, our results place ERMES as a regulator of acetic acid-induced cell death. Coupled to enhanced cell survival, null mutants revealed a late emergence of all studied apoptotic markers. Moreover, we found that not only the complex itself but also its individual subunits can mediate the cell process in different fashions. Notably, herein we demonstrated for the first time that ERMES actively participates in mitochondrial outer membrane permeabilization. Preliminary analysis also hinted that the mitochondrial porin appears to act as a negative regulator of ERMES-mediated cell death. As such, we propose that mitochondria outer membrane permeabilization and ensuing cytochrome *c* release are, at least partially, dependent on the ERMES complex in acetic acid-treated yeast.

With this work, we hope to lift the veil behind the molecular machinery that promotes mitochondrial outer membrane permeabilization in yeast. Whether this is due to the ERMES complex or the proteins themselves is still to be fully ascertained. However, our results so far suggest that both play a significant role in cell death. These results are also expected to encourage the study of ER-MCS on regulated cell death in mammals. Unraveling the role of these structures would be of great impact considering the link between disrupted ER-MCS and apoptosis in many pathologies. Evaluation of the mechanisms that control the impacted phenotypes herein reported, as well as others not yet disclosed, will aid to understand the cross-talk between ER-MCS and disease. We strive to continue in this line of research and to further explore the role of these structures in cell fate. Specifically, assessment of ERMES function and cross-talk with other interorganelle contact sites will help to understand how ERMES signaling can impact the survival outcome.

CHAPTER 7

REFERENCES

Acehan, D., Jiang, X., Morgan, D. G., Heuser, J. E., Wang, X., & Akey, C. W. (2002). Three-dimensional structure of the apoptosome: implications for assembly, procaspase-9 binding, and activation. *Molecular Cell, 9*(2), 423-432. DOI: 10.1016/S1097-2765(02)00442-2

Afonso, C. B. (2016). The role of endoplasmic reticulum-mitochondria contact sites and mitochondrial phospholipid composition in *Saccharomyces cerevisiae* acetic acid-induced apoptosis (Master Dissertation).

Alavian, K. N., Beutner, G., Lazrove, E., Sacchetti, S., Park, H. A., Licznerski, P., ... & Porter, G. A. (2014). An uncoupling channel within the c-subunit ring of the F1FO ATP synthase is the mitochondrial permeability transition pore. *Proceedings of the National Academy of Sciences*, *111*(29), 10580-10585. DOI: 10.1073/pnas.1401591111

Alberts, B., Johnson, A., Lewis, J., Raff, M., Roberts, K., & Walter, P. (2002). Programmed Cell Death. In B. Alberts (Ed), *Molecular Biology of the Cell*, (4th Edition, Chap. 17, pp. 2563-2575). New York, NY: Garland Science.

Almeida, B., Ohlmeier, S., Almeida, A. J., Madeo, F., Leão, C., Rodrigues, F., & Ludovico, P. (2009). Yeast protein expression profile during acetic acid-induced apoptosis indicates causal involvement of the TOR pathway. *Proteomics, 9*(3), 720-732. DOI: 10.1002/pmic.200700816

Baines, C. P., Kaiser, R. A., Purcell, N. H., Blair, N. S., Osinska, H., Hambleton, M. A., ... & Robbins, J. (2005). Loss of cyclophilin D reveals a critical role for mitochondrial permeability transition in cell death. *Nature*, *434*(7033), 658-662. DOI: 10.1038/nature03434

Baines, C. P., Kaiser, R. A., Sheiko, T., Craigen, W. J., & Molkentin, J. D. (2007). Voltage-dependent anion channels are dispensable for mitochondrial-dependent cell death. *Nature Cell Biology*, *9*(5), 550-555. DOI: 10.1038/ncb1575

Berger, K. H., Sogo, L. F., & Yaffe, M. P. (1997). Mdm12p, a component required for mitochondrial inheritance that is conserved between budding and fission yeast. *Journal of Cell Biology*, *136*(3), 545-553. DOI: 10.1083/jcb.136.3.545

Boehning, D., Van Rossum, D. B., Patterson, R. L., & Snyder, S. H. (2005). A peptide inhibitor of cytochrome c/inositol 1, 4, 5-trisphosphate receptor binding blocks intrinsic and extrinsic cell death pathways. *Proceedings of the National Academy of Sciences of the United States of America, 102*(5), 1466-1471. DOI: 10.1073/pnas.0409650102

Boldogh, I., Vojtov, N., Karmon, S., & Pon, L. A. (1998). Interaction between mitochondria and the actin cytoskeleton in budding yeast requires two integral mitochondrial outer membrane proteins, Mmm1p and Mdm10p. *The Journal of Cell Biology*, *141*(6), 1371-1381. DOI: 1010.1083/jcb.141.6.1371

Boldogh, I. R., Nowakowski, D. W., Yang, H. C., Chung, H., Karmon, S., Royes, P., & Pon, L. A. (2003). A protein complex containing Mdm10p, Mdm12p, and Mmm1p links mitochondrial

membranes and DNA to the cytoskeleton-based segregation machinery. *Molecular Biology of the Cell*, *14*(11), 4618-4627. DOI: 10.1091/mbc.E03-04-0225

Bonora, M., Bononi, A., De Marchi, E., Giorgi, C., Lebiedzinska, M., Marchi, S., ... & Wieckowski, M. R. (2013). Role of the c subunit of the FO ATP synthase in mitochondrial permeability transition. *Cell Cycle*, *12*(4), 674-683. DOI: 10.4161/cc.23599

Böckler, S., & Westermann, B. (2014). Mitochondrial ER contacts are crucial for mitophagy in yeast. *Developmental Cell, 28*(4), 450-458. DOI: 10.1016/j.devcel.2014.01.012

Brachmann, C. B., Davies, A., Cost, G. J., Caputo, E., Li, J., Hieter, P., & Boeke, J. D. (1998). Designer deletion strains derived from *Saccharomyces cerevisiae* S288C: a useful set of strains and plasmids for PCR-mediated gene disruption and other applications. *Yeast - Chichester*, *14*(2), 115-132. DOI: 10.1002/(SICI)1097-0061(19980130)14:2<115::AID-YEA204>3.0.CO;2-2

Bradford, M. M. (1976). A rapid and sensitive method for the quantitation of microgram quantities of protein utilizing the principle of protein-dye binding. *Analytical Biochemistry*, *72*(1-2), 248-254. DOI: 10.1016/0003-2697(76)90527-3

Budihardjo, I., Oliver, H., Lutter, M., Luo, X., & Wang, X. (1999). Biochemical pathways of caspase activation during apoptosis. *Annual Review of Cell and Developmental Biology, 15*(1), 269-290. DOI: 10.1146/annurev.cellbio.15.1.269

Burgess, S. M., Delannoy, M., & Jensen, R. E. (1994). MMM1 encodes a mitochondrial outer membrane protein essential for establishing and maintaining the structure of yeast mitochondria. *The Journal of Cell Biology*, *126*(6), 1375-1391. DOI: 10.1083/jcb.126.6.1375

Büttner, S., Eisenberg, T., Herker, E., Carmona-Gutierrez, D., Kroemer, G., & Madeo, F. (2006). Why yeast cells can undergo apoptosis: death in times of peace, love, and war. *Journal of Cell Biology*, *175*(4), 521-525. DOI: 10.1083/jcb.200608098

Büttner, S., Eisenberg, T., Carmona-Gutierrez, D., Ruli, D., Knauer, H., Ruckenstuhl, C., ... & Sigrist, S. (2007). Endonuclease G regulates budding yeast life and death. *Molecular Cell, 25*(2), 233-246. DOI: 10.1083/jcb.200608098

Büttner, S., Ruli, D., Vögtle, F. N., Galluzzi, L., Moitzi, B., Eisenberg, T., ... & Madeo, F. (2011). A yeast BH3-only protein mediates the mitochondrial pathway of apoptosis. *The EMBO Journal, 30*(14), 2779-2792. DOI: 10.1038/emboj.2011.197

Carmelo, V., Santos, H., & Sá-Correia, I. (1997). Effect of extracellular acidification on the activity of plasma membrane ATPase and on the cytosolic and vacuolar pH of *Saccharomyces cerevisiae*. *Biochimica et Biophysica Acta (BBA)-Biomembranes, 1325*(1), 63-70. DOI: 10.1016/S0005-2736(96)00245-3

Carmona-Gutierrez, D., Eisenberg, T., Büttner, S., Meisinger, C., Kroemer, G., & Madeo, F. (2010). Apoptosis in yeast: triggers, pathways, subroutines. *Cell Death & Differentiation, 17*(5), 763-773. DOI: 10.1038/cdd.2009.219

Carmona-Gutierrez, D., Bauer, M. A., Zimmermann, A., Aguilera, A., Austriaco, N., Ayscough, K., ... & Blondel, M. (2018). Guidelines and recommendations on yeast cell death nomenclature. *Microbial Cell, 5*(1), 4-31. DOI: 10.15698/mic2018.01.607

Carraro, M., & Bernardi, P. (2016). Calcium and reactive oxygen species in regulation of the mitochondrial permeability transition and of programmed cell death in yeast. *Cell Calcium, 60*(2), 102-107. DOI: 10.1016/j.ceca.2016.03.005

Casal, M., Cardoso, H., & Leão, C. (1998). Effects of ethanol and other alkanols on transport of acetic acid in *Saccharomyces cerevisiae*. *Applied and Environmental Microbiology, 64*(2), 665-668. DOI: 10.1099/13500872-142-6-1385

Cohen, Y., Klug, Y. A., Dimitrov, L., Erez, Z., Chuartzman, S. G., Elinger, D., ... & Schekman, R. (2014). Peroxisomes are juxtaposed to strategic sites on mitochondria. *Molecular BioSystems, 10*(7), 1742-1748. DOI: 10.1039/c4mb00001c

Copeland, D. E., & Dalton, A. J. (1959). An association between mitochondria and the endoplasmic reticulum in cells of the pseudobranch gland of a teleost. *The Journal of biophysical and biochemical cytology*, *5*(3), 393-396. DOI: 10.1083/jcb.5.3.393

Cosentino, K., & García-Sáez, A. J. (2014). Mitochondrial alterations in apoptosis. *Chemistry and Physics of Lipids, 181*, 62-75. DOI: 10.1016/j.chemphyslip.2014.04.001

Csordás, G., Várnai, P., Golenár, T., Roy, S., Purkins, G., Schneider, T. G., ... & Hajnóczky, G. (2010). Imaging interorganelle contacts and local calcium dynamics at the ER-mitochondrial interface. *Molecular Cell, 39*(1), 121-132. DOI: 10.1016/j.molcel.2010.06.029

Cui, Y., Zhao, S., Wu, Z., Dai, P., & Zhou, B. (2012). Mitochondrial release of the NADH dehydrogenase Ndi1 induces apoptosis in yeast. *Molecular Biology of the Cell, 23*(22), 4373-4382. DOI: 10.1091/mbc.E12-04-0281

Czabotar, P. E., Lee, E. F., Thompson, G. V., Wardak, A. Z., Fairlie, W. D., & Colman, P. M. (2011). Mutation to Bax beyond the BH3 domain disrupts interactions with pro-survival proteins and promotes apoptosis. *Journal of Biological Chemistry, 286*(9), 7123-7131. DOI: 10.1074/jbc.M110.161281

Day, M. (2013). Yeast petites and small colony variants: for everything there is a season. In Geoffrey Gadds and Sima Sariaslani (Eds), *Advances in Applied Microbiology* (1st edition, v. 85, pp. 1-41). Academic Press.

de Brito, O. M., & Scorrano, L. (2008). Mitofusin 2 tethers endoplasmic reticulum to mitochondria. *Nature*, *456*(7222), 605. DOI: 10.1038/nature07534

de Brito, O. M., & Scorrano, L. (2010). An intimate liaison: spatial organization of the endoplasmic reticulum–mitochondria relationship. *The EMBO Journal, 29*(16), 2715-2723. DOI: 10.1038/emboj.2010.177

De Stefani, D., Raffaello, A., Teardo, E., Szabò, I., & Rizzuto, R. (2011). A forty-kilodalton protein of the inner membrane is the mitochondrial calcium uniporter. *Nature, 476*(7360), 336-340. DOI: 10.1038/nature10230

Dejean, L. M., Martinez-Caballero, S., Manon, S., & Kinnally, K. W. (2006). Regulation of the mitochondrial apoptosis-induced channel, MAC, by BCL-2 family proteins. *Biochimica et Biophysica Acta (BBA) - Molecular Basis of Disease, 1762*(2), 191-201. DOI: 10.1016/j.bbadis.2005.07.002

Dejean, L. M., Ryu, S. Y., Martinez-Caballero, S., Teijido, O., Peixoto, P. M., & Kinnally, K. W. (2010). MAC and Bcl-2 family proteins conspire in a deadly plot. *Biochimica et Biophysica Acta (BBA) - Bioenergetics, 1797*(6), 1231-1238. DOI: 10.1016/j.bbabio.2010.01.007

Desagher, S., Osen-Sand, A., Nichols, A., Eskes, R., Montessuit, S., Lauper, S., ... & Martinou, J. C. (1999). Bid-induced conformational change of Bax is responsible for mitochondrial cytochrome c release during apoptosis. *The Journal of Cell Biology, 144*(5), 891-901. DOI: 10.1083/jcb.144.5.891

Dewson, G., & Kluck, R. M. (2009). Mechanisms by which Bak and Bax permeabilise mitochondria during apoptosis. *Journal of Cell Science, 122*(16), 2801-2808. DOI: 10.1242/jcs.038166

Doczi, J., Torocsik, B., Echaniz-Laguna, A., De Camaret, B. M., Starkov, A., Starkova, N., ... & Adam-Vizi, V. (2016). Alterations in voltage-sensing of the mitochondrial permeability transition pore in ANT1-deficient cells. *Scientific reports*, *6*. DOI: 10.1038/srep26700

Eble, K. S., Coleman, W. B., Hantgan, R. R., & Cunningham, C. C. (1990). Tightly associated cardiolipin in the bovine heart mitochondrial ATP synthase as analyzed by 31P nuclear magnetic resonance spectroscopy. *Journal of Biological Chemistry, 265*(32), 19434-19440. Retrieved from http://www.jbc.org/content/265/32/19434

Elbaz-Alon, Y., Rosenfeld-Gur, E., Shinder, V., Futerman, A. H., Geiger, T., & Schuldiner, M. (2014). A dynamic interface between vacuoles and mitochondria in yeast. *Developmental Cell, 30*(1), 95-102. DOI: 10.1016/j.devcel.2014.06.007

Elmore, S. (2007). Apoptosis: A Review of Programmed Cell Death. *Toxicologic Pathology, 35*(4), 495-516. DOI: 10.1080/01926230701320337

Erasmus, D. J., Cliff, M., & van Vuuren, H. J. (2004). Impact of yeast strain on the production of acetic acid, glycerol, and the sensory attributes of icewine. *American Journal of Enology and Viticulture, 55*(4), 371-378. Retrieved from http://www.ajevonline.org/content/55/4/371

Esposito, M., Piatti, S., Hofmann, L., Frontali, L., Delahodde, A., & Rinaldi, T. (2011). Analysis of the rpn11-m1 proteasomal mutant reveals connection between cell cycle and mitochondrial biogenesis. *FEMS Yeast Research, 11*(1), 60-71. DOI: 10.1111/j.1567-1364.2010.00690.x

Fadok, V. A., Bratton, D. L., Frasch, S. C., Warner, M. L., & Henson, P. M. (1998). The role of phosphatidylserine in recognition of apoptotic cells by phagocytes. *Cell Death & Differentiation, 5*(7), 551-562. DOI: 10.1038/sj.cdd.4400404

Fahrenkrog, B., Sauder, U., & Aebi, U. (2004). The *S. cerevisiae* HtrA-like protein Nma111p is a nuclear serine protease that mediates yeast apoptosis. *Journal of Cell Science, 117*(1), 115-126. DOI: 10.1242/jcs.00848

Fannjiang, Y., Cheng, W. C., Lee, S. J., Qi, B., Pevsner, J., McCaffery, J. M., ... & Hardwick, J. M. (2004). Mitochondrial fission proteins regulate programmed cell death in yeast. *Genes & Development*, *18*(22), 2785-2797. DOI: 10.1101/gad.1247904

Fernandes, T. R. (2013). The role of phospholipids and of the actin-binding protein cofilin in *Saccharomyces cerevisiae* acetic acid-induced apoptosis (Master Dissertation).

Ferro, S., Azevedo-Silva, J., Casal, M., Côrte-Real, M., Baltazar, F., & Preto, A. (2016). Characterization of acetate transport in colorectal cancer cells and potential therapeutic implications. *Oncotarget*, *7*(43), 70639. DOI: 10.18632/oncotarget.12156

Fleury, C., Pampin, M., Tarze, A., & Mignotte, B. (2002). Yeast as a model to study apoptosis?. *Bioscience Reports, 22*(1), 59-79. DOI: 10.1023/A:1016013123094

Foury, F. (1997). Human genetic diseases: a cross-talk between man and yeast. *Gene, 195*(1), 1-10. DOI: 10.1016/S0378-1119(97)00140-6

Friedman, J. R., Lackner, L. L., West, M., DiBenedetto, J. R., Nunnari, J., & Voeltz, G. K. (2011). ER tubules mark sites of mitochondrial division. *Science, 334*(6054), 358-362. DOI: 10.1126/science.1207385

Fulda, S., Galluzzi, L., & Kroemer, G. (2010). Targeting mitochondria for cancer therapy. *Nature reviews Drug discovery*, *9*(6), 447. DOI: 10.1038/nrd3137

Galluzzi, L., Bravo-San Pedro, J. M., Vitale, I., Aaronson, S. A., Abrams, J. M., Adam, D., ... & Jost, P. J. (2014). Essential versus accessory aspects of cell death: recommendations of the NCCD 2015. *Cell Death & Differentiation*, *22*(1), 58-73. DOI: 10.1038/cdd.2014.137

Galluzzi, L., Vitale, I., Senovilla, L., Eisenberg, T., Carmona-Gutiérrez, D., Vacchelli, E., ... & Servant, N. (2012). Independent transcriptional reprogramming and apoptosis induction by cisplatin. *Cell Cycle*, *11*(18), 3472-3480. DOI: 10.4161/cc.21789

García-Rodríguez, L. J., Crider, D. G., Gay, A. C., Salanueva, I. J., Boldogh, I. R., & Pon, L. A. (2009). Mitochondrial inheritance is required for MEN-regulated cytokinesis in budding yeast. *Current Biology*, *19*(20), 1730-1735. DOI: 10.1016/j.cub.2009.08.041

Gietz, R. D., & Woods, R. A. (2006). Yeast transformation by the LiAc/SS Carrier DNA/PEG method. *Methods in Molecular Biology (Clifton, NJ), 313*, 107-120. DOI: 10.1385/1-59259-958-3:107

Giorgio, V., Von Stockum, S., Antoniel, M., Fabbro, A., Fogolari, F., Forte, M., ... & Lippe, G. (2013). Dimers of mitochondrial ATP synthase form the permeability transition pore. *Proceedings of the National Academy of Sciences*, *110*(15), 5887-5892. DOI: 10.1073/pnas.1217823110

Ghibelli, L., & Diederich, M. (2010). Multistep and multitask Bax activation. *Mitochondrion*, *10*(6), 604-613. DOI: 10.1016/j.mito.2010.08.003

Giacomello, M., Drago, I., Pizzo, P., & Pozzan, T. (2007). Mitochondrial Ca^{2+} as a key regulator of cell life and death. *Cell Death & Differentiation, 14*(7), 1267-1274. DOI: 10.1038/sj.cdd.4402147

Giannattasio, S., Guaragnella, N., Côrte-Real, M., Passarella, S., & Marra, E. (2005). Acid stress adaptation protects *Saccharomyces cerevisiae* from acetic acid-induced programmed cell death. *Gene*, *354*, 93-98. DOI: 10.1016/j.gene.2005.03.030

Gomez, B., & Robinson, N. C. (1999). Phospholipase digestion of bound cardiolipin reversibly inactivates bovine cytochrome bc 1. *Biochemistry, 38*(28), 9031-9038. DOI: 10.1021/bi990603r

Guaragnella, N., Antonacci, L., Passarella, S., Marra, E., & Giannattasio, S. (2011). Achievements and perspectives in yeast acetic acid-induced programmed cell death pathways. *Biochemical Society Transactions, 39*(5), 1538-1544. DOI: 10.1042/BST0391538

Guaragnella, N., Pereira, C., Sousa, M. J., Antonacci, L., Passarella, S., Côrte-Real, M., ... & Giannattasio, S. (2006). YCA1 participates in the acetic acid induced yeast programmed cell death also in a manner unrelated to its caspase-like activity. *FEBS Letters*, *580*(30), 6880-6884. DOI: 10.1016/j.febslet.2006.11.050

Halestrap, A. P., & Davidson, A. M. (1990). Inhibition of Ca2+-induced large-amplitude swelling of liver and heart mitochondria by cyclosporin is probably caused by the inhibitor binding to mitochondrial-matrix peptidyl-prolyl cis-trans isomerase and preventing it interacting with the adenine nucleotide translocase. *Biochemical Journal, 268*(1), 153-160. DOI: 10.1042/bj2680153

Halestrap, A. P., McStay, G. P., Clarke, S. J. (2002). The permeability transition pore complex: another view. *Biochimie, 84*(2-3), 153-156. DOI: 10.1016/S0300-9084(02)01375-5

Halestrap, A. P. (2009). What is the mitochondrial permeability transition pore?. *Journal of Molecular and Cellular Cardiology*, *46*(6), 821-831. DOI: 10.1016/j.yjmcc.2009.02.021

Hanekamp, T., Thorsness, M. K., Rebbapragada, I., Fisher, E. M., Seebart, C., Darland, M. R., ... & Thorsness, P. E. (2002). Maintenance of mitochondrial morphology is linked to maintenance of the mitochondrial genome in *Saccharomyces cerevisiae*. *Genetics, 162*(3), 1147-1156. Retrieved from http://www.genetics.org/content/162/3/1147

He, J., Ford, H. C., Carroll, J., Ding, S., Fearnley, I. M., & Walker, J. E. (2017). Persistence of the mitochondrial permeability transition in the absence of subunit c of human ATP

synthase. *Proceedings of the National Academy of Sciences*, *114*(13), 3409-3414. DOI: 10.1073/pnas.1702357114

Hedskog, L., Pinho, C. M., Filadi, R., Rönnbäck, A., Hertwig, L., Wiehager, B., ... & Graff, C. (2013). Modulation of the endoplasmic reticulum–mitochondria interface in Alzheimer's disease and related models. *Proceedings of the National Academy of Sciences, 110*(19), 7916-7921. DOI: 10.1073/pnas.1300677110

Herrero, P., Fernández, R., & Moreno, F. (1985). Differential sensitivities to glucose and galactose repression of gluconeogenic and respiratory enzymes from *Saccharomyces cerevisiae*. *Archives of Microbiology*, *143*(3), 216-219. DOI: 10.1007/BF00411238

Hobbs, A. E. A., Srinivasan, M., McCaffery, J. M., & Jensen, R. E. (2001). Mmm1p, a mitochondrial outer membrane protein, is connected to mitochondrial DNA (mtDNA) nucleoids and required for mtDNA stability. *The Journal of Cell Biology*, *152*(2), 401-410. DOI: 10.1083/jcb.152.2.401

Hoppins, S., Collins, S. R., Cassidy-Stone, A., Hummel, E., DeVay, R. M., Lackner, L. L., ... & Nunnari, J. (2011). A mitochondrial-focused genetic interaction map reveals a scaffold-like complex required for inner membrane organization in mitochondria. *Journal of Cell Biology*, *195*(2), 323-340. DOI: 10.1083/jcb.201107053

Jan, G. B. A. S., Belzacq, A. S., Haouzi, D., Rouault, A., Metivier, D., Kroemer, G., & Brenner, C. (2002). Propionibacteria induce apoptosis of colorectal carcinoma cells via short-chain fatty acids acting on mitochondria. *Cell Death and Differentiation*, *9*(2), 179. DOI: 10.1038/sj.cdd.4400935

Jeong, H., Park, J., & Lee, C. (2016). Crystal structure of Mdm12 reveals the architecture and dynamic organization of the ERMES complex. *EMBO reports*, *17*(12), 1857-1871. DOI: 10.15252/embr.201642706

Jin, K., Musso, G., Vlasblom, J., Jessulat, M., Deineko, V., Negroni, J., ... & Minic, Z. (2015). Yeast mitochondrial protein–protein interactions reveal diverse complexes and disease-relevant functional relationships. *Journal of Proteome Research*, *14*(2), 1220-1237. DOI: 10.1021/pr501148q

Jung, D. W., Bradshaw, P. C., & Pfeiffer, D. R. (1997). Properties of a cyclosporin-insensitive permeability transition pore in yeast mitochondria. *Journal of Biological Chemistry, 272*(34), 21104-21112. DOI: 10.1074/jbc.272.34.21104

Kawazoe, N., Kimata, Y., & Izawa, S. (2017). Acetic Acid Causes Endoplasmic Reticulum Stress and Induces the Unfolded Protein Response in *Saccharomyces cerevisiae*. *Frontiers in Microbiology*, *8*, 1192. DOI: 10.3389/fmicb.2017.01192

Kayikci, Ö., & Nielsen, J. (2015). Glucose repression in *Saccharomyces cerevisiae*. *FEMS Yeast Research*, *15*(6). DOI: 10.1093/femsyr/fov068

Kerr, J. F., Wyllie, A. H., & Currie, A. R. (1972). Apoptosis: a basic biological phenomenon with wide-ranging implications in tissue kinetics. *British Journal of Cancer, 26*(4), 239-257. DOI: 10.1038/bjc.1972.33

Kinnally, K. W. & Antonsson, B. (2007). A tale of two mitochondrial channels, MAC and PTP, in apoptosis. *Apoptosis: An International Journal of Programmed Cell Death, 12*(5), 857-868. DOI: 10.1007/s10495-007-0722-z

Kokoszka, J. E., Waymire, K. G., Levy, S. E., Sligh, J. E., Cai, J., Jones, D. P., ... & Wallace, D. C. (2004). The ADP/ATP translocator is not essential for the mitochondrial permeability transition pore. *Nature, 427*(6973), 461-465. DOI: 10.1038/nature02229

Kopec, K. O., Alva, V., & Lupas, A. N. (2010). Homology of SMP domains to the TULIP superfamily of lipid-binding proteins provides a structural basis for lipid exchange between ER and mitochondria. *Bioinformatics, 26*(16), 1927-1931. DOI: 10.1093/bioinformatics/btq326

Kornmann, B. (2013). The molecular hug between the ER and the mitochondria. *Current Opinion in Cell Biology, 25*(4), 443-448. DOI: 10.1016/j.ceb.2013.02.010

Kornmann, B., Currie, E., Collins, S. R., Schuldiner, M., Nunnari, J., Weissman, J. S., & Walter, P. (2009). An ER-mitochondria tethering complex revealed by a synthetic biology screen. *Science, 325*(5939), 477-481. DOI: 10.1126/science.1175088

Kornmann, B., Osman, C., & Walter, P. (2011). The conserved GTPase Gem1 regulates endoplasmic reticulum–mitochondria connections. *Proceedings of the National Academy of Sciences, 108*(34), 14151-14156. DOI: 10.1073/pnas.1111314108

Kovács-Bogdán, E., Sancak, Y., Kamer, K. J., Plovanich, M., Jambhekar, A., Huber, R. J., ... & Mootha, V. K. (2014). Reconstitution of the mitochondrial calcium uniporter in yeast. *Proceedings of the National Academy of Sciences*, *111*(24), 8985-8990. DOI: 10.1073/pnas.1400514111

Kroemer, G., Galluzzi, L., Vandenabeele, P., Abrams, J., Alnemri, E. S., Baehrecke, E. H., ... & Hengartner, M. (2009). Classification of cell death: recommendations of the Nomenclature Committee on Cell Death 2009. *Cell death & Differentiation, 16*(1), 3-11. DOI: 10.1038/cdd.2008.150

Kuwana, T., Mackey, M. R., Perkins, G., Ellisman, M. H., Latterich, M., Schneiter, R., ... & Newmeyer, D. D. (2002). Bid, Bax, and lipids cooperate to form supramolecular openings in the outer mitochondrial membrane. *Cell, 111*(3), 331-342. DOI: 10.1016/S0092-8674(02)01036-X

Lahiri, S., Chao, J. T., Tavassoli, S., Wong, A. K., Choudhary, V., Young, B. P., ... & Prinz, W. A. (2014). A conserved endoplasmic reticulum membrane protein complex (EMC) facilitates phospholipid transfer from the ER to mitochondria. *PLoS Biology, 12*(10), e1001969. DOI: 10.1371/journal.pbio.1001969

Lamkanfi, M., & Dixit, V. M. (2010). Manipulation of host cell death pathways during microbial infections. *Cell Host & Microbe, 8*(1), 44-54. DOI: 10.1016/j.chom.2010.06.007

Lang, A. B., Peter, A. T. J., Walter, P., & Kornmann, B. (2015). ER–mitochondrial junctions can be bypassed by dominant mutations in the endosomal protein Vps13. *Journal of Cell Biology*, *210*(6), 883-890. DOI: 10.1083/jcb.201502105

Leung, A. W., Varanyuwatana, P., & Halestrap, A. P. (2008). The mitochondrial phosphate carrier interacts with cyclophilin D and may play a key role in the permeability transition. *Journal of Biological Chemistry*, *283*(39), 26312-26323. DOI: 10.1074/jbc.M805235200

Levine, T., & Loewen, C. (2006). Inter-organelle membrane contact sites: through a glass, darkly. *Current Opinion in Cell Biology*, *18*(4), 371-378. DOI: 10.1016/j.ceb.2006.06.011

Lewis S., Bethell S.S., Patel S., Martinou J.C., & Antonsson B. (1998). Purification and biochemical properties of soluble recombinant human Bax. *Protein Expression and Purification, 13*(1), 120-126. DOI: 10.1006/prep.1997.0871

Li, X. X., Tsoi, B., Li, Y. F., Kurihara, H., & He, R. R. (2015). Cardiolipin and its different properties in mitophagy and apoptosis. *Journal of Histochemistry & Cytochemistry*, *63*(5), 301-311. DOI: 10.1369/0022155415574818

Liu, X., Kim, C. N., Yang, J., Jemmerson, R., & Wang, X. (1996). Induction of apoptotic program in cell-free extracts: requirement for dATP and cytochrome *c*. *Cell*, *86*(1), 147-157. DOI: 10.1016/S0092-8674(00)80085-9

Lockshin, R. A., & Williams, C. M. (1964). Programmed cell death—II. Endocrine potentiation of the breakdown of the intersegmental muscles of silkmoths. *Journal of Insect Physiology*, *10*(4), 643-649. DOI: 10.1016/0022-1910(64)90034-4

Locksley, R. M., Killeen, N., & Lenardo, M. J. (2001). The TNF and TNF receptor superfamilies: integrating mammalian biology. *Cell, 104*(4), 487-501. DOI: 10.1016/S0092-8674(01)00237-9

Lodish, H., Berk, A., Zipursky, S. L., Matsudaira, P., Baltimore, D., & Darnell, J. (2000). Cell Death and its Regulation. In *Molecular Cell Biology*, (4th edition, Chap. 23, Section 8). New York, NY: W. H. Freeman.

López-Crisosto, C., Bravo-Sagua, R., Rodriguez-Peña, M., Mera, C., Castro, P. F., Quest, A. F., ... & Lavandero, S. (2015). ER-to-mitochondria miscommunication and metabolic diseases. *Biochimica et Biophysica Acta (BBA) - Molecular Basis of Disease*, *1852*(10), 2096-2105. DOI: 10.1016/j.bbadis.2015.07.011

Ludovico, P., Sousa, M. J., Silva, M. T., Leão, C. & Côrte-Real, M. (2001). *Saccharomyces cerevisiae* commits to a programmed cell death process in response to acetic acid. *Microbiology, 147*(9), 2409-2415. DOI: 10.1099/00221287-147-9-2409

Ludovico, P., Rodrigues, F., Almeida, A., Silva, M. T., Barrientos, A., & Côrte-Real, M. (2002). Cytochrome c release and mitochondria involvement in programmed cell death induced by acetic acid in *Saccharomyces cerevisiae*. *Molecular Biology of the Cell*, *13*(8), 2598-2606. DOI: 10.1091/mbc.E01-12-0161

Lutter, M., Fang, M., Luo, X., Nishijima, M., Xie, X. S., & Wang, X. (2000). Cardiolipin provides specificity for targeting of tBid to mitochondria. *Nature Cell Biology, 2*(10), 754-761. DOI: 10.1038/35036395

Lutter, M., Perkins, G. A., & Wang, X. (2001). The pro-apoptotic Bcl-2 family member tBid localizes to mitochondrial contact sites. *BMC Cell Biology, 2*(1), 1. DOI: 10.1186/1471-2121-2-22

Madeo, F., Carmona-Gutierrez, D., Ring, J., Büttner, S., Eisenberg, T., & Kroemer, G. (2009). Caspase-dependent and caspase-independent cell death pathways in yeast. *Biochemical and Biophysical Research Communications, 382*(2), 227-231. DOI: 10.1016/j.bbrc.2009.02.117

Madeo, F., Fröhlich, E., & Fröhlich, K. U. (1997). A yeast mutant showing diagnostic markers of early and late apoptosis. *The Journal of Cell Biology, 139*(3), 729-734. DOI: 10.1083/jcb.139.3.729

Madeo, F., Fröhlich, E., Ligr, M., Grey, M., Sigrist, S. J., Wolf, D. H., & Fröhlich, K. U. (1999). Oxygen stress: a regulator of apoptosis in yeast. *The Journal of Cell Biology, 145*(4), 757-767. DOI: 10.1083/jcb.145.4.757

Madeo, F., Herker, E., Maldener, C., Wissing, S., Lächelt, S., Herlan, M., ... & Fröhlich, K. U. (2002). A caspase-related protease regulates apoptosis in yeast. *Molecular Cell, 9*(4), 911-917. DOI: 10.1016/S1097-2765(02)00501-4

Marchi, S., Patergnani, S., & Pinton, P. (2014). The endoplasmic reticulum–mitochondria connection: one touch, multiple functions. *Biochimica et Biophysica Acta (BBA)-Bioenergetics, 1837*(4), 461-469. DOI: 10.1016/j.bbabio.2013.10.015

Marques, C., Oliveira, C. S. F., Alves, S., Chaves, S. R., Coutinho, O. P., Côrte-Real, M., & Preto, A. (2013). Acetate-induced apoptosis in colorectal carcinoma cells involves lysosomal membrane permeabilization and cathepsin D release. *Cell death & disease*, *4*(2), e507. DOI: 10.1038/cddis.2013.29

Martinez-Caballero, S., Dejean, L. M., Jonas, E. A., & Kinnally, K. W. (2005). The role of the mitochondrial apoptosis induced channel MAC in cytochrome c release. *Journal of Bioenergetics and Biomembranes, 37*(3), 155-164. DOI: 10.1007/s10863-005-6570-z

Mason, D. A., Shulga, N., Undavai, S., Ferrando-May, E., Rexach, M. F., & Goldfarb, D. S. (2005). Increased nuclear envelope permeability and Pep4p-dependent degradation of nucleoporins during hydrogen peroxide-induced cell death. *FEMS Yeast Research*, *5*(12), 1237-1251. DOI: 10.1016/j.femsyr.2005.07.008

Meisinger, C., Pfannschmidt, S., Rissler, M., Milenkovic, D., Becker, T., Stojanovski, D., ... & Pfanner, N. (2007). The morphology proteins Mdm12/Mmm1 function in the major β-barrel assembly pathway of mitochondria. *The EMBO Journal*, *26*(9), 2229-2239. DOI: 10.1038/sj.emboj.7601673

Meisinger, C., Rissler, M., Chacinska, A., Szklarz, L. K. S., Milenkovic, D., Kozjak, V., ... & Guiard, B. (2004). The mitochondrial morphology protein Mdm10 functions in assembly of the preprotein translocase of the outer membrane. *Developmental Cell, 7*(1), 61-71. DOI: 10.1016/j.devcel.2004.06.003

Michel, A. H., & Kornmann, B. (2012). The ERMES complex and ER-mitochondria connections. *Biochemical Society Transactions, 40*(2), 445-450. DOI: 10.1042/BST20110758

Michnick, S., Roustan, J., Remize, F., Barre, P., & Dequin, S. (1997). Modulation of glycerol and ethanol yields during alcoholic fermentation in *Saccharomyces cerevisiae* strains overexpressed or disrupted for GPD1 encoding glycerol 3-phosphate dehydrogenase. *Yeast, 13*(9), 783-793. DOI: 10.1002/(SICI)1097-0061(199707)13:9<783::AID-YEA128>3.0.CO;2-W

Murley, A., Lackner, L. L., Osman, C., West, M., Voeltz, G. K., Walter, P., & Nunnari, J. (2013). ER-associated mitochondrial division links the distribution of mitochondria and mitochondrial DNA in yeast. *Elife, 2*. DOI: 10.7554/eLife.00422

Murley, A., Sarsam, R. D., Toulmay, A., Yamada, J., Prinz, W. A., & Nunnari, J. (2015). Ltc1 is an ER-localized sterol transporter and a component of ER–mitochondria and ER–vacuole contacts. *Journal of Cell Biology*, *209*(4), 539-548. DOI: 10.1083/jcb.201502033

Nakagawa, T., Shimizu, S., Watanabe, T., Yamaguchi, O., Otsu, K., Yamagata, H., ... & Tsujimoto, Y. (2005). Cyclophilin D-dependent mitochondrial permeability transition regulates some necrotic but not apoptotic cell death. *Nature, 434*(7033), 652-658. DOI: 10.1038/nature03317

Nasmyth, K. (1996). At the heart of the budding yeast cell cycle. *Trends in Genetics*, *12*(10), 405-412. DOI: 10.1016/0168-9525(96)10041-X

Nguyen, T. T., Lewandowska, A., Choi, J. Y., Markgraf, D. F., Junker, M., Bilgin, M., ... & Shaw, J. M. (2012). Gem1 and ERMES do not directly affect phosphatidylserine transport from ER to mitochondria or mitochondrial inheritance. *Traffic, 13*(6), 880-890. DOI: 10.1111/j.1600-0854.2012.01352.x

Office Internationale de la Vigne et du Vin. (2017): International Code of Oenological Practices, Annex: Maximum Acceptable Limits, Issue 2017/01. Paris, France.

Ogur, M., John, R. S., & Nagai, S. (1957). Tetrazolium overlay technique for population studies of respiration deficiency in yeast. *Science, 125*(3254), 928-929. DOI: 10.1126/science.125.3254.928

Oliveira, C. S., Pereira, H., Alves, S., Castro, L., Baltazar, F., Chaves, S. R., ... & Côrte-Real, M. (2015). Cathepsin D protects colorectal cancer cells from acetate-induced apoptosis through autophagy-independent degradation of damaged mitochondria. *Cell Death & Disease*, *6*(6), e1788. DOI: 10.1038/cddis.2015.157

Osman, C., Haag, M., Potting, C., Rodenfels, J., Dip, P. V., Wieland, F. T., ... & Langer, T. (2009). The genetic interactome of prohibitins: coordinated control of cardiolipin and phosphatidylethanolamine by conserved regulators in mitochondria. *The Journal of Cell Biology*, *184*(4), 583-596. DOI: 10.1083/jcb.200810189

Ott, M., Norberg, E., Walter, K. M., Schreiner, P., Kemper, C., Rapaport, D., ... & Orrenius, S. (2007). The mitochondrial TOM complex is required for tBid/Bax-induced cytochrome *c* release. *Journal of Biological Chemistry*, *282*(38), 27633-27639. DOI: 10.1074/jbc.M703155200

Ottosson, L. G., Logg, K., Ibstedt, S., Sunnerhagen, P., Käll, M., Blomberg, A., & Warringer, J. (2010). Sulfate assimilation mediates tellurite reduction and toxicity in *Saccharomyces cerevisiae*. *Eukaryotic Cell*, *9*(10), 1635-1647. DOI: 0.1128/EC.00078-10

Paillusson, S., Stoica, R., Gomez-Suaga, P., Lau, D. H., Mueller, S., Miller, T., & Miller, C. C. (2016). There's Something Wrong with my MAM; the ER–Mitochondria Axis and Neurodegenerative Diseases. *Trends in Neurosciences, 39*(3), 146-157. DOI: 10.1016/j.tins.2016.01.008

Pampulha, M. E., & Loureiro-Dias, M. C. (1989). Combined effect of acetic acid, pH and ethanol on intracellular pH of fermenting yeast. *Applied Microbiology and Biotechnology, 31*(5), 547-550. DOI: 10.1007/BF00270792

Pampulha, M. E., & Loureiro-Dias, M. C. (1990). Activity of glycolytic enzymes of *Saccharomyces cerevisiae* in the presence of acetic acid. *Applied Microbiology and Biotechnology, 34*(3), 375-380. DOI: 10.1007/BF00170063

Pampulha, M. E., & Loureiro-Dias, M. C. (2000). Energetics of the effect of acetic acid on growth of *Saccharomyces cerevisiae*. *FEMS Microbiology Letters, 184*(1), 69-72. DOI: 10.1111/j.1574-6968.2000.tb08992.x

Pavlov, E. V., Priault, M., Pietkiewicz, D., Cheng, E. H. Y., Antonsson, B., Manon, S., ... & Kinnally, K. W. (2001). A novel, high conductance channel of mitochondria linked to apoptosis in mammalian cells and Bax expression in yeast. *The Journal of Cell Biology, 155*(5), 725-732. DOI: 10.1083/jcb.200107057

Pereira, C., Camougrand, N., Manon, S., Sousa, M. J., & Côrte-Real, M. (2007). ADP/ATP carrier is required for mitochondrial outer membrane permeabilization and cytochrome c release in yeast apoptosis. *Molecular Microbiology*, *66*(3), 571-582. DOI: 10.1111/j.1365-2958.2007.05926.x

Pereira, C., Chaves, S., Alves, S., Salin, B., Camougrand, N., Manon, S., ... & Côrte-Real, M. (2010). Mitochondrial degradation in acetic acid-induced yeast apoptosis: the role of Pep4

and the ADP/ATP carrier. *Molecular Microbiology*, *76*(6), 1398-1410. DOI: 10.1111/j.1365-2958.2010.07122.x

Perkins, G., Renken, C., Martone, M. E., Young, S. J., Ellisman, M., & Frey, T. (1997). Electron tomography of neuronal mitochondria: three-dimensional structure and organization of cristae and membrane contacts. *Journal of Structural Biology*, *119*(3), 260-272. DOI: 10.1006/jsbi.1997.3885

Pinto, I., Cardoso, H., Leão, C., & van Uden, N. (1989). High enthalpy and low enthalpy death in *Saccharomyces cerevisiae* induced by acetic acid. *Biotechnology and Bioengineering, 33*(10), 1350-1352. DOI: 10.1002/bit.260331019

Pinton, P., Giorgi, C., Siviero, R., Zecchini, E., & Rizzuto, R. (2008). Calcium and apoptosis: ER-mitochondria Ca^{2+} transfer in the control of apoptosis. *Oncogene*, *27*(50), 6407. DOI: 10.1038/onc.2008.308

Pfeiffer, K., Gohil, V., Stuart, R. A., Hunte, C., Brandt, U., Greenberg, M. L., & Schägger, H. (2003). Cardiolipin stabilizes respiratory chain supercomplexes. *Journal of Biological Chemistry, 278*(52), 52873-52880. DOI: 10.1074/jbc.M308366200

Polčic, P., Jaká, P., & Mentel, M. (2015). Yeast as a tool for studying proteins of the Bcl-2 family. *Microbial Cell, 2*(3), 74-87. DOI: 10.15698/mic2015.03.193

Rasola, A., Sciacovelli, M., Pantic, B., & Bernardi, P. (2010). Signal transduction to the permeability transition pore. *FEBS Letters, 584*(10), 1989–1996. DOI: 10.1016/j.febslet.2010.02.022

Raturi, A., & Simmen, T. (2013). Where the endoplasmic reticulum and the mitochondrion tie the knot: the mitochondria-associated membrane (MAM). *Biochimica et Biophysica Acta (BBA) - Molecular Cell Research, 1833*(1), 213-224. DOI: 10.1016/j.bbamcr.2012.04.013

Reggiori, F., & Klionsky, D. J. (2013). Autophagic processes in yeast: mechanism, machinery and regulation. *Genetics*, *194*(2), 341-361. DOI: 10.1534/genetics.112.149013

Remize, F., Roustan, J. L., Sablayrolles, J. M., Barre, P., & Dequin, S. (1999). Glycerol overproduction by engineered Saccharomyces cerevisiae wine yeast strains leads to substantial changes in by-product formation and to a stimulation of fermentation rate in stationary phase. *Applied and Environmental Microbiology*, *65*(1), 143-149. Retrieved from: http://aem.asm.org/content/65/1/143.long

Remize, F., Andrieu, E., & Dequin, S. (2000). Engineering of the Pyruvate Dehydrogenase Bypass in *Saccharomyces cerevisiae*: Role of the Cytosolic Mg2+ and Mitochondrial K+ Acetaldehyde Dehydrogenases Ald6p and Ald4p in Acetate Formation during Alcoholic Fermentation. *Applied and Environmental Microbiology, 66*(8), 3151-3159. DOI: 10.1128/AEM.66.8.3151-3159.2000

Ribéreau-Gayon, P., Dubourdieu, D., Donèche, B., & Lonvaud, A. (Eds.). (2006). Alcohols and other volatile compounds. In *Handbook of Enology: The Microbiology of Wine and Vinifications* (Vol. 2, 2nd ed, 51-64). John Wiley & Sons.

Rizzuto, R., Brini, M., Murgia, M., & Pozzan, T. (1993). Microdomains with high Ca^{2+} close to IP_3-sensitive channels that are sensed by neighboring mitochondria. *Science, 262*(5134), 744-748. DOI: 10.1126/science.8235595

Roucou, X., Manon, S., & Guérin, M. (1997). Conditions allowing different states of ATP-and GDP-induced permeability in mitochondria from different strains of *Saccharomyces cerevisiae*. *Biochimica et Biophysica Acta (BBA) - Biomembranes*, *1324*(1), 120-132. DOI: 10.1016/S0005-2736(96)00215-5

Saelens, X., Festjens, N., Walle, L. V., Van Gurp, M., van Loo, G., & Vandenabeele, P. (2004). Toxic proteins released from mitochondria in cell death. *Oncogene, 23*(16), 2861-2874. DOI: 10.1038/sj.onc.1207523

Saito, M., Korsmeyer S.J. & Schlesinger P.H. (2000). BAX-dependent transport of cytochrome c reconstituted in pure liposomes. *Nature Cell Biology, 2*(8), 553-555. DOI: 10.1038/35019596

Saraste, A., & Pulkki, K. (2000). Morphologic and biochemical hallmarks of apoptosis. *Cardiovascular Research, 45*(3), 528-537. DOI: 10.1016/S0008-6363(99)00384-3

Sattler, M., Liang, H., Nettesheim, D., Meadows, R. P., Harlan, J. E., Eberstadt, M., ... & Thompson, C. B. (1997). Structure of Bcl-xL-Bak peptide complex: recognition between regulators of apoptosis. *Science, 275*(5302), 983-986. DOI: 10.1126/science.275.5302.983

Schekman, R. (1992). Genetic and biochemical analysis of vesicular traffic in yeast. *Current Opinion in Cell Biology*, *4*(4), 587-592. DOI: 10.1016/0955-0674(92)90076-O

Segawa, K., & Nagata, S. (2015). An apoptotic 'eat me'signal: phosphatidylserine exposure. *Trends in Cell Biology*, *25*(11), 639-650. DOI: 10.1016/j.tcb.2015.08.003

Shamas-Din, A., Brahmbhatt, H., Leber, B., & Andrews, D. W. (2011). BH3-only proteins: Orchestrators of apoptosis. *Biochimica et Biophysica Acta (BBA) - Molecular Cell Research, 1813*(4), 508-520. DOI: 10.1016/j.bbamcr.2010.11.024

Silva, A., Almeida, B., Sampaio-Marques, B., Reis, M. I. R., Ohlmeier, S., Rodrigues, F., ... & Ludovico, P. (2011). Glyceraldehyde-3-phosphate dehydrogenase (GAPDH) is a specific substrate of yeast metacaspase. *Biochimica et Biophysica Acta (BBA) - Molecular Cell Research, 1813*(12), 2044-2049. DOI: 10.1016/j.bbamcr.2011.09.010

Simmen, T., Aslan, J. E., Blagoveshchenskaya, A. D., Thomas, L., Wan, L., Xiang, Y., ... & Thomas, G. (2005). PACS-2 controls endoplasmic reticulum–mitochondria communication and Bid-mediated apoptosis. *The EMBO Journal, 24*(4), 717-729. DOI: 10.1038/sj.emboj.7600559

Sinzel, M., Tan, T., Wendling, P., Kalbacher, H., Özbalci, C., Chelius, X., ... & Dimmer, K. S. (2016). Mcp3 is a novel mitochondrial outer membrane protein that follows a unique IMP-dependent biogenesis pathway. *EMBO Reports*, *17*(7), 965-981. DOI: 10.15252/embr.201541273

Skulachev, V. P. (2000). Mitochondria in the programmed death phenomena; a principle of biology: "it is better to die than to be wrong". *IUBMB Life, 49*(5), 365-373. DOI: 10.1080/152165400410209

Sogo, L. F., & Yaffe, M. P. (1994). Regulation of mitochondrial morphology and inheritance by Mdm10p, a protein of the mitochondrial outer membrane. *The Journal of Cell Biology*, *126*(6), 1361-1373. DOI: 10.1083/jcb.126.6.1361

Sousa, M. J., Ludovico, P., Rodrigues, F., Leão, C., & Côrte-Real, M. (2012). Stress and cell death in yeast induced by acetic acid. In *Cell Metabolism – Cell Homeostasis and Stress Response*. InTech. DOI: 10.5772/27726

Sousa, M., Duarte, A. M., Fernandes, T. R., Chaves, S. R., Pacheco, A., Leão, C., ... & Sousa, M. J. (2013). Genome-wide identification of genes involved in the positive and negative regulation of acetic acid-induced programmed cell death in Saccharomyces cerevisiae. *BMC Genomics, 14*(1), 838. DOI: 10.1186/1471-2164-14-838

Stroud, D. A., Oeljeklaus, S., Wiese, S., Bohnert, M., Lewandrowski, U., Sickmann, A., ... & Wiedemann, N. (2011). Composition and topology of the endoplasmic reticulum–mitochondria encounter structure. *Journal of Molecular Biology, 413*(4), 743-750. DOI: 10.1016/j.jmb.2011.09.012

Suen, D. F., Norris, K. L., & Youle, R. J. (2008). Mitochondrial dynamics and apoptosis. *Genes & Development, 22*(12), 1577-1590. DOI: 10.1101/gad.1658508

Susin, S. A., Lorenzo, H. K., Zamzami, N., & Marzo, I. (1999). Molecular characterization of mitochondrial apoptosis-inducing factor. *Nature*, *397*(6718), 441. DOI: 10.1038/17135

Suzuki, M., Youle, R. J., & Tjandra, N. (2000). Structure of Bax: coregulation of dimer formation and intracellular localization. *Cell*, *103*(4), 645-654. DOI: 10.1016/S0092-8674(00)00167-7

Szklarz, L. K. S., Kozjak-Pavlovic, V., Vögtle, F. N., Chacinska, A., Milenkovic, D., Vogel, S., ... & Borner, C. (2007). Preprotein transport machineries of yeast mitochondrial outer membrane are not required for Bax-induced release of intermembrane space proteins. *Journal of Molecular Biology*, *368*(1), 44-54. DOI: 10.1016/j.jmb.2007.01.016

Tait, S. W., & Green, D. R. (2010). Mitochondria and cell death: outer membrane permeabilization and beyond. *Nature Reviews Molecular Cell Biology*, *11*(9), 621-632. DOI: 10.1038/nrm2952

Tait, S. W., Ichim, G., & Green, D. R. (2014). Die another way–non-apoptotic mechanisms of cell death. *Journal of Cell Science, 127*(10), 2135-2144. DOI: 10.1242/jcs.093575

Tan, T., Özbalci, C., Brügger, B., Rapaport, D., & Dimmer, K. S. (2013). Mcp1 and Mcp2, two novel proteins involved in mitochondrial lipid homeostasis. *Journal of Cell Science*, *126*(16), 3563-3574. DOI: 10.1242/jcs.121244

Terrones, O., Antonsson, B., Yamaguchi, H., Wang, H. G., Liu, J., Lee, R. M., ... & Basañez, G. (2004). Lipidic pore formation by the concerted action of pro-apoptotic BAX and tBID. *Journal of Biological Chemistry, 279*(29), 30081-30091. DOI: 10.1074/jbc.M313420200

Trindade, D., Pereira, C., Chaves, S. R., Manon, S., Côrte-Real, M., & Sousa, M. J. (2016). VDAC regulates AAC-mediated apoptosis and cytochrome *c* release in yeast. *Microbial Cell*, *3*(10), 500. DOI: 10.15698/mic2016.10.533

Tsiatsiani, L., Van Breusegem, F., Gallois, P., Zavialov, A., Lam, E., & Bozhkov, P. V. (2011). Metacaspases. *Cell Death & Differentiation, 18*(8), 1279-1288. DOI: 10.1038/cdd.2011.66

Ušaj, M. M., Brložnik, M., Kaferle, P., Žitnik, M., Wolinski, H., Leitner, F., ... & Petrovič, U. (2015). Genome-wide localization study of yeast Pex11 identifies peroxisome–mitochondria interactions through the ERMES complex. *Journal of Molecular Biology, 427*(11), 2072-2087. DOI: 10.1016/j.jmb.2015.03.004

van den Berg, M. A., de Jong-Gubbels, P., Kortland, C. J., van Dijken, J. P., Pronk, J. T., & Steensma, H. Y. (1996). The two acetyl-coenzyme A synthetases of *Saccharomyces cerevisiae* differ with respect to kinetic properties and transcriptional regulation. *Journal of Biological Chemistry*, *271*(46), 28953-28959. DOI: 10.1074/jbc.271.46.28953

van Vliet, A. R., Verfaillie, T., & Agostinis, P. (2014). New functions of mitochondria associated membranes in cellular signaling. *Biochimica et Biophysica Acta (BBA) - Molecular Cell Research*, *1843*(10), 2253-2262. DOI: 10.1016/j.bbamcr.2014.03.009

Vance, J. E. (1990). Phospholipid synthesis in a membrane fraction associated with mitochondria. *Journal of Biological Chemistry, 265*(13), 7248-7256. Retrieved from http://www.jbc.org/content/265/13/7248

Velours, J., Rigoulet, M., & Guerin, B. (1977). Protection of yeast mitochondrial structure by phosphate and other H+-donating anions. *FEBS Letters, 81*(1), 18-22. DOI: 10.1016/0014-5793(77)80918-6

Vilela-Moura, A., Schuller, D., Mendes-Faia, A., Silva, R. D., Chaves, S. R., Sousa, M. J., & Côrte-Real, M. (2011). The impact of acetate metabolism on yeast fermentative performance and wine quality: reduction of volatile acidity of grape musts and wines. *Applied Microbiology and Biotechnology*, *89*(2), 271-280. DOI: 10.1007/s00253-010-2898-3

Vo, T. T., & Letai, A. (2010). BH3-only proteins and their effects on cancer. In Claudio Hetz (Ed), *BCL-2 Protein Family* (Chap. 3, pp. 49-63). New York, NY: Springer.

Wang, H. J., Guay, G., Pogan, L., Sauvé, R., & Nabi, I. R. (2000). Calcium regulates the association between mitochondria and a smooth subdomain of the endoplasmic reticulum. *The Journal of Cell Biology, 150*(6), 1489-1498. DOI: 10.1083/jcb.150.6.1489

Wang, P., Wang, P., Liu, B., Zhao, J., Pang, Q., Agrawal, S. G., ... & Liu, F. T. (2015). Dynamin-related protein Drp1 is required for Bax translocation to mitochondria in response to irradiation-induced apoptosis. *Oncotarget, 6*(26), 22598. DOI: 10.18632/oncotarget.4200

Weinberger, M., Ramachandran, L., & Burhans, W. (2003). Apoptosis in yeasts. *IUBMB Life, 55*(8), 467-472. DOI: 10.1080/15216540310001612336

Westermann, B. (2008). Molecular machinery of mitochondrial fusion and fission. *Journal of Biological Chemistry, 283*(20), 13501-13505. DOI: 10.1074/jbc.R800011200

Westermann, B. (2012). Bioenergetic role of mitochondrial fusion and fission. *Biochimica et Biophysica Acta (BBA) - Bioenergetics*, *1817*(10), 1833-1838. DOI: 10.1016/j.bbabio.2012.02.033

Wideman, J. G. (2015). The ubiquitous and ancient ER membrane protein complex (EMC): tether or not?. *F1000Research, 4*, 624. DOI: 10.12688/f1000research.6944.2

Winderickx, J., Delay, C., De Vos, A., Klinger, H., Pellens, K., Vanhelmont, T., ... & Zabrocki, P. (2008). Protein folding diseases and neurodegeneration: lessons learned from yeast. *Biochimica et Biophysica Acta (BBA) - Molecular Cell Research, 1783*(7), 1381-1395. DOI: 10.1016/j.bbamcr.2008.01.020

Wissing, S., Ludovico, P., Herker, E., Büttner, S., Engelhardt, S. M., Decker, T., ... & Madeo, F. (2004). An AIF orthologue regulates apoptosis in yeast. *The Journal of Cell Biology, 166*(7), 969-974. DOI: 10.1083/jcb.200404138

Wong, A. H. H., Yan, C., & Shi, Y. (2012). Crystal structure of the yeast metacaspase Yca1. *Journal of Biological Chemistry, 287*(35), 29251-29259. DOI: 10.1074/jbc.M112.381806

Woodcock, J. (2006). Sphingosine and ceramide signalling in apoptosis. *IUBMB life*, *58*(8), 462-466. DOI: 10.1080/15216540600871118

Yadav, V., Shitiz, K., Pandey, R., & Yadav, J. (2011). Chlorophenol stress affects aromatic amino acid biosynthesis — a genome-wide study. *Yeast*, *28*(1), 81-91. DOI: 10.1002/yea.1825

Yamano, K., Tanaka-Yamano, S., & Endo, T. (2010). Tom7 regulates Mdm10-mediated assembly of the mitochondrial import channel protein Tom40. *Journal of Biological Chemistry, 285*(53), 41222-41231. DOI: 10.1074/jbc.M110.163238

Zamora, F. (2009). Biochemistry of alcoholic fermentation. In M. V. Moreno-Arribas & M. C. Polo (Ed), *Wine Chemistry and Biochemistry* (Vol. 223, 3-26). New York: Springer.

Zampese, E., Fasolato, C., Kipanyula, M. J., Bortolozzi, M., Pozzan, T., & Pizzo, P. (2011). Presenilin 2 modulates endoplasmic reticulum (ER)–mitochondria interactions and Ca2+ cross-talk. *Proceedings of the National Academy of Sciences, 108*(7), 2777-2782. DOI: 10.1073/pnas.1100735108

Zhou, W., Marinelli, F., Nief, C., & Faraldo-Gómez, J. D. (2017). Atomistic simulations indicate the c-subunit ring of the F1Fo ATP synthase is not the mitochondrial permeability transition pore. *Elife*, *6*, e23781. DOI: 10.7554/eLife.23781